Integrin Signaling is a Novel Regulator of Hepatic Insulin Action

By

Ashley Silberman Williams

Dissertation

Submitted to the Faculty of the

Graduate School of Vanderbilt University

in partial fulfillment of the requirements

for the degree of

DOCTOR OF PHILOSOPHY

in

Molecular Physiology and Biophysics

May, 2015

Nashville, Tennessee

Approved:

Maureen Gannon, Ph.D.
Alan D. Cherrington, Ph.D.
Ambra Pozzi, Ph.D.
John M. Stafford, M.D., Ph.D.

ACKNOWLEDGEMENTS

I would like to acknowledge the many people who have been so instrumental to the completion of these studies as well as my personal and professional growth over the past six years. First, I would like to thank my mentor, Dr. David Wasserman, for his guidance and support. I am very grateful to have had the experience to work with him as a student in the laboratory. David has provided many great opportunities for me to grow and learn as a scientist, for which I will always be thankful. Under his mentorship, I have learned so much about physiology and what it means to be a scientist at the cutting edge of biomedical research. He has also taught me the invaluable lesson to see the humor in everything.

These studies would also not have been possible without the technical support and input from past and present members of the laboratory: Deanna (Bing) Bracy, Jeff Bonner, Mickael Goelzer, Clinton Hasenour, Curtis Hughey, Freyja James, Li Kang, Louise Lantier, Dan Lark, Elijah Trefts, Ian Williams, Azeem Ansari and Jenny Zheng. I would especially like to thank Bing Bracy, Li Kang and Louise Lantier for their support and friendship over the years. The technical support from the Vanderbilt Mouse Metabolic Phenotyping Core, Translational Pathology Shared Resource Core, Lipid Core and Hormone Assay Core were essential for the completion of these studies.

I would like to thank the members of my dissertation committee: Drs. Maureen Gannon, Alan Cherrington, Ambra Pozzi and John Stafford, for their time, guidance, patience and support. I have learned so much from each of them and truly appreciate their contributions to these projects and my professional development. Intellectual discussions with Dr. Owen McGuinness were also critical to these projects and my scientific development. Finally, I would like to thank my family for their never ending support throughout this journey.

TABLE OF CONTENTS

Page

LIST OF FIGURES

LIST OF TABLES

Table **Page**

Chapter I

INTRODUCTION

The prevalence of obesity is increasing and it is projected to get worse with approximately 50% of the US population becoming obese by the year 2030. Obesity is a primary risk factor for Type 2 diabetes (T2D). As body mass increases so does the risk of developing T2D. Consequently, the number of individuals with T2D has risen to epidemic proportions. It is estimated that approximately 9.3% of the United States population had T2D in 2012 with an estimated 1.7 million new diagnoses occurring every year (http://www.diabetes.org/diabetes-basics/statistics).

Insulin resistance precedes the development of T2D (1,2). In healthy individuals, insulin secreted by the β-cells of the pancreas facilitates glucose homeostasis by suppressing hepatic glucose production and increasing glucose disposal by peripheral tissues. In the insulin resistant state, the skeletal muscle and liver are no longer able to respond to insulin. This results in an elevation of blood glucose due in part to impaired peripheral glucose uptake and increased hepatic glucose production despite high levels of circulating insulin. The insulin resistant state is characterized by hyperglycemia. However T2D does not occur until the β-cells of the pancreas fail to produce sufficient insulin. The liver is integral to maintaining whole-body glucose homeostasis; therefore understanding the mechanisms underlying hepatic adaptations to obesity are critical to developing potential therapeutic targets and treating T2D.

The liver is essential for whole-body glucose homeostasis

The liver is central for maintaining glucose homeostasis. This is achieved through its ability to regulate glucose output, uptake and storage depending on the metabolic state of the body. The liver is a major insulin-responsive organ. In the presence of insulin, hepatic glucose disposal is enhanced and hepatic glucose production (also termed endogenous glucose production or EGP) is suppressed (1,3,4). Both processes greatly contribute to whole-body glucose homeostasis. The contribution of insulin-mediated suppression of hepatic glucose production to the regulation of glucose homeostasis was originally demonstrated in a study by Basu et al. (5). In this study, EGP was determined in nondiabetic and T2D subjects in the postprandial state. Blood glucose was clamped at postprandial levels (~8mmol/l) and insulin was infused at different physiological doses. EGP was higher in individuals with T2D compared to nondiabetic individuals despite the same experimental glucose and insulin concentrations. This original study was subsequently expanded into another study that included individuals with both "mild" diabetes (fasting glucose ~8mmol/l) and "severe" diabetes (fasting glucose ~12mmol/l) (6). In this study, hyperinsulinemic-euglycemic (insulin) clamps were performed and EGP was measured in the fasted state and during the insulin clamp. As previously reported, EGP was increased in the fasted state in patients with severe diabetes. However, there was no difference in fasting EGP between mild diabetic and nondiabetic individuals. The lack of differences in fasting endogenous glucose production between individuals with mild diabetes and nondiabetic individuals was attributed to higher fasting insulin levels in individuals with mild diabetes. Most importantly, EGP during the insulin clamp was higher in individuals with mild and severe diabetes compared to nondiabetic individuals. Collectively, these studies demonstrate that

abnormal regulation of hepatic glucose metabolism occurs early in the development of T2D and individuals with T2D have hepatic insulin resistance.

Mechanisms of hepatic insulin action

Defects in hepatic insulin signaling can lead to insulin resistance and eventually T2D (1,2). In nondiabetic individuals, dietary glucose stimulates insulin secretion from pancreatic β-cells. Insulin then travels directly to the liver through the portal vein. The liver is a major site of insulin clearance. It is estimated that 50% of insulin is extracted by the liver during the first pass via a receptor-mediated process (7-9). The majority of liver insulin uptake is attributed to hepatocytes and a small portion, approximately 15%, is due to Kupffer cells (8).

The uptake of insulin into the liver can vary depending on several physiological or pathophysiological factors including nutrient status, obesity and hyperinsulinemia. Insulin clearance rates by the liver are decreased in obesity and glucose intolerance (10). Moreover, hepatic insulin extraction is decreased in the ob/ob mouse model (11). This is attributed to hyperinsulinemia and the subsequent downregulation of hepatic insulin receptors. Hence, the ability of the liver to extract insulin from the circulation may impact its ability to properly respond to an insulin stimulus.

Insulin exerts its biological effects through the insulin receptor (12). The insulin receptor is a tetrameric protein that consists of two extracellular α subunits and two transmembrane β subunits bound by disulfide bonds. Once insulin reaches the hepatocyte and binds its receptor, a conformational change occurs resulting in the activation and subsequent tyrosine kinase autophosphorylation of the β subunits. This leads to the recruitment of receptor substrates such as insulin receptor substrate (IRS) proteins. IRS proteins are recruited to the membrane and

activated receptors where they are subsequently phosphorylated on multiple tyrosine residues (13). Along with the IRS proteins, the insulin receptor can phosphorylate other substrates such as Shc proteins involved in the activation of the Ras/ERK signaling cascade (14).

Both IRS1 and IRS2 are critical for activation of the PI3-kinase-Akt signaling cascade. Akt can be phosphorylated at 2 sites by its activating kinases that are important for insulin signaling, Ser473 and Thr308. There are three described isoforms of Akt encoded by different genes: Akt1, Akt2 and Akt3 (15). In mouse liver, Akt2 is the predominant isoform which constitutes approximately 84% of all Akt protein. The remaining Akt protein consists entirely of Akt1 as Akt3 cannot be detected. Upon Akt activation, it phosphorylates and either activates or inactivates several downstream proteins to modulate distinct metabolic pathways. One pathway modulates protein synthesis and cell growth through the inactivation of tuberous sclerosis (TSC) 1-2 complex. Another pathway facilitates glycogen storage through the inactivation of glycogen synthase kinase (GSK)-3β. A third pathway, and the most important for insulin action in the liver, facilitates the phosphorylation and nuclear exclusion of a key modulator of gluconeogenic gene expression, forkhead box O1 (Foxo1) (16). Akt phosphorylates Foxo1 at several sites including Ser253, Ser316 and Thr24. This provides docking sites for proteins of the 14-3-3 family and blocks the entry of Foxo1 into the nucleus. The nuclear exclusion of Foxo1 prohibits gene expression of the gluconeogenic genes glucose 6-phosphatase (*G6pase*) and phosphoenolpyruvate carboxykinase (*Pepck*) resulting in a decrease in hepatic glucose production.

In the insulin resistant state, insulin fails to produce its desired biological effect due to defects in insulin receptor autophosphorylation and/or decreased activation of its downstream effectors (17). This results in the hallmark of hepatic insulin resistance which is increased

hepatic glucose production despite an insulin stimulus. Multiple mechanisms have been described for the downregulation of insulin signaling within the hepatocyte (Figure 1.1). These include decreased phosphorylation of the insulin receptor and/or IRS proteins, suppressor of cytokine signaling (SOCS) protein upregulation/activation, phosphatases, and inhibitory serine phosphorylation of IRS proteins as well as the insulin receptor (18). Much of this has been established through the use of genetic manipulations in mouse models. Liver-specific insulin receptor knockout (LIRKO) mice and liver-specific IRS1 and IRS2 double knockout (DKO) mice develop hyperinsulinemia, glucose intolerance and severe insulin resistance associated with impaired insulin signaling (19,20).

Most interestingly, of all the proposed regulators of hepatic insulin action, it appears that Foxo1 regulation by Akt is particularly important for the suppression of insulin-mediated hepatic glucose production. In the insulin resistant liver, Foxo1 translocates to the nucleus where it promotes the transcriptional upregulation of G6Pase and PEPCK. Transgenic mice expressing a Foxo1 dominant negative mutant (Foxo1-Δ256) exhibit a significant reduction in hepatic G6pase and Pepck mRNA (21). Both G6Pase and PEPCK are regulated at the transcriptional level and are not subject to post-translational modifications (22). PEPCK catalyzes the conversion of oxaloacetate to phosphoenolpyruvate. Phosphoenolpyruvate is then converted into glucose through several enzyme-mediated reactions. The PEPCK reaction is a rate limiting step for gluconeogenesis. In contrast, G6Pase catalyzes the hydrolysis of glucose-6-phosphate to glucose. The glucose is then transported across the ER and plasma membranes through the glucose T2 and GLUT2 transporters where it is then released into the circulation.

The contribution of Foxo1 to hepatic glucose production in the insulin resistant state was addressed in a study by Lu et al. (23). In this study, mice with a hepatic deletion of Akt1, Akt2

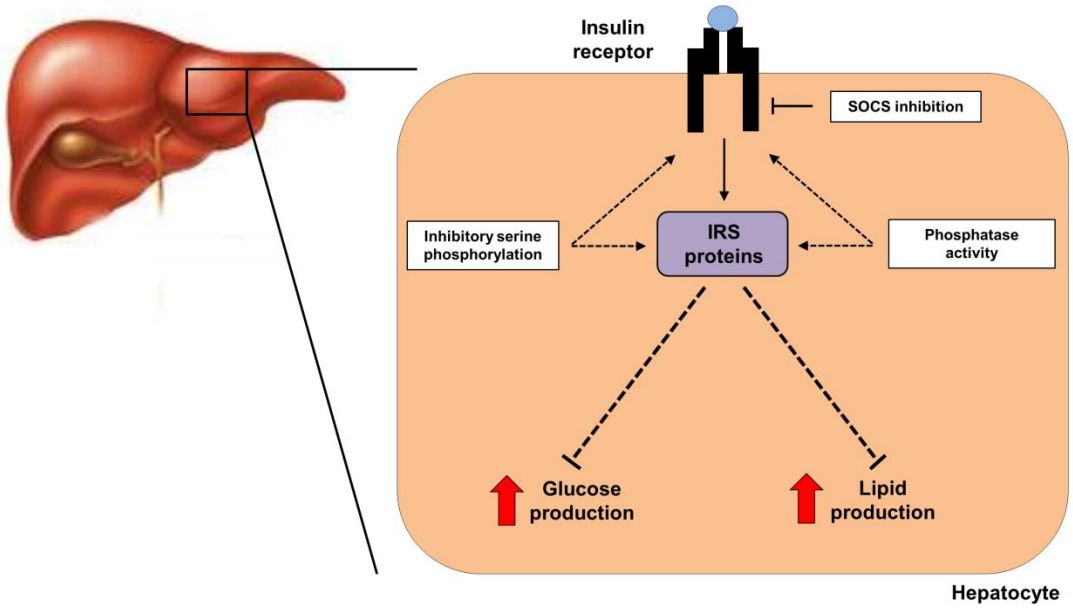

Figure 1.1 – Intracellular mechanisms of hepatic insulin resistance. In the insulin resistant state, there are multiple mechanisms that exist for down regulating insulin signaling such as SOCS proteins, phosphatases and inhibitory serine phosphorylation of IRS proteins and the insulin receptor. This results in decreased hepatic insulin signaling and the hallmarks of hepatic insulin resistance including increased hepatic glucose production and lipid production.

and both Akt and Foxo1 were studied to determine their relative contributions to the suppression of hepatic glucose production in the presence of insulin. The mice with a hepatic deletion of Akt1 and Akt2 were insulin resistant. Strikingly, the insulin resistance was normalized and hepatic glucose production was suppressed when Foxo1 was also deleted. This indicates that hepatic Akt plays a major role in preventing the activation of Foxo1 and when Foxo1 is absent, Akt is not necessary for the suppression of hepatic glucose production.

The termination of insulin action occurs upon the internalization and degradation of insulin-receptor complexes (24). This process happens within minutes of receptor binding. Studies in either isolated hepatocytes (25) or perfused livers (26) have shown that insulin is initially localized to the plasma membrane and by 10 min, over half of the insulin is internalized. Receptor-bound insulin can also be released from the cell where it re-enters the circulation (27).

Mechanisms of hepatic lipid accumulation and nonalcoholic fatty liver disease (NAFLD)

Insulin promotes hepatic triglyceride (TG) synthesis and storage within the liver. In times of excess caloric intake, a disproportionate amount of hepatic fat accumulation occurs within the liver. When more than 5-10% of the liver's weight consists of fat, then it is referred to as a fatty liver. This is also referred to as nonalcoholic fatty liver disease (NAFLD). NAFLD is the leading cause of liver dysfunction in the US (28). It is estimated that approximately 25% of the US population has NAFLD (http://www.liverfoundation.org/abouttheliver/info/nafld/).

There are several metabolic pathways that contribute to increased hepatic lipid accumulation in the presence of over nutrition (Figure 1.2). These include: increased fat delivery, increased fat synthesis, reduced fat export, and decreased cellular utilization of fats (28-30). High circulating levels of serum free fatty acids (FFA) are positively correlated with NAFLD (31).

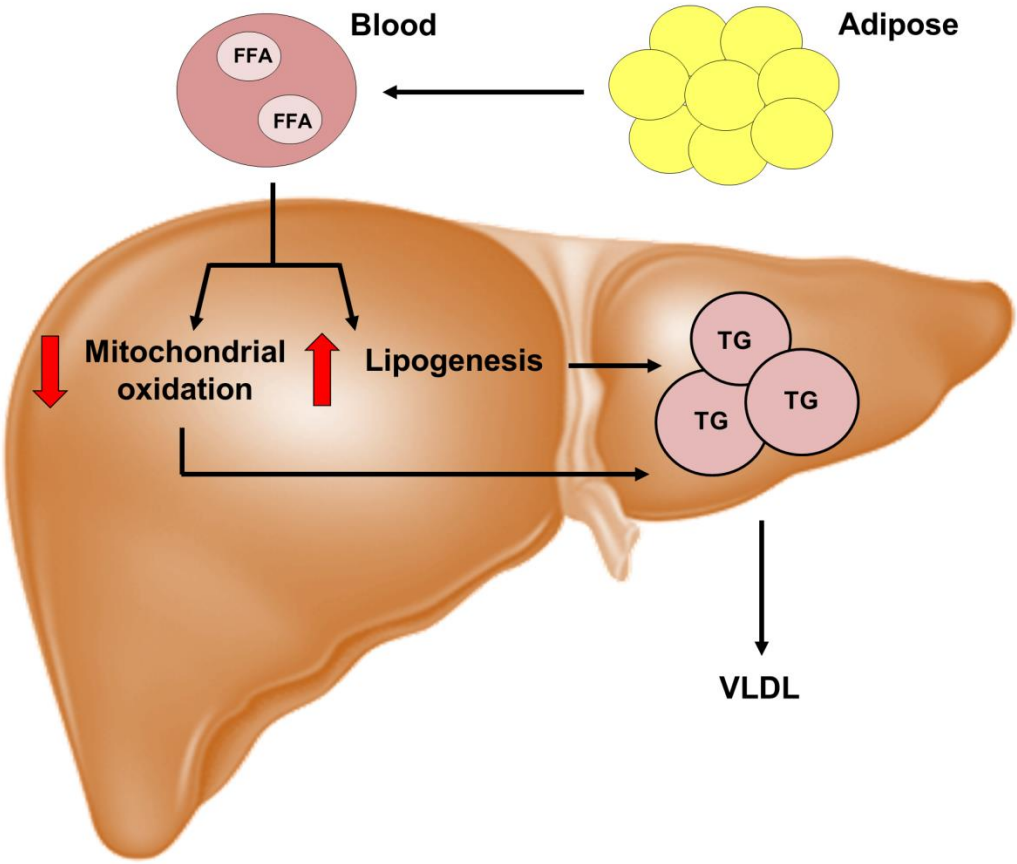

Figure 1.2 – Metabolic pathways leading to hepatic triglyceride accumulation. There are several metabolic pathways that lead to hepatic TG accumulation. Under conditions of insulin resistance, lipolysis in white adipose tissue is not suppressed. This leads to increased FFA flux into the circulation. In addition, hyperglycemia and hyperinsuinemia promote lipogenesis and mitochondrial oxidation is impaired. After the esterification step TGs can then be stored as lipid droplets within hepatocytes or secreted into the blood as VLDL.

Increased circulating FFAs can occur due to increased lipolysis (the hydrolysis of TGs) or increased dietary intake of fat. Under normal conditions, insulin suppresses lipolysis in the adipose tissue. In insulin resistant human patients with NAFLD, insulin fails to suppress lipolysis in white adipose tissue to the same extent as healthy patients (32). This results in increased FFA release from the adipose tissue and a subsequent higher rate of entry into the circulation due in part to the failure of insulin to adequately inhibit hormone sensitive lipase (HSL) (33). Studies in HSL-null mice exhibit decreased circulating FFAs and a concomitant decrease in liver TG levels (34).

FFAs are taken up from the circulation by fatty acid transporters located on the cell surface of the hepatocyte such as CD36/FAT. CD36 is a transmembrane protein that promotes fatty acid uptake via facilitated diffusion. CD36 is an important regulator of fatty acid uptake into the hepatocyte and its expression is positively correlated with liver fat in patients with NAFLD (35). In the basal state, the expression of CD36 on hepatocytes is low; however its expression increases significantly with HF feeding (36). Mice fed a HF diet (60%) for 5 weeks displayed a 2.6-fold increase in CD36 protein expression. This correlated with a 1.7-fold increase in hepatic TG content suggesting that increased CD36 expression correlates with increased TG accumulation in mice fed a HF diet. Moreover, overexpression of CD36 via adenovirus resulted in an increase in hepatic fatty acid uptake and TG storage. These data suggest that CD36 expression regulates fatty acid uptake into the liver and a rise in CD36 expression that occurs with HF feeding is associated with increased hepatic TG accumulation. Once FFAs enter into the liver, they can be esterified into TGs where they can be stored as lipid droplets within hepatocytes.

Increased fat delivery via high levels of circulating FFAs is a major determinant of hepatic TG accumulation (30,37). The relative contribution of FFAs to liver TGs in human patients with NAFLD was determined in a study by Donnelly et al. (30). In this study, a multiple stable isotope approach was used to estimate the relative contributions of circulating FFAs, de novo lipogenesis and the diet to liver fat accumulation. Their results showed that approximately 59% was due to FFAs, 26% arose from de novo lipogenesis and the remaining 15% was from the diet. This suggests that although there are many pathways that can lead to TG accumulation in the liver, elevated circulating FFAs are the largest contributor to the development of NAFLD.

As stated above, increased de novo lipogenesis (DNL) is the second largest contributor of hepatic TG accumulation in humans with NAFLD (30). DNL is an integrated metabolic pathway comprised of glycolysis (conversion of glucose to acetyl-CoA), synthesis of saturated fatty acid followed by desaturation, and the formation of TGs (28). There are several key enzymes that regulate DNL. These include acetyl-CoA carboxylase (ACC), fatty acid synthase (FAS), long chain fatty acid elongase 6 (ELOVL6), stearoyl-CoA desaturase (SCD), glycerol-3-phosphate acyltransferase (GPAT) and diacylglycerol acyltransferase (DGAT). ACC and FAS are involved in fatty acid synthesis. ELOVL6 and SCD facilitate the formation of monounsaturated fatty acids. GPAT and DGAT regulate the formation of TGs.

The enzymes responsible for DNL are transcriptionally regulated by both carbohydrate responsive element-binding protein (ChREBP) and sterol regulatory element-binding protein-1c (SREBP-1c). These pathways are regulated by nutritional status and synergistically respond to glucose and carbohydrate, respectively. Glucose activates ChREBP by regulating its entry into the nucleus from the cytosol where it regulates the transcription of its target genes as part of a heterodimeric complex with Mlx (Max-like protein X) (38,39). In contrast, SREBP-1c is

transcriptionally regulated by insulin and it regulates gene expression through its ability to bind sterol regulatory elements (SREs) within the promoter of its target genes (40). This is evidenced by a rise in SREBP-1c gene and protein expression when insulin levels are high, such as during refeeding with a high carbohydrate diet (41). Collectively, ChREBP and SREBP-1c regulate the transcription of enzymes involved in fatty acid synthesis such as ACC, FAS, ELOVL6, and SCD1 as well as enzymes involved in TG synthesis such as GPAT.

Genetic manipulations in mice have added a great amount to the understanding of the regulation of lipogenic gene expression in response to glucose and/or insulin. ChREBP-1c overexpressing mice on either a chow and HF diet exhibit increased liver fat accumulation and increased expression of genes involved in lipogenesis such as *Acc, Elovl6* and *Scd1* compared to controls (42). Transgenic mice that overexpress SREBP-1c in the liver display increased lipogenic gene expression and increased lipid accumulation (43). Additionally, the synergistic regulation of lipogenic gene expression by both ChREBP and SREBP-1c was established in a study using mice with a genetic deletion of SREBP-1c (44). In this study, the deletion of SREBP-1c resulted in only a 50% reduction in hepatic gene expression of *Acc* and *Fas*. When these mice were fasted and refed, thus generating an insulin response, it was observed that there was no induction of gene expression of *Gpat*. This suggests that SREBP-1c is only partially responsible for gene expression of *Acc* and *Fas*, while it may be completely responsible for the transcriptional regulation of *Gpat.* It is also interesting to note that the SREBP-1c null mice exhibit a marked decrease in hepatic TG accumulation compared to the wild-type control mice in response to a high carbohydrate meal.

Mitochondria are metabolically flexible organelles that can adapt to increased fatty acid oxidation to a limited extent when provided with excess substrate (45). Mitochondrial β-

oxidation of fatty acids serves to shorten the fatty acids into acetyl-CoA where they are either converted into ketone bodies (β-hydroxybutyrate) or enter the TCA cycle. The NADH and $FADH_2$ produced by both β-oxidation and the TCA cycle are used as substrates for oxidative phosphorylation. When the supply of FFAs exceeds the amount the mitochondria can oxidize, hepatic fat accumulation occurs. In light of this, mitochondrial dysfunction is associated with the development of NAFLD. Mice with a heterozygous deletion of mitochondrial trifunctional protein (MTP) developed hepatic steatosis (46). Adiponectin knock out mice exhibit mitochondrial dysfunction and increased hepatic TG accumulation (47). Additionally, genetically obese rats display impaired mitochondrial function, decreased mitochondrial content and heightened liver TG content (48). Together these studies highlight the role of mitochondrial oxidation in the regulation of liver TG levels.

Fat export or secretion of TGs from the liver is also a key regulatory point for the determination of hepatic lipid accumulation in the presence of a HF diet. TGs are secreted from the liver in the form of very low density lipoproteins (VLDL). VLDL consists of a hydrophobic core containing TGs and cholesterol esters covered by hydrophilic phospholipids and apolipoprotein B (apoB). It is initially assembled in the rough endoplasmic reticulum and is transported into the Golgi before release from the liver through exocytosis. The ability of the liver to export TGs through VLDL is important for reducing hepatic lipid accumulation. Human patients with mutations in apoB that result in dysfunctional VLDL transport have elevated hepatic fat accumulation (49). It is also important to note that in the insulin resistant state, VLDL secretion from the liver is elevated. This results in hypertriglyceridemia in humans but not in mice. However, increased TG secretion is unable to mitigate the upregulation of TG synthesis and this ultimately results in hepatic TG accumulation (50).

A strong correlation exists between HF feeding, increased hepatic TG accumulation and insulin resistance (29,51,52). Rats fed a HF diet for three days developed hepatic insulin resistance in the absence of an observable impairment in peripheral insulin sensitivity (53). A study later conducted by Samuel et al. set forth to use a similar feeding paradigm and reported a similar finding (51). In this study, rats were fed either a chow or HF diet (59% fat) for three days. Three days of HF feeding nearly tripled hepatic TG and fatty acyl-CoA content. The rats fed a HF diet developed hepatic insulin resistance as evidenced by increased hepatic glucose production during an insulin clamp. This finding was associated with diminished insulin-stimulated Akt2 and IRS-1 and IRS-2 associated PI3-kinase activation/activity in the HF-fed rats. Moreover, rodent models designed to modulate fat uptake into the liver also support this correlation (54). The hepatic overexpression of lipoprotein lipase, which causes increased fatty acid uptake into the liver, results in hepatic insulin resistance and liver fat accumulation. The antisense oligonucleotide knockdown of the lipogenic genes ACC1 and ACC2 reduces hepatic lipid accumulation and improves insulin sensitivity. As a consequence, it was proposed in these studies and widely accepted that an increase in hepatic TGs leads to the development of hepatic insulin resistance.

Despite the correlation between hepatic TG accumulation and insulin resistance, a causal relationship has recently become a point of contention in the literature. This is the direct result of several studies that show that insulin resistance can exist in the absence of increased hepatic lipid accumulation (28,55-58). For example, transgenic mice overexpressing DGAT2 in the liver (*Liv-dgat2* mice) exhibit full suppression of endogenous glucose production during an insulin clamp despite significant hepatic steatosis (56). Overexpression of hepatic ChREBP in HF-fed mice display increased hepatic steatosis as well as improved insulin signaling and glucose tolerance

compared to wild-type controls (42). ELOVL6-null mice are protected against hepatic insulin resistance when fed a high fat/high carbohydrate diet despite increased hepatic palmitate concentrations (58). This has led to an alternate hypothesis whereby hepatic TGs actually protect the liver from lipotoxicity by incorporating potentially harmful lipid metabolites or deleterious fatty acids into neutral lipid droplets. Moreover, the results from these studies also suggest that hepatic TG accumulation and hepatic insulin resistance can occur via independent mechanisms and are not necessarily linked by a common mechanism.

Components of the hepatic extracellular matrix are upregulated in the insulin resistant state

The pathology of NAFLD ranges from fatty liver to a more progressive form of the disease called nonalchoholic steatohepatisis (NASH). NASH is characterized by the presence of hepatocellular injury (ballooning, degeneration, Mallory bodies, as well as elevated AST and ALT) and liver fibrosis. The prevalence of NASH is much lower than NAFLD (59). It is estimated that approximately 3% of the general population is affected by NASH. Moreover, while NAFLD is generally asymptomatic, the consequences of NASH are much steeper as it can eventually lead to progressive liver damage with complications of cirrhosis, liver failure, hepatocellular carcinoma and liver-related death.

The liver is a heterogeneous tissue comprised of several different cell types including hepatocytes, endothelial lining cells, Kupffer cells (tissue macrophages), and stellate cells (previously known as Ito cells). Hepatocytes are the most abundant cell type, making up approximately 80% of the cells in the liver (60). Liver cells are organized into microvascular units called sinusoids (Figure 1.3). The sinusoidal endothelium is separated from hepatocytes by

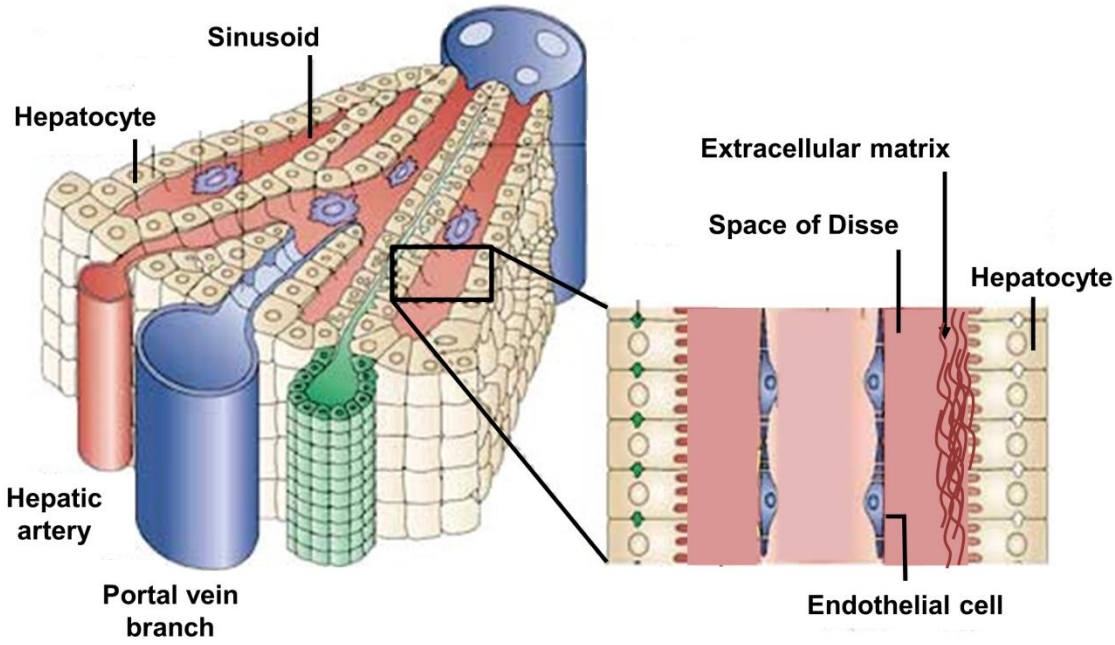

Figure 1.3 – Liver architecture. In the liver, blood from the portal vein and hepatic artery drain into the sinusoids. The sinusoids are lined by endothelial cells. The space between the endothelial cells and the hepatocytes is called the Space of Disse. This portion contains extracellular matrix proteins.

the space of Disse where all metabolites from the bloodstream must pass through to reach the hepatocytes. The surface area of hepatocytes exposed to the space of Disse is greatly enhanced by the presence of microvilli (61). Under normal conditions, the space of Disse is filled with loosely assembled, low density extracellular matrix (ECM) proteins.

The ECM is composed of a diverse array of proteins and proteoglycans including collagens, laminins, fibronectin and hyaluronic acid (62). The ECM is important for the liver as it provides a scaffold for hepatocytes and modulates many biological processes including differentiation, cell migration, repair and development (63,64). Collagens are the most abundant protein in humans and represent approximately 5-10% of the total hepatic protein (63). They consist of three α polypeptide chains folded into a triple helix formation. Moreover, collagen can be divided into subgroups depending on their organization and/or molecular size (63). These are referred to as collagen types. In the normal liver, the space of Disse consists of small bundles of collagen type I and fibers of collagen types III, IV and V. Collagen type I is a fibril forming collagen that serves as a site where other collagen types, glycoproteins and proteoglycans can attach. Collagen type III is similar to collagen type I as it is a member of the fibrillar collagen family and it often colocalizes with collagen type I in the same fibril (65). Collagen type IV is structurally longer than the fibrillary collagens and it surrounds the perisinusoidal surface in the normal liver (66). It has the ability to polymerize into a network on which other ECM components such as laminin and heparan sulfate proteoglycan can bind and assemble (67). Collagen IV is generally associated with basement membranes; however hepatic sinusoids lack a continuous basement membrane. This allows a site of contact between the blood and hepatocytes. Deposits of collagen type IV can be found in the sinusoidal space of the normal liver (63). Additionally, collagen type V is a minor component of the hepatic ECM. It is a fibril-

forming collagen that forms fibrils with collagen type I and is most abundant near the central veins and portal triad (68).

In addition to collagens, glycoproteins are vital elements in the organization of the ECM. There are several different types of glycoproteins which include fibronectin and laminin. Fibronectin is a key component of the hepatic ECM. It consists of two polypeptide chains connected by disulfide bonds. Fibronectin is predominant in the hepatic ECM and is the most abundant ECM component in the space of Disse. In the liver, it has been detected in all extracellular compartments and is a central adhesion site for collagens, fibrin and heparin. Studies show that it is required *in vitro* for the assembly of a collagen matrix (69).

Laminin is the major glycoprotein found in basement membranes. It is a large, noncollagenous heterotrimeric glycoprotein made up of individual α, β and γ subunits (70). Laminin can polymerize with collagen IV to provide a scaffold for adjacent cells. Twelve different heterotrimers of laminin have been identified from various combinations of five α, three β and three γ chains (71). The distribution of different laminin chains depends on the location where they are expressed. In the liver, laminin α1 is present along the sinusoids and space of Disse while laminin α2 is present along the blood vessels.

The ECM is a dynamic structure that is constantly changing and remodeling during times of injury and repair (72). ECM remodeling or fibrosis occurs in the liver in response to chronic liver injury. Chronic hepatocellular injury is a common feature in both NAFLD and NASH. The specific process as to how this occurs is currently undefined. However, one prevailing hypothesis is the "two hit" hypothesis proposed by Day et al (73). The "first hit" is the accumulation of lipid metabolites in hepatocytes. This leads to a series of events including lipotoxicity, oxidative stress, and inflammation that produce a "second hit". The "second hit" promotes tissue injury

and the activation of stellate cells. Under normal conditions, stellate cells are quiescent vitamin A rich cells (74,75). Following liver injury, stellate cells undergo an activation process that transforms them from quiescent cells into proliferative and fibrogenic myofibroblasts. This process is initiated by autocrine and paracrine stimuli including inflammatory cytokines and growth factors such as platelet-derived growth factor (PDGF), endothelin-1, fibroblast growth factors (FGF), insulin-like growth factor (IGF) I, tumor necrosis factor (TNF)-α and transforming growth factor (TGF)-β (74,76,77).

TGF-β has been heavily implicated in stellate cell activation (75). Treatment of cultured stellate cells with TGF-β results in an increase in type I pro-collagen gene expression (78). TGF-β is upregulated in both rodent and human models of hepatic fibrosis (79,80). Gene expression for TGF-β is increased in parallel with collagen type I gene expression in two models of hepatic fibrosis (79). Liver biopsies from human patients with liver disease and increased collagen type I gene expression exhibited a 120% increase in TGF-β gene expression compared to controls (80). Once activated, stellate cells deposit ECM proteins in the space of Disse as part of a wound healing response resulting in subsequent changes in the liver ECM and fibrosis (81).

It has been widely proposed that stellate cells are the main contributor to ECM deposition in the liver (82). This notion was based on *in vitro* studies performed in cell culture (83,84) and it is still unknown whether this occurs *in vivo*. However, several cell types of cells in the liver are capable of ECM synthesis (63). These are hepatocytes, endothelial cells and stellate cells. Hepatocytes are able to synthesize collagen types I, III, and IV, laminin and fibronectin. Endothelial cells are able to synthesize collagen type IV and laminin and stellate cells are able to synthesize collagen types I, III and IV in addition to laminin. Considering that hepatocytes

comprise approximately 80% of the liver, it is feasible that they may also contribute a great amount to the hepatic ECM under pathological conditions.

Fibrosis is characterized by both a quantitative and qualitative change in the composition of the ECM. During this process, there is a several-fold (~3-5) increase in ECM proteins in addition to a shift from low-density ECM proteins to more fibril-forming collagens such as collagen type I. Hepatocytes become encased in type V collagen. Fibronectin accumulation is also markedly increased (66). It has been proposed that fibronectin deposition may actually precede collagen type I deposition and as fibrosis progresses, fibronectin disappears when mature collagen is formed (85). Additionally, ECM proteins accrue in the abluminal space and the sinusoids become enclosed in a sheath of ECM proteins (61). This process is referred to as sinusoidal capillarization. Increased perisinusoidal deposition of laminin allows for the formation of a complete basement membrane and this facilitates the capillarization process (66). Type IV collagen and laminin have also been implicated in this process.

Although NASH is associated with heightened levels of liver damage and fibrosis, it is possible that ECM remodeling in the liver occurs early on as an adaptation to over nutrition. A study by Wada et al. showed that wild-type C57BL/6 mice fed a 60% HF diet with high fructose water for 12 weeks exhibit increased hepatic collagen I α1 gene expression compared to control chow fed mice (86). In addition, wild-type C57BL/6 mice fed a 42% HF diet display increased hepatic immunohistochemical staining for α-smooth muscle actin (SMA) and collagen as well as increased collagen I α1 gene expression compared to controls (87).

Moreover, studies show that ECM remodeling is associated with T2D (88,89). In one study, the histology of liver biopsies was assessed in obese patients with NAFLD with and without T2D using immunohistochemistry. Patients with T2D had increased staining for collagen

IV, α-SMA and a tendency towards an increase in laminin staining. In a separate study, liver biopsies from patients with T2D showed increased perisinusoidal fibrosis characterized by immunostaining for laminin in the sinusoidal spaces as well as collagen IV and αSMA in the space of Disse (89). It is important to note that none of the subjects in these studies had marked liver fibrosis or cirrhosis. Collectively, this suggests that early markers of ECM remodeling occur in patients with T2D prior to more advanced fibrosis and cirrhosis.

It is evident that a diet high in fat is associated with hepatic insulin resistance and ECM remodeling. However, only one study to date has demonstrated a causal link between the two (90). A study from our laboratory showed that depletion of systemic hyaluronan via chronic tail vein injection of a long-acting hyaluronidase reverses HF diet induced muscle and liver insulin resistance (90). It is reasonable to speculate that the cellular and microcirculatory changes (i.e. sinusoidal capillarization) that occur with HF feeding sensitize the liver to further damage and may facilitate maladaptive changes in hepatic insulin action (91). Patients with cirrhosis and chronic hepatitis have been shown to display decreased hepatic insulin extraction compared to normal subjects (24). This decrease in clearance can be attributed to either liver damage or shunting of the portal-systemic circulation (24). A direct end result of decreased insulin extraction is impaired insulin action and ultimately insulin resistance. Another possibility is that hepatic ECM remodeling promotes changes in cell signaling through ECM receptors called integrins.

Integrins are receptors for ECM proteins

Integrins are transmembrane cell surface receptors (92). They facilitate communication between cells and the surrounding ECM. The extracellular domains of integrins constitute the

ligand binding domain while the cytoplasmic domain transduces intracellular signals and interacts with the cytoskeleton (Figure 1.4). Integrins are heterodimers comprised of non-covalently bound α and β subunits (93). In mammals, there are 18α and 8β subunits that can form a total of 24 distinct integrins. Generally, the β subunits are synthesized in excess compared with α subunits, thus heterodimer expression is regulated by the rate limiting synthesis of the α subunit (94). Once synthesized, the two subunits associate intracellularly before they are transported to the cell surface.

The ligand specificity of integrins depends on the combination of α and β subunits (92). Integrins can be divided into subgroups based on the ligands they bind. These subgroups include collagen receptors, laminin receptors, RGD receptors and leukocyte-specific receptors. The primary collagen binding receptors are integrins α1β1, α2β1, α10β1 and α11β1. Integrins α3β1, α6β1, α6β4 and α7β1 are the major laminin binding receptors. The RGD sequence is a major integrin binding sequence found in ligands such as fibronectin. The RGD receptors include integrins α5β1, α8β1, αIIbβ3 and the αvβ integrins. Lastly, the leukocyte-specific receptors consist of the β2 integrins.

The integrin α1 subunit is the largest of the α subunits with a molecular weight around 190-210 kDa (95). Collagen type IV is the preferred ligand of integrin α1β1, however it is able to bind to several other ligands including collagen type I and laminin (96-98). This was demonstrated in a study by Gardner et al. in which embryonic fibroblasts isolated from integrin α1 null mice were plated on either collagen IV, collagen I or laminin (98). The integrin α1 null fibroblasts were unable to spread on collagen IV. In contrast, there was a slight effect on laminin and little to no effect of spreading on collagen I indicating that collagen IV is a preferred ligand. As a result, integrin α1β1 is important for survival on collagen substrates (99). Other integrin α1

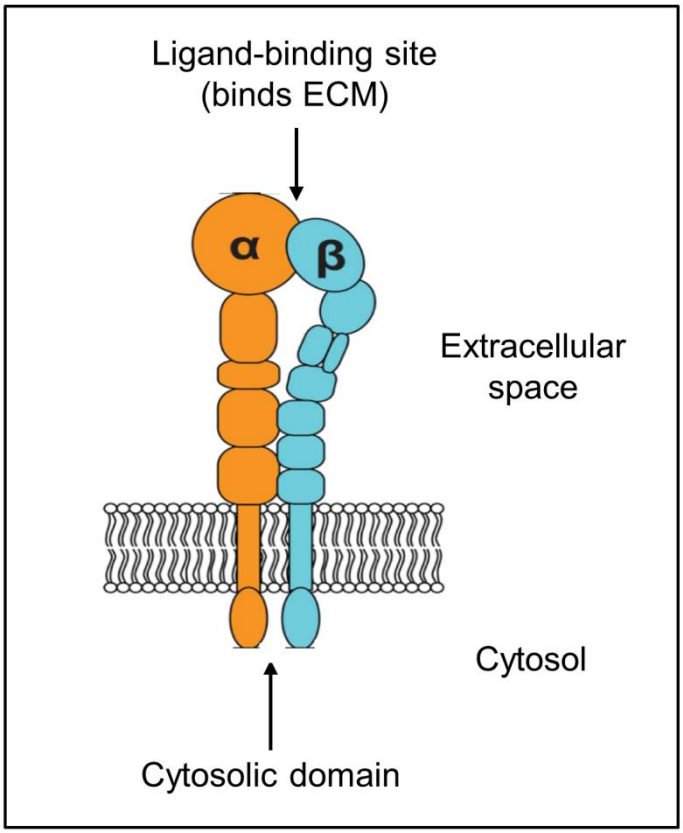

Modified from: http://www.ks.uiuc.edu/Research/dbps/

Figure 1.4 – Integrin structure. Integrins are receptors for extracellular matrix proteins. They are heterodimeric transmembrane proteins that consist of an alpha and beta subunit. The extracellular portion contains the ligand-binding site that binds the ECM and the cytosolic portion modulates cell signaling.

ligands include the cartilage protein matrilin-1, TCPTP, galectins 1, 3, and 8 as well as semaphorin 7A expressed on macrophages (100,101).

The integrin α1 subunit is expressed in several different tissue types including vascular smooth muscle, kidney, brain, skin and liver (98). In the liver, it is expressed in several different cell types including hepatocytes, stellate cells, vascular endothelium, connective tissue stroma and sinusoidal lining cells (102,103). Notably, it is the only collagen binding integrin expressed on the hepatocyte. There are six α subunits (α1, α2, α3, α4, α5 and α6) expressed in the liver and they are all associated with the β1 integrin (102). Only two integrin heterodimers have been shown to be expressed on the hepatocyte: integrin α1β1 and α5β1. Integrin α5β1 is a fibronectin receptor, thus integrin α1β1 is the sole collagen binding integrin on the hepatocyte.

The genetic whole body deletion of integrin α1 in mice exists and is viable (98). These mice develop normally and are visibly indistinguishable from wild-type mice. Early studies in the integrin α1 null mouse demonstrated that integrin α1 null mice synthesize excess dermal collagen *in vivo* (99) as a result of increased steady state levels of collagen synthesis (104). The apparent increase in collagen synthesis in integrin α1 null mice is attributed to decreased MAPK signaling (99). The activation of integrin α1β1 signaling via ligand binding activates the MAP kinases Erk1 and 2 through Shc. Erk1/2 activation then reduces collagen synthesis. Collectively, this demonstrates that integrin α1β1 is a negative regulator of collagen synthesis via its ability to activate the MAPK pathway.

Various stimuli and growth factors regulate integrin α1β1 expression (98,106-108). These include retinoic acid (106), cytokines (107,108), and the growth factors NGF, TGF-β, PDGF and TNF (98). TGF-β is a particularly potent stimulus of integrin α1 expression (109). Incubation of mesangial cells with TGF-β for 48 hours increases mRNA and protein synthesis of the integrin

α1 subunit in a dose-dependent manner (109). Moreover, integrin α1β1 expression is altered under conditions of liver injury as well as in disease states associated with fibrosis (102,103,110,111). Patients with chronic hepatitis C display increased integrin α1 expression (110). Male Wistar rats with diet-induced liver cirrhosis exhibit increased integrin α1 expression on hepatocytes and sinusoidal lining cells (112). Human liver biopsy specimens from patients with either inflammatory or cholestatic liver disease show increased integrin α1 expression in hepatocytes and connective tissue stroma (102). Additionally, two weeks of ethanol feeding in rats leads to increased hepatocellular expression of integrin α1 (111). Collectively, these studies suggest that integrin α1 is upregulated during times of ECM remodeling.

Integrins transduce signals from the ECM to the intracellular space

Integrins are capable of bidirectional signaling. Integrin activation is regulated from the cytosol through 'inside-out' signaling. Additionally, integrin binding to the ECM transduces signals to the cytosol through 'outside-in' signaling. Inside-out signaling is important for integrin activation (i.e. the transition from a low to high affinity state) (113). This process is primarily mediated by two protein families, the talins and the kindlins. During inside-out signaling, talins or kindlins bind to the β-integrin cytoplasmic tail. This leads to conformational changes that result in integrin activation (114). Talins are large (~270 kDa) cytoplasmic proteins (115). Several factors have been described to modulate talin binding to integrins. These include the lipid second messenger PIP2 and tyrosine phosphorylation by members of the Src family of kinases. The kindlin family of proteins consists of three members: kindlin-1, kindlin-2 and kindlin-3. Kindlin-1 is found primarily in epithelial cells. Kindlin-2 is ubiquitously expressed. While kindlin-3 is widely expressed in several different tissue types including the spleen, thymus

and lymph nodes, but not in the heart, brain, liver or skeletal muscle (116). Both talins and kindlins are able to bind to distinct regions of integrins and modulate integrin affinity and activation through their cooperative ability to separate integrin cytoplasmic tails.

Integrin ligand binding facilitates the transduction of signals from the ECM to the inside of the cell (i.e. outside-in cell signaling) (Figure 1.5). The cytoplasmic domains of integrins are critical for their ability to modulate intracellular signaling. The signals generated by integrins regulate a variety of cellular processes including, but not limited to, motility, proliferation, differentiation and gene expression. Upon ligand binding, integrins cluster in the plane of the plasma membrane and this triggers the generation of focal adhesion complexes. Focal adhesions are signaling centers composed of over 150 proteins and they provide links from the ECM to the cytoskeleton (117). This initiates the assembly of the cytoskeleton, namely actin, and the activation of several diverse downstream signaling pathways.

Integrins themselves lack kinase activity. Thus they are reliant on downstream kinases and scaffolding proteins for signal transduction. Integrins signal through various proteins including Src-family kinases, Abl, focal adhesion kinase (FAK) and integrin-linked kinase (ILK). FAK is a cytoplasmic tyrosine kinase found in focal adhesions. It is targeted to focal adhesions through a region in its C-terminal domain called the FAT region (118). FAK localizes with integrin receptors at sites where cells attach to the ECM (119) and is activated by antibody crosslinking of β1 integrins (120). It has at least five tyrosine phosphorylation sites (Tyr397, 407, 576, 577 and 925) (121). Moreover, FAK has also been shown to bind the integrin α1 cytoplasmic tail (122).

FAK undergoes rapid autophosphorylation at Tyr397 upon integrin-mediated cell adhesion (123) and this is associated with increased catalytic activity. Tyr397 phosphorylation

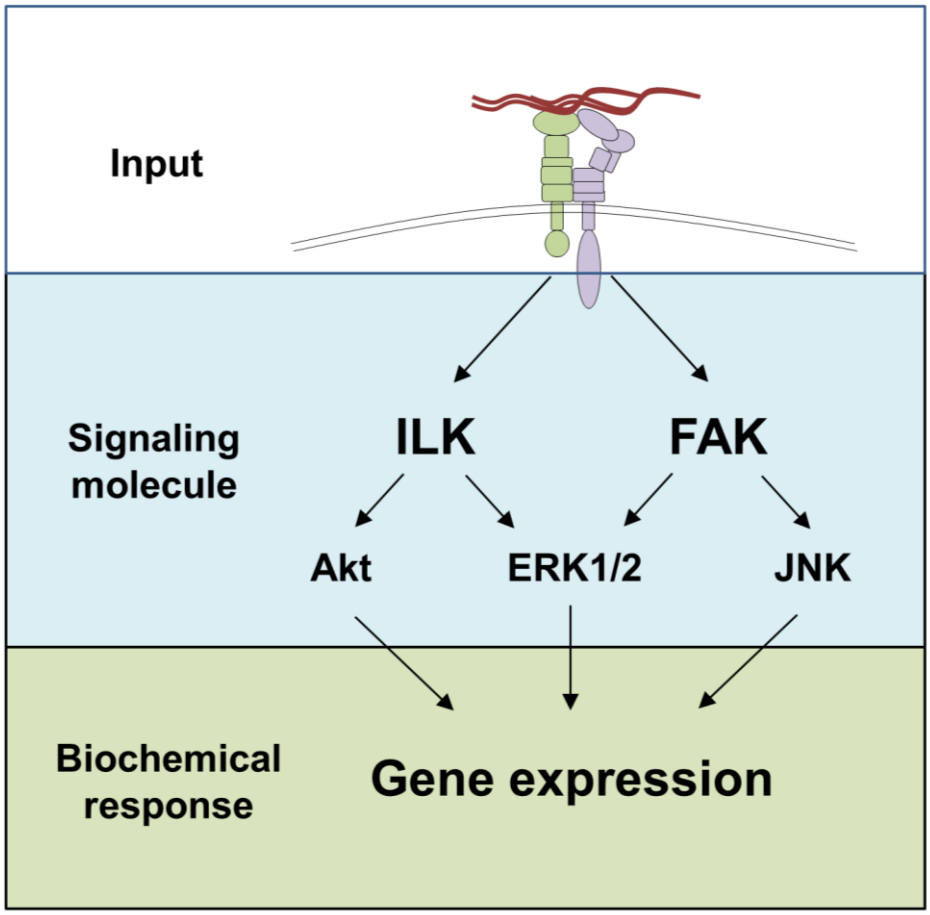

Modified from: Legate et al., *Genes and Dev.* 2009

Figure 1.5 – Integrin signaling. Upon ligand binding, integrins transduce signals across the plasma membrane to facilitate cell signaling. Integrin signaling can be divided into 3 portions: the input, signaling molecule and biochemical response. The input is the extracellular ligand it binds. The signaling molecule can be very diverse and integrins can signal to many different molecules including ILK and FAK. These can then signal to some well-known insulin signaling molecules including Akt, ERK and JNK. Finally, one example of the biochemical response is gene expression.

promotes the recruitment of Src-family tyrosine kinases to focal adhesions. In turn, Src further promotes FAK phosphorylation at Tyr407, 576 and 577 and this leads to the recruitment of Src and phosphatidyl inositol 3-kinase (PI3K) as well as other proteins. Additionally, FAK has been shown to be regulated by the growth factor receptors EGFR, FGFR and the insulin receptor (124,125). This results in the activation of several downstream signaling cascades including the MAPK and PI3K signaling pathways (124,125). In addition to its signaling properties, FAK is important for cytoskeletal stabilization and focal adhesion turnover (126).

ILK is a highly conserved intracellular scaffolding protein. It interacts with the β1, β2 and β3-integrin cytoplasmic domains and numerous cytoskeleton-associated proteins. It is composed of three distinct domains: an N-terminus that contains five ankyrin repeats, a pleckstrin homology-like domain and a pseudokinase domain at the C-terminus. ILK is a component of the ILK-pinch-parvin (IPP) protein complex located at focal adhesions (127,128). The ankyrin repeats facilitate the interaction with pinch and the C-terminal domain binds the adaptor protein, parvin. It is expressed in most mammalian cell types and tissues with the greatest expression in cardiac and skeletal muscle (129).

ILK was originally identified as a kinase due to the significant sequence homology of the C-terminus to other Ser/Thr protein kinases (129). Since then, several lines of evidence have confirmed that ILK does not possess an active kinase domain and it has since been classified as a *bona fide* pseudokinase (130,131). The identification as a pseudokinase arose as the result of genetic studies in *C. elegans* and *D. melanogaster* in which kinase dead mutants were capable of rescuing the phenotypes caused by ILK deletion (132,133). The pseudokinase domain of ILK is an essential domain for the recruitment of several adaptor proteins and signaling molecules including several proteins involved in insulin action such as PKB/Akt, PDK1 and GSK-3β.

Moreover, ILK is connected to growth factor receptors through the adaptor protein Nck2 (134). Therefore although ILK lacks intrinsic kinase activity, it has been shown to regulate the activation of numerous intracellular growth factor signaling cascades (135-137).

Integrins regulate insulin signaling and insulin action in several metabolic tissues

Integrins can work with growth factors to promote phosphorylation or activation of receptor tyrosine kinases (138). Engagement of the αvβ3 integrin results in an increase in insulin-stimulated DNA synthesis (139-141). Insulin receptors rapidly associate with integrins at focal adhesions upon tyrosine phosphorylation (141). Additionally, integrin engagement is thought to play a stimulatory role in insulin signaling (142). Integrin engagement promotes the activation of both insulin receptor substrate (IRS)-1-associated phosphatidylinositol-3 (PI3)-kinase activity and Akt activity (142).

Several studies have established a role for FAK in the regulation of insulin signaling (125,143-145). A mammalian two-hybrid system showed that FAK binds to IRS-1 and FAK co-immunoprecipitates with IRS-1 in 293 cells suggesting this interaction may occur *in vivo* (146). FAK has also been shown to phosphorylate IRS-1 in both a Src-dependent and Src-independent manner. FAK interacts with Src in CHO cells and this facilitates IRS-1 phosphorylation (146). Moreover, FAK has also been shown to phosphorylate IRS-1 in the absence of Src in human embryo kidney cells (146).

FAK has been implicated in the regulation of glucose homeostasis and insulin action in both muscle and liver (144,147-149). FAK tyrosine phosphorylation is decreased in muscle from HF-fed Sprague-Dawley rats (147). The *in vivo* siRNA-mediated knockdown of FAK results in hyperglycemia, hyperinsulinemia, and impaired glucose tolerance in mice fed a chow diet (144).

The metabolic impairments in these mice were associated with decreased IRS-1 tyrosine and Akt Ser473 phosphorylation in both the muscle and liver. The overexpression of FAK in C2C12 cells increases insulin-stimulated glucose uptake (150). Conversely, C2C12 skeletal muscle cells transfected with siRNA against FAK exhibit decreased insulin-stimulated glucose uptake (147). L6 myocytes transfected with antisense FAK display decreased insulin-stimulated IRS-1, IRS-2, Akt and GSK-3 phosphorylation associated with decreased insulin-stimulated glucose uptake, decreased glycogen synthesis and impaired Glut4 translocation (148). Moreover, FAK undergoes rapid tyrosine phosphorylation in livers from healthy rats upon insulin stimulation under euglycemic conditions *in vivo* (149). This is consistent with another study showing that HepG2 cells transfected with mutant FAK constructs display decreased Akt Ser473 and GSK-3 Ser9 phosphorylation (125). The observed decrease in GSK-3 phosphorylation was associated with decreased insulin-stimulated glycogen synthase activity. There was no difference in the phosphorylation of insulin receptor β or PI3K activity upon insulin stimulation. This suggests that the effect of FAK on insulin-stimulated glycogen synthesis is downstream of the insulin receptor and PI3K. The absence of FAK affecting insulin receptor phosphorylation is consistent with other studies indicating that FAK exterts its actions on insulin signaling downstream of the insulin receptor (151). Finally, *fa/fa* rats treated with a TNF-α neutralizing agent exhibited increased hepatic FAK phosphorylation associated with decreased hepatic glucose output during an insulin clamp (149,152).

Little is known about the role of ILK in the regulation of insulin action. Considering that it is a scaffolding protein, it has been proposed that ILK modulates intracellular signaling through its ability to recruit a kinase or multiple kinases into a multiprotein complex. This complex then facilitates the activation of downstream signaling molecules upon insulin

stimulation. Nonetheless, the presence of ILK has been shown to modulate the activation of key insulin signaling molecules such as Akt and GSK-3β. Overexpression of ILK or insulin treatment results in increased GSK-3 and Akt phosphorylation (153). Cotransfection of Akt with wild-type ILK in 293 cells resulted in an enhancement of phosphorylation of Akt Ser473 (153). Several studies have shown that the ablation of ILK results in decreased Akt Ser473 phosphorylation (154-156). For example, knockdown of ILK expression in HEK-293 and PC3 cells or the genetic deletion of ILK using Cre recombinase in macrophages resulted in decreased Akt Ser473 phosphorylation (154,157). The activation of hepatic stellate cells in rats using CCl4 resulted in increased ILK protein expression associated with enhanced phosphorylation of Akt, p38, and ERK1/2 while the inhibition of ILK by siRNA prevented these signaling changes (158). In contrast, the phosphorylation of Akt Ser473 is not affected in mice with a hepatocyte-specific deletion of ILK (159) and ILK-deficient cells are capable of phosphorylating Akt at both Thr308 and Ser473 upon insulin stimulation in a robust manner similar to control cells (160). Thus the role of ILK in the regulation of Akt and GSK-3 phosphorylation is debatable and more studies need to be performed to address whether ILK mediates phosphorylation of Akt and GSK-3 upon insulin stimulation *in vivo*.

Hypotheses

The liver extracellular matrix (ECM) expands with high fat (HF) feeding as evidenced by increased collagen gene expression and protein expression. Integrins transduce signals from the ECM to the cytosol. I hypothesize that the ECM contributes to the pathogenesis of hepatic insulin resistance through integrin signaling. As a corollary, I hypothesize that integrin signaling regulates hepatic insulin action and lipid metabolism in the context of HF feeding. Integrin α1β1

is the only known collagen binding integrin expressed on the hepatocyte. The results of the dissertation show that integrin α1 protein expression is upregulated with HF feeding in hepatocytes. Thus I hypothesize that integrin α1 is upregulated in hepatocytes as an important adaptive response to over nutrition and this protects the liver against metabolic impairments in HF-fed C57BL/6J mice. To address this, mice with a deletion of the integrin α1 subunit were utilized to determine the role of integrin α1β1 in hepatic glucose and lipid metabolism *in vivo*. Integrins signal through two main proteins: FAK and ILK. The results in Chapter III show that there is no difference in FAK activation between HF-fed integrin α1-null mice and wild-type littermates. Thus, I hypothesize in Chapter IV that integrin α1β1 signals through ILK to protect against hepatic insulin resistance in HF fed mice. To test this hypothesis, mice with a hepatocyte-specific deletion of ILK were generated and hepatic insulin action and lipid metabolism were assessed *in vivo*. This study was significant as it showed that integrin α1β1 does not signal through ILK to protect against hepatic insulin resistance and ILK is in fact a major contributor to diet-induced hepatic insulin resistance and lipid accumulation in high fat fed mice.

Chapter II

RESEARCH MATERIALS AND METHODS

Mouse Models

All animal protocols were approved by the Vanderbilt University Institutional Animal Care and Use Committee and conducted in Association for Assessment and Accreditation of Laboratory Animal Care-accredited facilities. Mice were housed in a temperature and humidity controlled environment with a 12:12-h light-dark cycle. Mice with a global deletion of integrin α1 were studied in Chapter III. Littermate wild-type (*itgα1*$^{+/+}$) and integrin α1-null (*itgα1*$^{-/-}$) male mice were kindly provided by Dr. Ambra Pozzi (98). Mice were backcrossed on to a C57BL/6J background for at least 10 generations. Mice with a hepatocyte-specific deletion of integrin-linked kinase (ILK) were studied in Chapter IV. Mice carrying an ILK allele flanked by loxP sites (ILK$^{lox/lox}$, kindly provided by Dr. Roy Zent) (161) were crossed to transgenic mice expressing Cre recombinase under the control of the albumin (Alb) promoter (purchased from Jackson Laboratory) to generate ILK$^{lox/lox}$Alb*cre* mice and wild-type littermates, ILK$^{lox/lox}$ mice. The efficiency of recombination of the Alb promoter increases progressively with age (60). The efficiency at birth is approximately 40%. It increases to 75% at weaning (3 weeks of age) and completes by 6 weeks of age. For all studies, mice were weaned at 3 weeks of age and separated by gender. Mice were fed a standard chow diet (5.5% fat by weight; 5001 Purina Laboratory Rodent Diet) or high fat diet (60% kcal from fat; F3282 BioServ) for 16 weeks. All studies were performed between 19-24 weeks of age. Mice were weighed and handled weekly to monitor body weight and minimize stress due to handling during studies.

Surgical Procedures and Body Composition

A detailed protocol of the surgical procedure is available online through the Vanderbilt Mouse Metabolic Phenotyping Center website for their annual course titled: Glucose Clamping the Conscious Mouse (www.mc.vanderbilt.edu/mmpc)(162). Briefly, mice were anesthetized using isofluorane. The surgical site was prepared by removing hair and washing the skin with betadine followed by alcohol. Ketoprofen (5-10 mg/kg) was administered subcutaneously. A small midline incision was made 5 mm to the xiphoid process. The left carotid artery was exposed, isolated and the cephalic end was ligated with silk suture. Another piece of suture was loosely knotted on the caudal end of the exposed artery. The vessel was clamped with micro-serrefine and cut below the ligated end with spring scissors. The catheter was inserted as far as possible prior to the release of the clamp. The catheter was then inserted into the tip of the aortic arch. Both ligatures were securely tied and catheter sampling was confirmed. A separate incision was made 5 mm to the right of the midline and about 2 mm caudal to the first incision. The right jugular vein was exposed and the cephalic end was ligated with silk suture. Another piece of suture was loosely tied at the caudal end of the exposed vein and a cut was made below the cephalic ligature with spring scissors. The catheter was inserted into the bead and sampling was confirmed. The mouse was turned over onto its stomach and a small incision was made between the shoulder blades. A 14-gauge needle was tunneled under the skin and through the incision on the back. Catheters were threaded through the needle to exteriorize them to the back of the mouse. The ventral incisions were closed with nylon suture. The venous catheter was clamped with micro-serrefine at the incision site between the shoulder blades. The catheter was cut 1 cm above the clamp and connected to a MASA^{TM}. The venous catheter and arterial catheters were secured to the MASA^{TM} with silk suture. The dorsal incision was closed with nylon and the

patency of both catheters was confirmed. The mouse was placed in a warmed, clean cage and allowed to recover for 5-6 days prior to study. Body composition was assessed using a mq10 nuclear magnetic resonance analyzer (Bruker Optics) in 5-h fasted mice.

In Vivo Experiments

Hepatocyte Isolation

Mice were anesthetized and their livers were perfused via the portal vein with pre-warmed (30°C) Liver Perfusion Medium (Gibco) for 10-15 min at a rate of 4-5 mL/min. The livers were then perfused with Liver Digest Medium containing collagenase (Gibco) for 15-20 min at a rate of 4-5 mL/min. After digestion, the livers were removed from the mice, placed in a dish containing Liver Digest Media and the hepatic capsule was torn and shaken to free the dissociated cells. The cell suspension was filtered through a sterile 150-mesh nylon screen into a 50 mL sterile Falcon tube and centrifuged at 50g for 2 min at 4°C to collect the cells. The cell pellet was resuspended and washed 3 times in HBSS prior to a final resuspension in lysis buffer. The supernatant from each centrifugation was collected and combined into a single tube. The tube containing the supernatant was centrifuged at 650g for 7 min at 4°C. This pellet consists of the non-parenchymal cells including Kupffer cells, stellate cells, erythrocytes and cell debris. Proteins were extracted and the cellular protein content was measured using the Bradford Protein Assay (Bio-Rad).

Glucose Tolerance Tests (GTTs)

Indwelling carotid artery and gastric catheters were surgically implanted for sampling and glucose administration, respectively. The gastric catheter allows mice to absorb glucose via physiological mechanisms and avoids a stress response from intraperitoneal injection or gavage. Mice were fasted for 5-hs and baseline arterial glucose and insulin measurements were obtained through the arterial catheter to prevent handling the mice. Glucose was administered through the gastric catheter at a dose of 2g/kg body weight. Arterial glucose was measured at 5, 10, 15, 20, 30, 45, 60, 90 and 120 min after glucose administration. Arterial insulin levels were assessed during the GTT at 10, 30, 60 and 120 min. Plasma insulin was determined by radioimmunoassay with assistance from the Vanderbilt Hormone Assay Core.

Hyperinsulinemic-euglycemic clamp (Insulin Clamp)

Indwelling carotid artery and jugular vein catheters were surgically implanted for sampling and infusion 5-6 days before the insulin clamp. Mice were fasted for 5 hours before the start of the study. [3-^{3}H]glucose was primed (2.4 μCi) and continuously infused for a 90-min equilibration period (0.04 μCi/min). Baseline measurements were determined in arterial blood samples collected at -15 and -5 min for analysis of glucose, [3-^{3}H]glucose, free fatty acids (FFAs) and insulin. A schematic of the insulin clamp is depicted in Figure 2.1. At t = 0, insulin ($4mU \bullet kg^{-1} \bullet min^{-1}$) was infused at a fixed rate and glucose (D50 mixed with [3-^{3}H]glucose) was infused at a variable rate to maintain euglycemia. The mixing of D50 with [3-^{3}H]glucose prevents deviations in specific activity during the insulin clamp (163). Blood glucose was clamped at 150-160 mg/dL in the integrin α1β1 studies (Chapter III) and at 130-140 mg/dL in the ILK studies (Chapter IV). Heparinized saline-washed erythrocytes were infused to prevent a

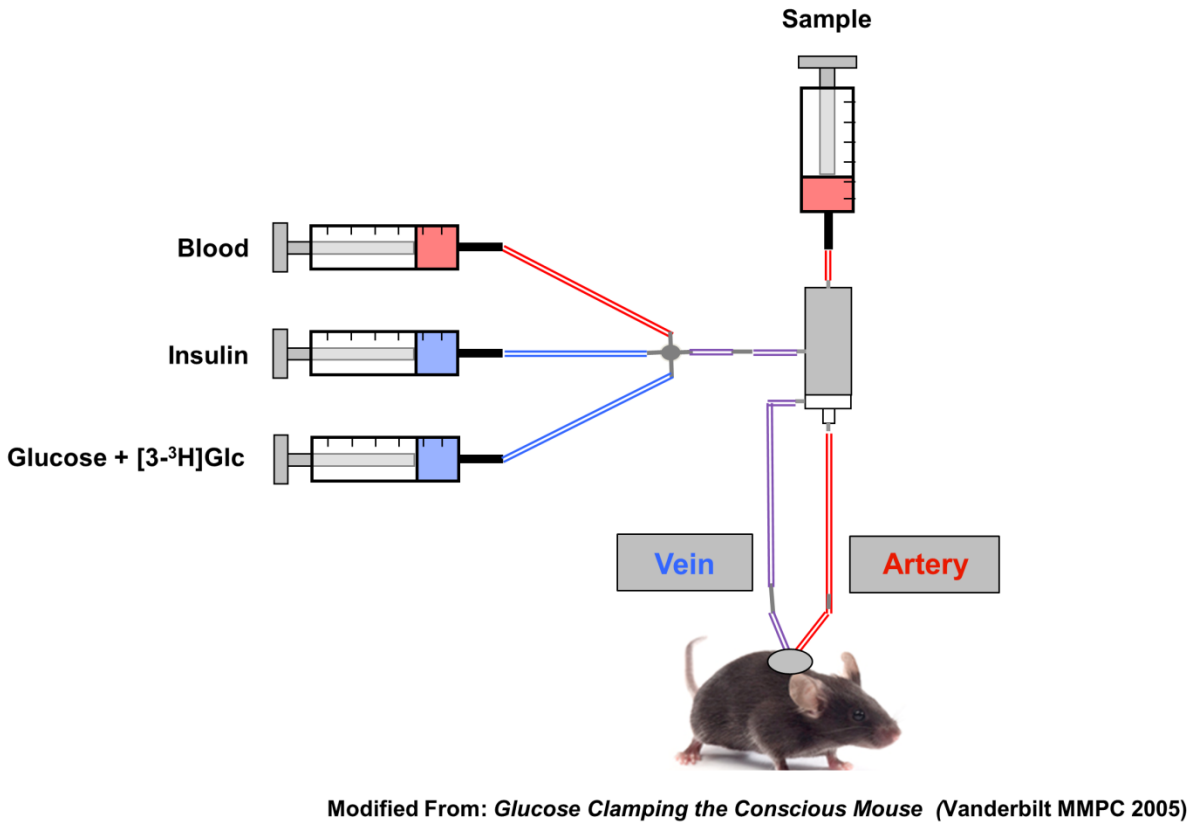

Figure 2.1 – Experimental setup for the hyperinsulinemic-euglycemic (insulin clamp).

fall in hematocrit. Blood was taken at 80-120 min for the determination of [3-^{3}H]glucose. Samples for the measurement of arterial insulin and FFAs during the insulin clamp were taken at 80 and 120 min.

Hepatic Triglyceride Secretion

Mice with indwelling carotid artery and jugular vein catheters were fasted for 8-hours. Baseline arterial plasma triglycerides were determined in samples collected at -30 and 0 min. After the 0 min sample, VLDL-TG clearance was blocked by an intravenous injection of tyloxapol (500 mg/kg, Sigma). Blood samples were collected at 45 min intervals (0, 45, 90, 135, and 180 min post-injection). Plasma triglycerides were assessed using Triglycerides-GPO Reagent (Raichem) as described below in the section titled *Ex Vivo* Experiments.

Ex Vivo Experiments

Processing of Insulin Clamp Plasma Samples

Plasma Radioactivity

Plasma samples from the insulin clamp studies were deproteinized using equal volumes of 0.3N barium hydroxide and 0.3N zinc sulfate. The $^{3}H_2O$ that resulted from glycolysis of the radioactive glucose tracer was removed from the plasma through drying under vacuum. Radioactivity of [3-^{3}H]glucose was determined by liquid (Ultima Gold; Packard) scintillation counting (Packard TRI-CARB 2900TR) (164). R_a and R_d were calculated using non-steady-state equations (165). Endogenous (endo) R_a was determined by subtracting the glucose infusion rate

(GIR) during the insulin clamp from the total R_a. Assuming steady state conditions, the equation for total R_a can be simplified as:

$R_a = I/SA$

where I is the tracer infusion rate and SA is the specific activity of the tracee (dpm/mg).

Plasma Insulin

Arterial insulin was determined by sandwich ELISA (ALPCO) per manufacturer's instructions. Ten µl of plasma, standard or control was added to the appropriate well into a 96-well plate supplied by the manufacturer. The wells of the plate were coated with mouse monoclonal antibodies specific for insulin. After addition of the samples, an anti-insulin monoclonal antibody conjugated horseradish peroxidase enzyme was added to each well. Unbound conjugate was washed from the plate and the wells were incubated with TMB substrate. A stop solution was added and the optical density was determined at 450 nm and 590 nm. The intensity of the optical density read at 450 nm was proportional to the amount of insulin in the plasma sample. Basal 5-h fasted insulin levels were calculated as an average of samples taken at t = -15 and -5 min. The levels during the insulin clamp were calculated as an average between the samples taken at t = 80 and 120 min

Plasma Non-Esterified Free Fatty Acids

Free fatty acids (FFAs) were assessed using an enzymatic assay (NEFA C Kit; Wako Chemicals). Arterial blood samples were collected in EDTA tubes. The tubes were centrifuged at 13,000 rpm for 1 min and 5 µl of the plasma was pipetted into a tube containing dried down THL solution. The NEFA assay is based on the following chemical reactions:

$$\text{NEFA} + \text{ATP} + \text{CoA-SH} \xrightarrow{\text{ACS}} \text{Acyl-CoA} + \text{AMP} + \text{P}$$

$$\text{Acyl-CoA} + \text{O}_2 \xrightarrow{\text{ACOD}} \text{2,3-trans-Enoyl-CoA} + \text{H}_2\text{O}_2$$

$$2\ \text{H}_2\text{O}_2 + \text{4-Aminophenazone} + \text{MEHA} \xrightarrow{\text{POD}} \text{Quinoneimine-color} + 4\ \text{H}_2\text{O}$$

The plate was incubated for 10 min at 37°C and the optical density was determined at 550 nm. The intensity of the red coloration was proportional to the NEFA concentration in the plasma sample. Basal FFA levels were calculated as an average of samples taken at t = -15 and -5 min. The levels during the insulin clamp were calculated as an average between the samples taken at t = 80 and 120 min.

Plasma Triglycerides

Plasma triglycerides were assessed using Triglycerides-GPO Reagent (Raichem) per the manufacturer's protocol. Plasma samples were diluted in water as follows:

Baseline (-30 and 0 min): 1:40

45 and 90 min: 1:100

135 and 180 min: 1:200

The triglyceride standards were prepared and 50 µl of either diluted sample or standard were added to the appropriate well of a 96-well plate. Seventy five µl of triglyceride reagent was added to the plate. The plate was incubated for 10 min at 37°C.

$$\text{Triglycerides} \xrightarrow{\text{Lipase}} \text{Glycerol} + \text{Fatty Acids}$$

$$\text{Glycerol} + \text{ATP} \xrightarrow{\text{Glycerol kinase}} \text{Glycerol-3-Phosphate} + \text{ADP}$$

Glycerol-3-Phosphate + O_2 $\xrightarrow{GPO}$ Dihydroxyacetone phosphate + H_2O_2

H_2O_2 + 3-hydroxy-2,4,6-tribomobenzoic acid $\xrightarrow{Peroxidase}$ Quinoneimine dye + $2H_2O$

The absorbance of the quinoneimine dye was determined at 540 nm. The intensity of the color produced is directly proportional to the concentration of triglycerides in the sample. The triglyceride levels were calculated according to their respective dilutions. For the tyloxapol studies, the triglyceride production rate was determined according to the following formula:

TG flux = slope * 0.475 μmol/kg*hour

where slope (mg/dL/hour) [y-axis is the concentration of triglyceride (mg/dL) and x-axis is time (hours)]

Hepatic Triglyceride Content

Liver triglycerides were quantified using the Triglycerides-Glycerophosphate oxidase (GPO) Reagent Set according to the manufacturer's protocol (Pointe Scientific, Inc.). Seventy to ninety mg of frozen liver tissue was digested for 1 hour at 70°C in an equal volume of a 3M KOH/Ethanol solution. The tubes were incubated at room temperature overnight at 1g. The next day, the total volume of the solution was brought up to a total volume of 500 μl with 2M Tris-HCl (pH 7.5). In a new set of tubes, each sample was diluted 1:5 with 2M Tris-HCl (pH 7.5). In a third set of tubes, 1 mL of GPO reagent was prewarmed at 37°C for 5 min. Ten μl of the diluted sample was added to each tube and the reaction was incubated for another 5 min at 37°C. A standard curve was prepared in a separate set of tubes with prewarmed GPO reagent. Two hundred μl of the reagent mixture was added to a 96-well plate. The GPO assay is based on the

chemical reactions as described above under the section titled Plasma Triglycerides. The absorbance of the quinoneimine dye was determined at 540 nm. The intensity of the color produced is directly proportional to the concentration of triglycerides in the sample.

Hepatic Diglyceride Content

Liver diglycerides were extracted with the assistance from the Vanderbilt Lipid Core using the method of Folch-Lees (166). Phospholipids, diglycerides, triglycerides and cholesteryl esters were scraped from the plates and methylated using BF3 /methanol as described by Morrison and Smith (167). The methylated fatty acids were extracted and analyzed by gas chromatography. Gas chromatographic analyses were carried out on an Agilent 7890A gas chromatograph equipped with flame ionization detectors, a capillary column (SP2380, 0.25 mm x 30 m, 0.25 µm film, Supelco, Bellefonte, PA). Helium was used as a carrier gas. The oven temperature was programmed from 160°C to 230°C at 4°C/min. Inclusion of lipid standards with odd chain fatty acids permitted quantitation of the amount of lipid in the sample. Dipentadecanoyl phosphatidylcholine (C15:0), diheptadecanoin (C17:0), trieicosenoin (C20:1), and cholesteryl eicosenoate (C20:1) were used as standards.

Plasma β-hydroxybutyrate

Plasma β-hydroxybutyrate (β-OH) levels were determined in samples from 5-h fasted mice using the β-OH (Ketone Body) Colormetric Assay Kit (Cayman Chemical Company) per the manufacturer's protocol. Plasma was diluted 1:5 in assay buffer. Fifty µl of the plasma mixture or standard was added to the appropriate well of a 96-well plate. The β-OH assay is based on the following chemical reactions:

$$\beta\text{-OH} + NAD^{+} \xrightarrow{\beta\text{-OH dehydrogenase}} \text{Acetoacetate} + NADH + H^{+}$$

$$\text{WST-1} + NADH \xrightarrow{\text{Diaphorase}} \text{WST-1 Formazan} + NAD^{+}$$

The absorbance of the formazan dye was determined spectrophotometrically at 445 nm. The absorbance of the dye was directly proportional to the β-OH concentration in the plasma.

Oil Red O Staining

Neutral lipids were stained with oil red O with assistance from the Vanderbilt Translational Pathology Shared Resource Core. Fresh liver pieces were embedded in OCT, flash frozen on dry ice and stored at -80°C until processing. Liver sections were cut and mounted to slides. Slides with liver samples were incubated in 100% propylene glycol prior to a 4 hour incubation in a filtered oil red o solution. The samples were washed in 85% propylene glycol, counterstained in hematoxylin and mounted. Images were obtained using an Olympus upright microscope.

Hepatic Glycerol-3-Phosphate

Glycerol-3-Phosphate (G3P) was determined in frozen liver tissue from 5-h fasted mice using the Glycerol-3-Phosphate Colormetric Assay Kit (BioVision) per the manufacturer's protocol. Approximately 30 mg of frozen liver tissue from 5-h fasted mice was homogenized in 200 µl G3P assay buffer on ice. The lysate was centrifuged at 12000 rpm at 4°C. Five µl of the supernatant was added to the appropriate well of a 96-well plate and the volume was brought up to 50 µl with G3P assay buffer. Fifty µl of the G3P reaction mix was added to each well containing the standard and sample wells. The plate was incubated at 37°C for 40 min and the

absorbance was determined at 450 nm. The G3P assay is based on the following chemical reactions:

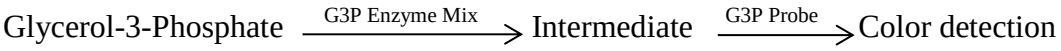

Mitochondrial Oxygen Consumption and Enzymatic Activity

Mice were fasted for 5-h prior to cervical dislocation. For the integrin α1 studies (Chapter III), fresh liver samples were mechanically permeabilized (168). Mechanically permeabilized liver pieces were used in lieu of isolated mitochondria to ensure the cytoskeletal attachments are conserved and the mitochondria are not stressed during the functional measurements. For the ILK studies (Chapter IV), mitochondria were isolated from fresh liver tissue using standard homogenization and differential centrifugation methods as previously described (169). Briefly, liver tissue was minced in 5 mL ice-cold mitochondrial isolation buffer containing 250 mM sucrose, 2 mM KH_2PO_4, 1 mM EGTA and 20 mM Tris-HCL (pH 7.2). The minced liver tissue was rinsed twice and resuspended in 4.5 mL ice-cold mitochondrial isolation buffer. The tissue was homogenized at 150 rpm in a pre-chilled Teflon Potter-Elvehjem pestle for 2 up and down passes. The homogenate was centrifuged for 10 min at 2200 rpm at 4°C. The mitochondria-enriched supernatant was centrifuged for 10 min at 9400 rpm at 4°C. The mitochondrial pellet was resuspended in 1 mL mitochondrial isolation buffer and centrifuged for a second time for 10 min at 9400 rpm at 4°C. The final pellet was resuspended in 200 µl mitochondrial isolation buffer. Mitochondrial protein concentration was determined using the BCA protein assay. In all studies, oxygen consumption was measured in air-saturated MiR05 (pH 7.4, 30°C) with a Clark-type oxygen electrode (Oroboros Instruments Corp., Innsbruck, Austria). State 2 respiration was

measured in the presence of either 10 mM glutamate and 2 mM malate or 2 mM malate and 50 μM palmitoyl carnitine prior to the addition of ADP. State 3 respiration was measured upon the addition of 0.5 mM ADP. Cytochrome c (10 μM) was added at the end of each measurement to ensure the outer mitochondrial membrane was intact. The following criteria were applied for the inclusion of each respiration measurement: a respiratory control ratio (RCR) at or above 4 and less than 10% response to cytochrome c addition. The RCR was calculated as state 3/state 2. Citrate synthase activity (CSA) was measured in liver homogenate according to the method of Srere (170). Respiration measurements were normalized to CSA for the integrin α1 studies. For the ILK studies, respiration measurements were normalized to mitochondrial protein concentration.

Hepatic Glycogen Content

Liver glycogen content was determined in 5-h fasted and insulin clamped livers as previously described (171). Approximately 40-60 mg of frozen liver tissue was homogenized in 0.03N HCl (0.1 mg tissue/ul HCl) and incubated at 80°C for 10 min. Two hundred μl of the digest was transferred to chromatography paper strips. The paper strips were washed 3x for 40 min per wash in 70% ethanol using a stir plate. After the last wash, the ethanol was poured off and the strips were briefly rinsed with acetone. The strips were dried in a ventilation hood overnight. The next day, the dried strips were placed in tubes containing 5 mL of aminoglucosidase solution (20 mg aminoglucosidase, 100 mL 0.2 M NaOAc buffer and 400 mL distilled water) and incubated in a 37°C shaking water bath for 3 hours. For both the 5-h fasted and insulin clamped livers, the glucose concentration was determined enzymatically in a 96-well place at 340 nm at the end of the incubation period. The following reaction was used:

$$\text{Glucose + ATP} \xrightarrow{\text{Hexokinase}} \text{Glucose-6-phosphate +ADP}$$

$$\text{Glucose-6-phosphate +ADP} \xrightarrow{\text{G6PDH}} \text{phospho-D-gluconolactone + NADPH}$$

Standard glucose concentrations were used to measure known equivalent NADPH, which was used to generate a standard curve for the measurement of the absorbance for the glucose concentrations of each sample. For the insulin clamped livers, the rate of glucose incorporated into glycogen during the insulin clamp was also determined by liquid scintillation counting. Briefly, 3 mL of the solution from the aminoglucosidase incubation was added to a scintillation vial with 15 mL scintillation fluid (Ultima Gold; Packard) and counted.

Hepatic Hydroxyproline Content

Hydroxyproline was determined in frozen livers from 5-h fasted mice using the Hydroxyproline Assay Kit (Sigma-Aldrich) per manufacturer's instructions. Approximately 50 mg of frozen liver tissue from 5-h fasted mice was homogenized in distilled water. Two hundred µl of the lysate was combined with 200 µl 12N HCl. The samples were hydrolyzed at 120°C for 3 hours. Twenty µl of lysate was added to a 96-well plate. The plate was incubated in an oven at 60°C for 1 hour to dry the samples. One hundred µl of the ChloramineT/Oxidation buffer was added to each sample and standard well, and the plate was incubated at room temperature for 5 min. One hundred µl of Diluted 4-(Dimethylamino) benzaldehyde (DMAB) Reagent was added to each standard and sample well, and the plate was incubated for 90 min at 60°C. The absorbance was determined at 560 nm. Hydroxyproline concentration was determined by the reaction of oxidized hydroxyproline with DMAB.

Immunoprecipitation and Immunoblotting

Frozen liver tissue was homogenized in a buffer containing 25 mM Tris-HCl (pH 7.4), 10 mM EDTA, 10% glycerol, 1% Triton X, 50 mM sodium pyrophosphate, 100 mM sodium fluoride, 1 mM PMSF and Halt Protease and Phosphatase Inhibitor (Thermo Scientific). For immunoprecipitation of the insulin receptor, 1 mg of protein was incubated with antibodies against the insulin receptor (Cell Signaling). Samples were incubated at 4°C overnight with Protein A/G PLUS-Agarose Immunoprecipitation Reagent (Santa Cruz Biotechnology). The immunoprecipitates were collected via centrifugation, applied to SDS-PAGE gels and transferred to PVDF membranes. Immunoblots were incubated with primary antibodies against the insulin receptor (Cell Signaling) and phosphotyrosine (Santa Cruz Biotechnology). For traditional immunoblots, the following primary antibodies were used: pAkt (Ser^{473} and Thr^{308}, Cell Signaling), total Akt (Cell Signaling), pIRS1 (Tyr^{612}, Life Technologies), total IRS1 (Cell Signaling), pERK1/2 (Thr^{202}/Tyr^{204} Cell Signaling), total ERK 1/2 (Cell Signaling), pJNK1/2 (Thr^{183}/Tyr^{185}, Cell Signaling) pFAK (Tyr^{397}, Abcam), total FAK (Santa Cruz), pFoxo1 Ser^{253}, total Foxo1 (Santa Cruz), integrin α1 (Chemicon), collagen I (Santa Cruz Biotechnology), collagen IV (Meridian), α-parvin (Cell Signaling), PINCH (BD Biosciences) and β-actin (Cell Signaling). Imaging and densitometry were performed using the ImageJ program and Odyssey imaging system (LI-COR Biosciences).

Immunohistochemistry

Collagen I was assessed by immunohistochemistry in paraffin-embedded tissue sections with assistance from the Vanderbilt Translational Shared Pathology Resource Core. Sections (5μm) were incubated with anti-collagen I antibody for 60 min prior to staining with

hematoxylin. The EnVision+HRP/DAB System (DakoCytomation) was used to produce staining. Images were obtained using a Q-Imaging Micropublisher camera mounted on an Olympus upright microscope.

Real-time Polymerase Chain Reaction

RNA was extracted using the RNeasy Mini Kit (Qiagen). RNA was reverse transcribed using the iScript cDNA synthesis kit (Bio-Rad). Quantitative PCR was performed using TaqMan Universal PCR Master Mix and commercially available TaqMan Assays (Applied Biosystems) on the CFX Real Time PCR Instrument (Bio-Rad) for all genes except for *Dgat1* and *Dgat2*. Data were normalized to the 18S ribosomal protein. Gene expression for *Dgat1* and *Dgat2* was measured using SYBR Green as previously described (172). Data were analyzed using the $2^{-\Delta\Delta Ct}$ method (173).

Kinexus Assay

The Kinex Kam-850 Antibody Microarray Kit (Kinexus) was used to monitor expression levels and phosphorylation states of signaling proteins per manufacturer's instructions. Two-hundred and fifty mg of pooled frozen 5-h fasted insulin clamped liver tissue from each genotype was homogenized and needle sheered in 1 mL of lysis buffer. The homogenate was centrifuged at 13000 rpm for 30 min at 4°C. The supernatant was collected and the protein concentration was determined using the BCA protein assay. Fifty μg of lysate from each genotype was labeled with the Kinex 543 Labeling Dye and the proteins were purified using Microspin G-25 Columns. The full amount of each labeled protein sample was applied to the microarray slide. The slide was incubated in a humidity chamber in the dark on a table top shaker for 2 hours at room

temperature. The slide was washed several times and dried in a swing-bucket bench top centrifuge. The microarray slide was shipped to Kinexus for quantitation and data analysis. Signal quantification was performed using *ImaGene* 9.0 from BioDiscovery. Z scores were calculated by subtracting the overall average intensity of all spots within a sample from the raw intensity for each spot, and dividing it by the standard deviations of all measured intensities within each sample (174). A Z ratio of ± 1.2 to 1.5 is considered significant.

Statistical analysis

Data are presented as means ± SEM. Statistical analyses were performed using Student *t* test or two-way ANOVA followed by Tukey post hoc tests as appropriate. The significance level was $P \leq 0.05$.

Chapter III

INTEGRIN α1-NULL MICE EXHIBIT IMPROVED FATTY LIVER WHEN FED A HIGH FAT DIET DESPITE SEVERE HEPATIC INSULIN RESISTANCE

Aims

Hepatic insulin resistance is associated with increased collagen. Integrin α1β1 is the only collagen binding receptor expressed on hepatocytes. The studies described in this chapter show that integrin α1 protein expression is increased in hepatocytes isolated from HF-fed mice compared to chow fed controls. The goal of Chapter III was to determine whether the upregulation of integrin α1 in response to a HF diet exerts a protective effect against the detrimental effects of a HF diet in the liver through increased signal transduction (Figure 3.1).

Introduction

The prevalence of Type 2 diabetes (T2D) has increased dramatically in parallel with excess caloric intake and sedentary lifestyles. Insulin resistance precedes the development of T2D (1,2). The liver, as one of the major insulin responsive organs, contributes to the pathogenesis of insulin resistance (32,175). Hepatic insulin resistance is strongly correlated with hepatic lipid accumulation. In rats, three days of high fat (HF) feeding leads to a 3-fold increase in hepatic triglyceride (TG) accumulation and decreased suppression of hepatic glucose production during an insulin clamp (51). In addition, hepatic lipid accumulation is associated with liver damage and increases in extracellular matrix (ECM) collagen proteins (32,73,86,175). Liver biopsies from humans with and without T2D demonstrate that the livers from diabetic patients exhibit severe steatosis associated with increased collagen IV protein expression (88).

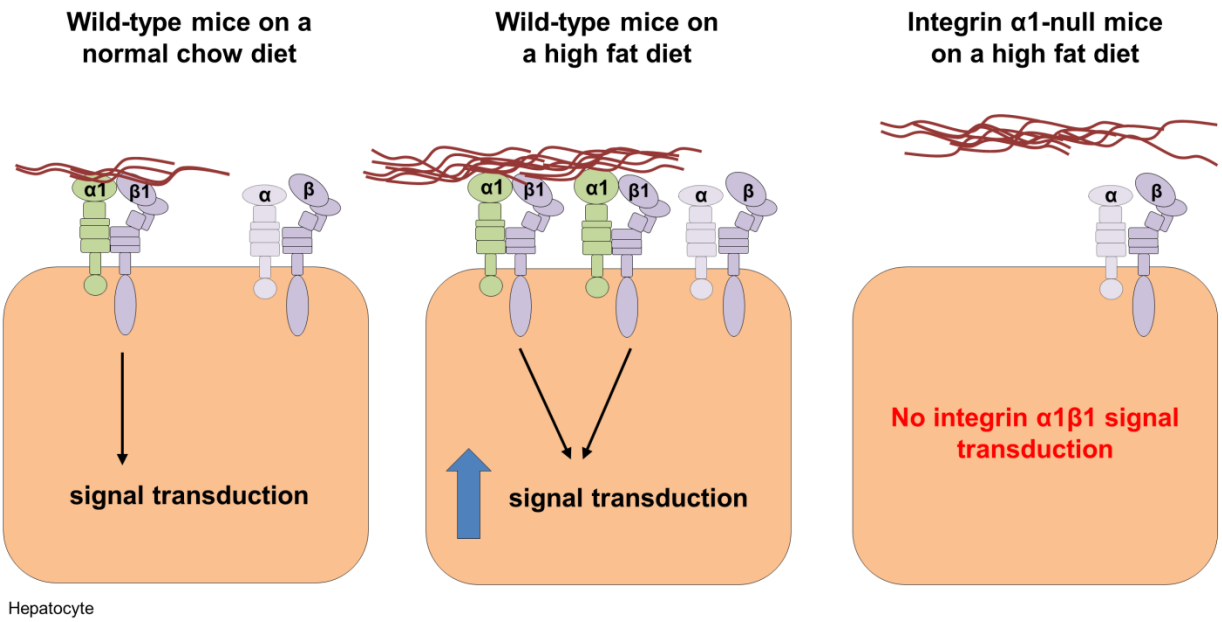

Figure 3.1 – Scheme of the hypothesis presented in Chapter III. In wild-type C57BL/6J mice on a normal chow diet, there is some collagen present and when bound to integrin α1β1, this results in signal transduction in the hepatocyte. Under conditions of high fat feeding, hepatic collagen content expands and there is increased integrin α1 protein expression on hepatocytes. This results in increased hepatocyte signal transduction. When integrin α1-null mice are fed on a high fat diet, there is an increase in hepatic collagen content but there is no integrin α1β1 present. This results in no integrin α1β1 signal transduction within the hepatocyte and metabolic impairments within the liver.

ECM production and degradation are controlled by integrins, transmembrane receptors for ECM proteins that consist of an α and β subunit (92). Upon ligand binding, integrins transduce signals across the plasma membrane to facilitate outside-in cell signaling (113). Several studies have suggested a role for integrins in the promotion of insulin action (92,142,146,176,177). Integrin α5β1 binding to its ligand fibronectin enhances insulin-stimulated tyrosine phosphorylation of both the insulin receptor and IRS1 (176). β1-integrin activation through its engagement with an anti-β1-integrin antibody or fibronectin leads to IRS1, PI3-kinase and subsequent Akt activation in isolated rat adipocytes (142). The integrin signaling molecule, focal adhesion kinase (FAK) has been shown to directly bind to IRS-1 and lead to IRS-1 tyrosine phosphorylation in intact cells (146). Finally, the loss of the integrin β1 subunit in striated muscle leads to insulin resistance and decreased muscle glucose uptake (177).

Integrin α1β1 is a major collagen receptor expressed on various cell types, including hepatocytes (102). The expression of integrin α1β1 is upregulated in the course of hepatic injury and ECM remodeling (110). We previously showed that the global deletion of the integrin α1 subunit leads to severe impairments in insulin-induced suppression of glucose production in HF-fed mice (178). However, the mechanism for this effect and the broader role of integrin α1 in the pathogenesis of HF diet-induced hepatic insulin resistance and lipid accumulation is unknown.

In these studies we show that integrin α1 protein expression is upregulated with HF feeding in hepatocytes. Thus, we assessed glucose tolerance and insulin sensitivity in HF-fed integrin α1-null (*itga1*$^{-/-}$) and wild-type littermates (*itgα1*$^{+/+}$) to determine whether this response belies a protective effect against hepatic metabolic impairments in C57BL/6J mice. We show that deletion of integrin α1 results in severe hepatic insulin resistance as evidenced by complete alleviation of the insulin-mediated suppression of hepatic glucose production and decreased

hepatic insulin signaling. The severe hepatic insulin resistance in HF-fed *itga1-/-* mice was present despite a ~50% decrease in hepatic TG and DAG accumulation. The reduction in hepatic lipids was associated with a combination of decreased FFA availability upon insulin stimulation, decreased gene expression of the fatty acid transporter *Cd36* and increased mitochondrial fatty acid utilization. This indicates that the decrease in hepatic lipid accumulation in HF-fed *itga1-/-* mice may be attributed to altered fatty acid metabolism.

Experimental Design

Littermate wild-type ($itga1^{+/+}$) and integrin α1-null ($itga1^{-/-}$) male mice on a C57BL/6J background were fed either a standard chow diet (5.5% fat by weight; 5001 Purina Laboratory Rodent Diet) or HF diet (60% kcal from fat; F3282 BioServ) for 16 weeks. All studies were performed between 19 and 24 weeks of age. Insulin action was assessed using the insulin clamp combined with tracer techniques to determine sites of insulin resistance. See Chapter II for detailed methods.

Results

Collagen gene expression and hydroxyproline content are elevated in livers from HF-fed C57BL/6J mice

Gene expression for collagen I α1, collagen I α2 and collagen III α1 was increased in HF-fed mice compared to chow-fed mice (Figure 3.2A). The increase in collagen gene expression correlated with an increase in hydroxyproline content (Figure 3.2B).

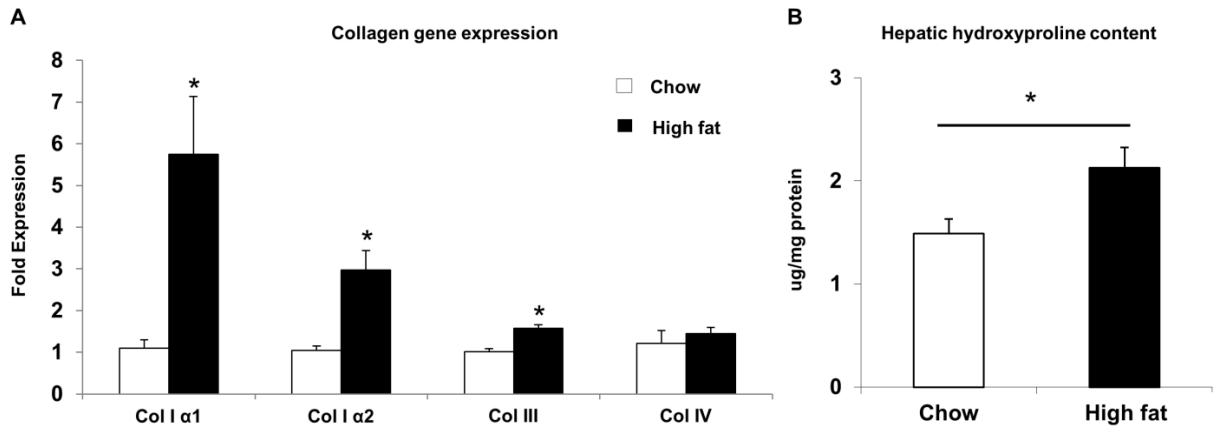

Figure 3.2 – Collagen gene expression and hydroxyproline content in livers from 5-h fasted wild-type C57BL/6J mice on a chow or high fat diet. Data are represented as means ± SEM; n = 4-5/group. *$p < 0.05$ chow vs. high fat fed.

Integrin α1 protein expression is increased in hepatocytes isolated from HF-fed C57BL/6J mice

The upregulation of the integrin α1 subunit has been described in several states of chronic liver disease associated with inflammation and fibrosis (110). To determine the effect of HF feeding on hepatocyte integrin α1 expression, hepatocytes were isolated from both chow and HF-fed C57BL/6J wild-type mice. Integrin α1 protein expression was increased ~2 fold in isolated hepatocytes from HF-fed mice (Figure 3.3A and B). TGF-β signaling is associated with the synthesis of hepatic collagen in rodents fed a HF diet (179). In addition, this cytokine promotes the expression of integrin α1 (109). Thus, we analyzed the activation of the TGF-β signaling cascade by evaluating TGF-β gene expression and the phosphorylation status of the downstream activator Smad2. We found that TGF-β gene expression was increased in the livers of HF fed mice (Figure 3.3C). In support of the notion that TGF-β signaling is increased with HF-feeding along with our observation that integrin α1 protein expression is increased in HF-fed mice, we also found that Smad2 activation (represented as the ratio of pSmad2/Smad2) was increased in the livers of HF-fed mice compared to their lean littermate controls (Figure 3.3D and E).

Adaptations to the genetic deletion of integrin α1 in both chow and HF-fed mice

To determine the role of integrin α1 in the livers of HF-fed mice, *itgα1*$^{+/+}$ and *itga1-/-* mice were fed a HF-diet for 16 weeks. HF feeding increased body weight, % fat mass and fasting blood glucose (Table 3.1). Body weight did not differ between genotypes on their respective diets. Fat mass was decreased in the HF-fed *itga1-/-* mice compared to HF-fed *itgα1*$^{+/+}$ mice. HF feeding increased fasting glucose and fasting insulin in wild-type mice. Fasting glucose was not different between the genotypes on their respective diets. Fasting insulin was not different

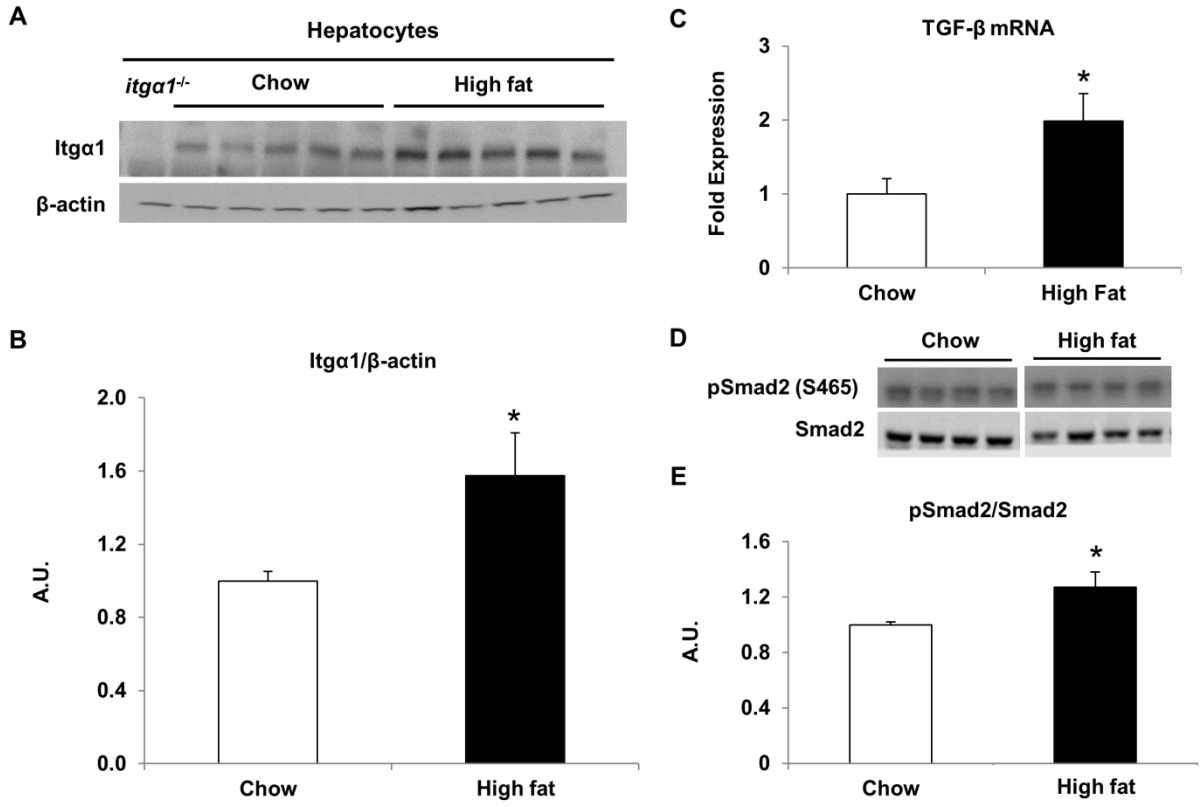

Figure 3.3 – Integrin α1 protein expression is increased in hepatocytes isolated from high fat fed mice. (A) Western blot analysis for integrin α1 protein expression in isolated hepatocytes (*n* = 5/group). (B) Quantitative analysis of data from A. (C) TGF-β gene expression in whole liver homogenate from 5-h fasted mice fed either a chow or high fat diet for 16 weeks (*n* = 5-6/group). (D) Smad2 activation in whole liver homogenate from 5-h fasted mice fed either a chow or high fat diet for 16 weeks (*n* = 4/group). (E) Quantitative analysis of data from D. Integrated intensities were obtained by the Odyssey and Image J software. Integrin α1 protein expression was normalized to β-actin. Smad2 activated was calculated as the ratio of p-Smad2 to total Smad2. Data are represented as means ± SEM; n = 4-5. *$p < 0.05$ chow vs. high fat fed.

Table 3.1
Characteristics of wild-type (*itgα1*$^{+/+}$) and integrin α1 null mice (*itgα1*$^{-/-}$) mice on both a chow and high fat (HF) diet.

	Chow		**High fat**	
	itgα1$^{+/+}$	***itgα1***$^{-/-}$	***itgα1***$^{+/+}$	***itgα1***$^{-/-}$
Weight (g)	26.1 ± 0.5	27.0 ± 0.5	48.4 ± 0.9 *	48.9 ± 1.3†
Fat mass (%)	10.4 ± 0.5	11.5 ± 2.0	41.6 ± 0.7 *	39.0 ± 1.8 §
Fasting glucose (mg/dL)	118 ± 3	111 ± 7	147 ± 12 *	151 ± 5†
Fasting insulin (ng/mL)	0.80 ± 0.2	0.82 ± 0.1	2.12 ± 0.21*	3.44 ± 0.72 §

Body composition, fasting glucose and insulin were determined in basal 5-h fasted mice (n = 6-8/group). Data are represented as means ± SEM. *$p < 0.05$ chow-fed *itgα1*$^{+/+}$ vs. HF-fed *itgα1*$^{+/+}$, $^{\dagger}p < 0.05$ chow-fed *itgα1-/-* vs. HF-fed *itgα1*$^{-/-}$and $^{\S}p < 0.05$ HF-fed *itgα1*$^{+/+}$ vs. HF-fed *itgα1*$^{-/-}$.

between the genotypes on a chow diet, however it was elevated in HF-fed *itga1-/-* mice compared to HF-fed *itgα1*$^{+/+}$ mice indicating insulin resistance.

HF feeding leads to excessive accumulation of collagen in the liver (86,87). Integrin α1β1 down regulates collagen synthesis, however its contribution to hepatic collagen gene expression in the HF-fed state has not been investigated (180). Therefore we measured collagen gene expression in *itgα1*$^{+/+}$ and *itga1-/-* mice on both a chow and HF-fed diet (Table 3.2). Gene expression for collagen I α1, collagen I α2 and collagen III α1 was increased in chow-fed *itga1-/-* mice compared to chow-fed *itgα1*$^{+/+}$ mice. Gene expression for collagen I α1 and collagen I α2 was increased by HF feeding in *itgα1*$^{+/+}$ mice. There was no difference in collagen mRNA levels between chow-fed and HF-fed *itga1-/-* mice. Next, we investigated whether the changes in collagen I gene expression resulted in differences in protein expression through western blot analysis and immunohistochemistry (Figure 3.4). Consistent with the collagen I gene expression results, we found that collagen I protein expression was also increased in the *itga1-/-* mice compared to *itgα1*$^{+/+}$ mice regardless of diet using western blot analysis (Figure 3.4A). Collagen I immunohistochemistry in the liver was used to determine the localization of the collagen deposition (Figure 3.4B). Collagen I staining was most prevalent around the vessels and within the sinusoidal spaces in all conditions. Thus, deletion of integrin α1 leads to increased hepatic collagen gene and protein expression independent of diet.

Integrin α1-null mice on a HF diet exhibit severe hepatic insulin resistance

Fasting insulin levels are increased in HF-fed *itga1-/-* mice compared to HF-fed *itgα1*$^{+/+}$ mice indicating impaired glucose metabolism. Therefore we examined glucose tolerance in both chow and HF-fed *itgα1*$^{+/+}$ and *itga1-/-* mice using gastric catheters for the delivery of glucose

Table 3.2
Collagen mRNA levels: interaction of gene and diet.

	Chow		High fat	
	itgα1$^{+/+}$	***itgα1***$^{-/-}$	***itgα1***$^{+/+}$	***itgα1***$^{-/-}$
Col I α1	1.1 ± 0.2	3.0 ± 0.6 *	1.5 ± 0.1 *	4.2 ± 1.2 §
Col I α2	1.1 ± 0.3	9.6 ± 3.0 *	2.6 ± 0.6 *	13.6 ± 5.1 §
Col III α1	1.2 ± 0.2	4.0 ± 0.6 *	1.1 ± 0.3	4.5 ± 1.6 §
Col IV α1	1.0 ± 0.1	2.3 ± 0.4 *	1.8 ± 0.5	3.4 ± 1.0

Total RNA was extracted from the livers of 5-h fasted mice and reverse transcribed into cDNA. Quantitative PCR was used to determine gene expression of several collagen chains (n = 5-7/group). Data are represented as means ± SEM. *$p < 0.05$ compared to chow-fed *itgα1*$^{+/+}$ mice and $^{\S}p < 0.05$ HF-fed *itgα1*$^{+/+}$ vs. HF-fed *itgα1*$^{-/-}$.

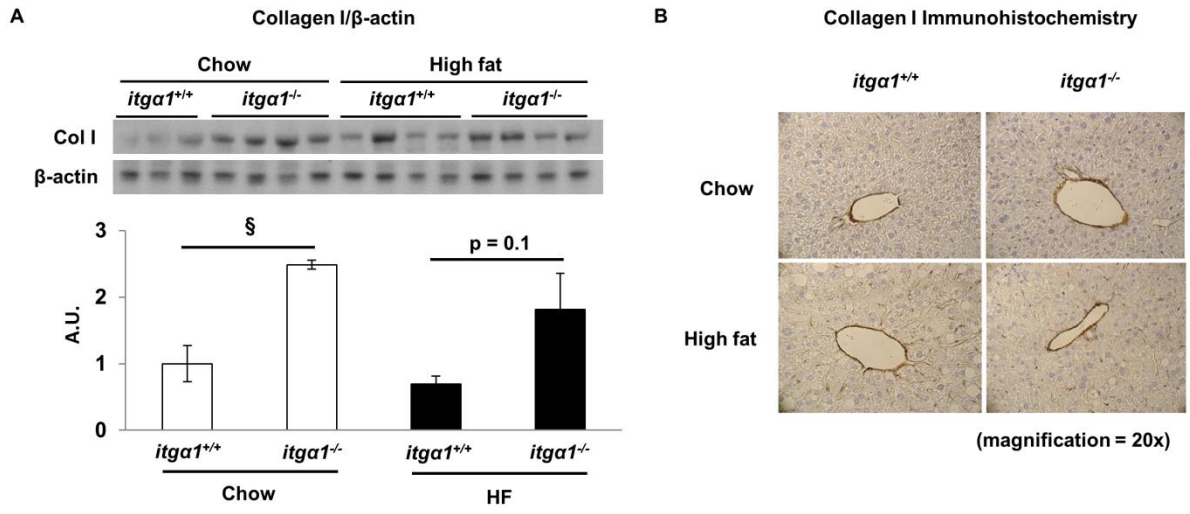

Figure 3.4 – Collagen I protein expression is increased in integrin α1 null mice. (A) Western blot analysis of collagen I performed on liver homogenates from basal 5-h fasted mice (n = 4/group). Integrated intensities were obtained using the Image J software and collagen I protein expression was normalized to β-actin. (B) Representative images from immunohistochemical staining of collagen I in livers from basal 5-h fasted mice (n = 5-7/group). Data are represented as means ± SEM. $^{\S}p < 0.05$ compared to chow-fed $itg\alpha 1^{+/+}$ mice.

directly into the stomach. The results from the GTTs indicate that there is no difference in glucose tolerance or the insulin response to a glucose challenge (insulin excursion) between the genotypes on their respective diets (Figure 3.5A-D). Considering that whole-body glucose tolerance can appear normal despite impaired insulin action (181), we next assessed insulin action in HF-fed *itgα1*$^{+/+}$ and *itga1-/-* mice using the hyperinsulinemic-euglycemic (insulin) clamp. During the insulin clamp, blood glucose was maintained between 150-160 mg/dL (Figure 3.5E). The steady state glucose infusion rate (GIR) was lower in HF-fed *itga1-/-* mice (Figure 3.5F). There was no difference in fasting endogenous glucose production ($endoR_a$) (Figure 3.5G). $EndoR_a$ during the insulin clamp was suppressed by ~50% in HF-fed *itgα1*$^{+/+}$ mice. In contrast, $endoR_a$ was not suppressed at all in HF-fed *itga1-/-* mice (Figure 3.5G) indicating complete resistance to insulin suppression of endogenous glucose production. There was no difference in basal or insulin-clamped whole body glucose disappearance (R_d) (Figure 3.5H). Plasma insulin during the insulin clamp was not different between the groups (9.65 ± 1.22 vs. 9.35 ± 1.20 ng/mL). The severe hepatic insulin resistance in HF-fed *itga1-/-* mice is independent of its effects on the transcriptional regulation of collagen as there is no difference in collagen gene expression between the chow and HF-fed *itga1-/-* mice (Table 3.2).

Integrins, including integrin α1β1, can regulate the phosphorylation and activation state of receptor tyrosine kinases and their downstream modulators (139,180,182-184). To determine whether genetic deletion of the integrin α1 subunit affected insulin receptor phosphorylation, we assessed insulin receptor phosphorylation in insulin clamped livers from HF-fed *itgα1*$^{+/+}$ and *itga1-/-* mice. There was no difference in insulin receptor phosphorylation (Figure 3.6A), suggesting that integrin α1β1 does not affect insulin-mediated activation of its receptor. To determine whether integrin α1β1 affected insulin signaling downstream of the insulin receptor,

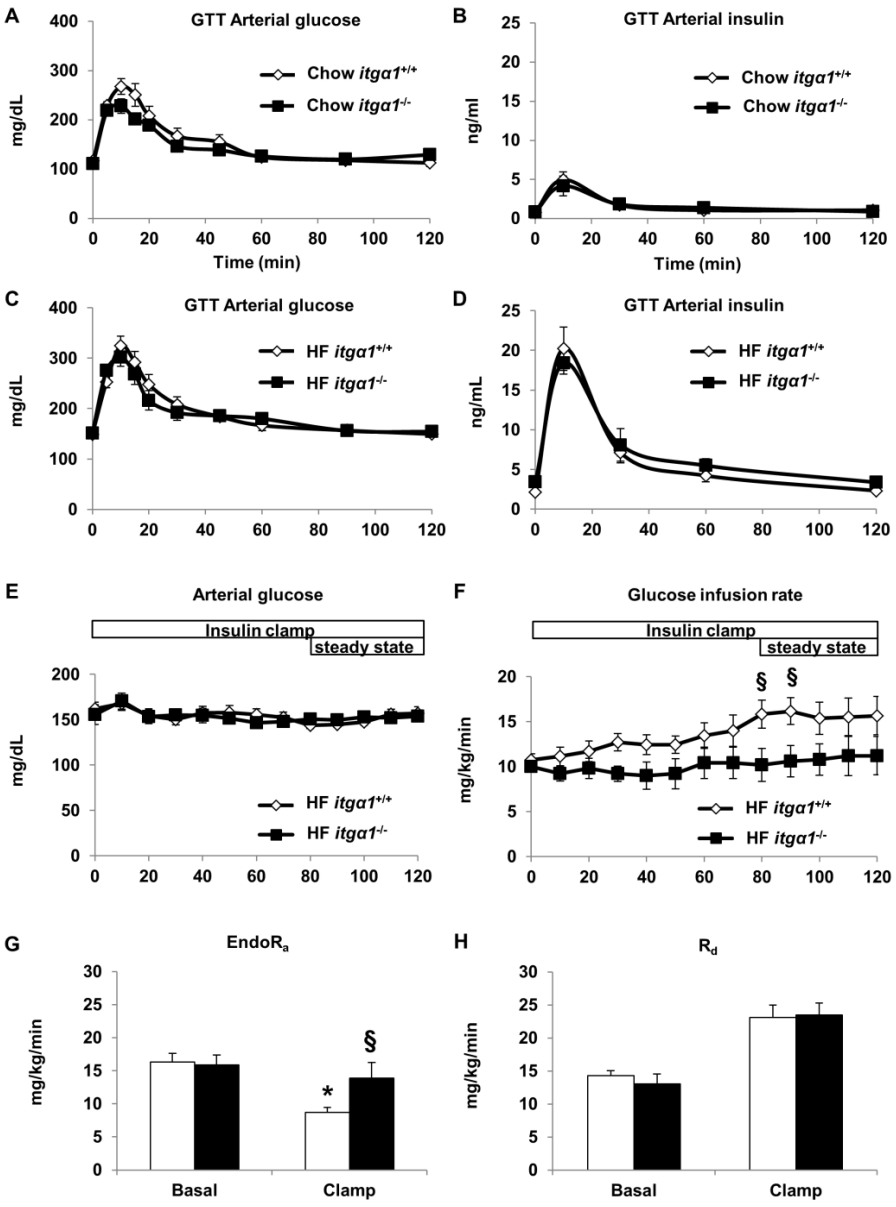

Figure 3.5 – Integrin α1β1 protects against diet-induced hepatic insulin resistance. Glucose tolerance tests (GTT) were performed on chow and HF fed *itgα1*$^{+/+}$ and *itga1-/-* mice. Arterial glucose (A and C) and insulin (B and D) were measured during the GTTs (n = 5-7/group). Arterial glucose (E) and glucose infusion rate (F) during the hyperinsulinemic-euglycemic (insulin) clamp (n = 5-6/group). Mice were fasted for 5-h prior to the start of the insulin clamp. Blood glucose was maintained between 150-160 mg/dL during the steady state (80-120 min). Glucose (50%) was infused to maintain euglycemia. Endogenous glucose production ($endoR_a$) (G) and whole-body disappearance (R_d) (H) were determined during the steady state period of the insulin clamp. Data are represented as means ± SEM. *$p < 0.05$ compared to the basal measurement in HF-fed *itgα1*$^{+/+}$ mice and $^{§}p < 0.05$ compared to HF-fed *itgα1*$^{+/+}$ mice during the insulin clamp.

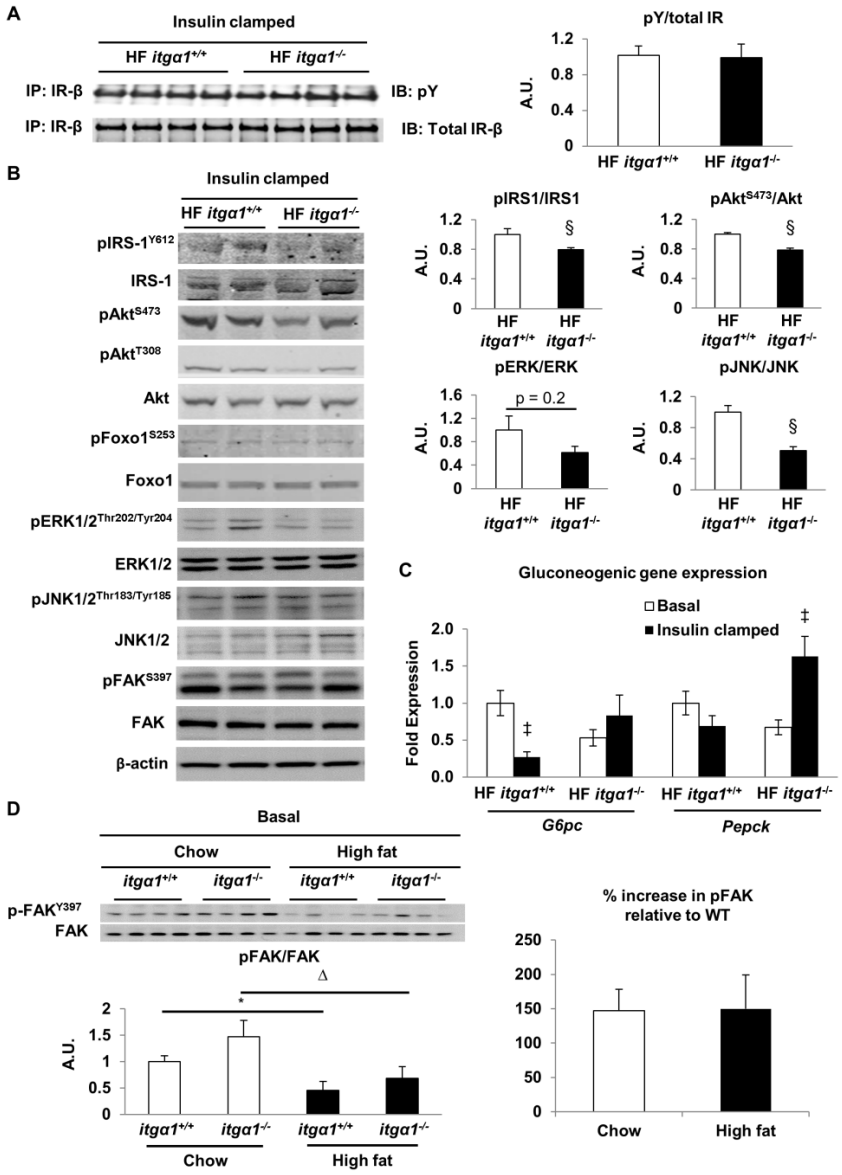

Figure 3.6 – Integrin α1β1 facilitates hepatic insulin action in HF-fed mice. (A) Immunoprecipitation (IP) of the insulin receptor (IR) was performed on liver homogenates after the insulin clamp prior to an immunoblot for phosphotyrosine (pY) (*n* = 4/group). IR phosphorylation was determined as the ratio of pY to total IR. (B) Representative blots of liver insulin signaling after the insulin clamp (*n* = 4-5/group). (C) mRNA was extracted from both basal 5-h fasted and 5-h fasted insulin clamped livers. qPCR was performed to determine gene expression of the gluconeogenic genes *G6pc* and *Pepck*. (D) Focal adhesion kinase (FAK) and FAK phosphorylation was determined in liver homogenates from basal 5-h fasted mice (*n* = 4/group). FAK phosphorylation was quantified as the ratio of p-FAK to FAK. Percent increase of FAK phosphorylation was calculated relative to wild-type (WT) mice. Integrated intensities were obtained by the odyssey and Image J software. Data are represented as means ± SEM. $^{\S}p< 0.05$ compared to HF-fed *itgα1*$^{+/+}$ mice. $^{*}p< 0.05$ compared to chow-fed *itgα1*$^{+/+}$ mice. $^{\Delta}p < 0.05$ compared to chow-fed *itgα1-/-* mice. $^{\ddagger}p < 0.05$ compared to basal 5-h fasted mice.

we assessed several markers of insulin signaling in insulin stimulated livers from HF-fed *itgα1*$^{+/+}$ and *itga1-/-* mice. Consistent with the hepatic glucose flux measurements, phosphorylation of IRS-1 at Tyr^{612} and Akt at Ser^{473} were decreased in HF-fed *itga1-/-* mice indicating decreased insulin action (Figure 3.6B). There was no difference in the insulin-mediated phosphorylation of Akt at Thr^{308}, Foxo1 at Ser^{253} or FAK at Ser^{397}. To determine the effect of integrin α1β1 on hepatic gluconeogenic gene expression in the HF-fed state, we used qPCR to determine gene expression of glucose-6-phosphatase (*G6pc*) and phosphoenol pyruvate carboxylase (*Pepck*) in the livers from basal 5-h fasted and insulin clamped mice (Figure 3.6C). Consistent with the severe hepatic insulin resistance in the HF-fed *itga1-/-* mice, insulin failed to suppress *G6pc* gene expression and there was a striking insulin-mediated increase in *Pepck* gene expression. In contrast, insulin-mediated *G6pc* gene expression was significantly decreased in the HF-fed *itgα1*$^{+/+}$mice. Consistent with other reports (105,185), we found that deletion of integrin α1 reduced activation of the MAPK signaling pathway as evidenced by a slight yet non-significant decrease in ERK1/2 activation and a significant decrease in JNK1/2 activation (Figure 3.6B).

Integrin α1β1 signals to activate several downstream targets including FAK (144) and the integrin α1 subunit has been shown to bind FAK (122). In addition, FAK has been shown to interact with IRS1 (146). Thus we sought to determine whether decreased insulin signaling in the HF-fed *itga1-/-* mice is associated with decreased FAK phosphorylation in both insulin clamped and basal 5-h fasted livers. We found that there was no difference in insulin-stimulated FAK phosphorylation between the HF-fed *itgα1*$^{+/+}$ and *itga1-/-* mice (Figure 3.6B). In the basal state, there was a significant decrease in FAK phosphorylation in HF-fed mice compared to chow-fed mice independent of genotype (Figure 3.6D). However, there was no difference in the percent increase in pFAK/FAK relative to WT in either the chow-fed or HF-fed mice in the basal 5-h

fasted state. Thus, integrin α1β1 appears to mediate insulin signaling in a FAK-independent manner.

Genetic deletion of integrin α1 improves fatty liver through changes in fatty acid metabolism

HF feeding leads to increased hepatic lipid accumulation and severe hepatic insulin resistance associated with decreased insulin stimulated IRS1 tyrosine phosphorylation (51). Thus, we wanted to assess whether the severe hepatic insulin resistance in HF-fed *itga1-/-* mice could be attributed to increased lipid accumulation. To determine the role of integrin α1 on hepatic lipid accumulation, we assessed hepatic triglyceride (TG) and diglyceride (DAG) accumulation in the livers from both chow and HF-fed $itg\alpha1^{+/+}$ and *itga1-/-* mice. HF feeding increased liver TG and DAG content ~ 5 fold in $itg\alpha1^{+/+}$ mice compared to chow-fed $itg\alpha1^{+/+}$ mice (Figure 3.7A, B and C). Liver TG and DAG content was decreased by ~ 50% in HF-fed *itga1-/-* mice compared to HF-fed $itg\alpha1^{+/+}$ mice (Figure 3.7A, B and C). This was supported by the finding that lipid droplets were smaller in HF-fed *itga1-/-* mice compared to HF-fed $itg\alpha1^{+/+}$ mice (Figure 3.7A).

To examine the potential mechanisms whereby HF-fed *itga1-/-* mice exhibit decreased TG and DAG accumulation, we first investigated several parameters that regulate hepatic triglyceride metabolism. Circulating plasma TGs were increased in HF-fed *itga1-/-* mice (Figure 3.8A). Thus, we tested the hypothesis that the reduction in liver TGs was due to increased secretion from the liver. This hypothesis, however, was not supported by the results as no difference in TG secretion was observed between the HF-fed $itg\alpha1^{+/+}$ and *itga1-/-* mice (Figure 3.8B and C). Next we examined the expression of several genes associated with hepatic lipogenesis. Despite decreased lipid accumulation, gene expression for the lipogenic genes

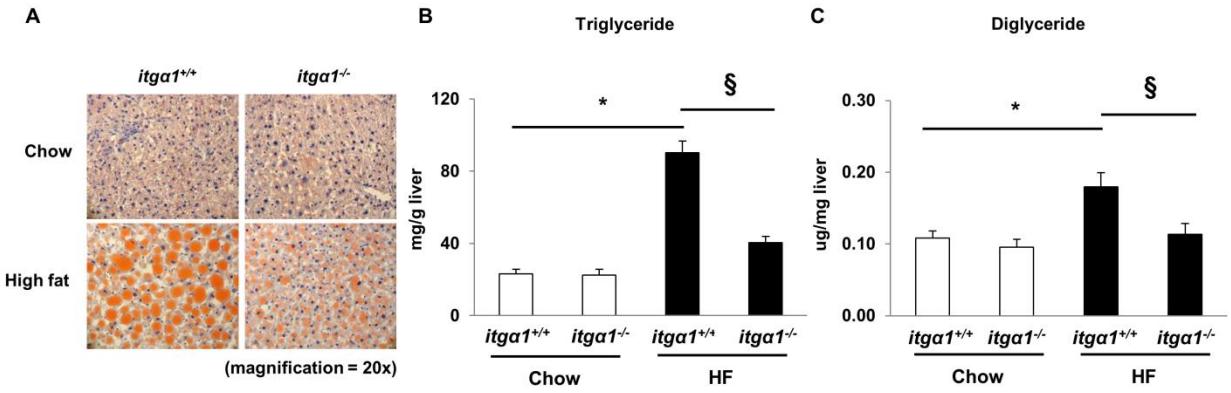

Figure 3.7 – Integrin α1 promotes hepatic lipid accumulation. (A) Oil red O staining of liver neutral lipid droplets. Liver triglyceride (TG) (B) and diglyceride (DAG) (C) content was quantified in 5-h fasted mice (n = 5/group). Data are represented as means ± SEM. *$p < 0.05$ compared to chow-fed $itg\alpha1^{+/+}$ mice and $^{\S}p < 0.05$ compared to HF-fed $itg\alpha1^{+/+}$ mice.

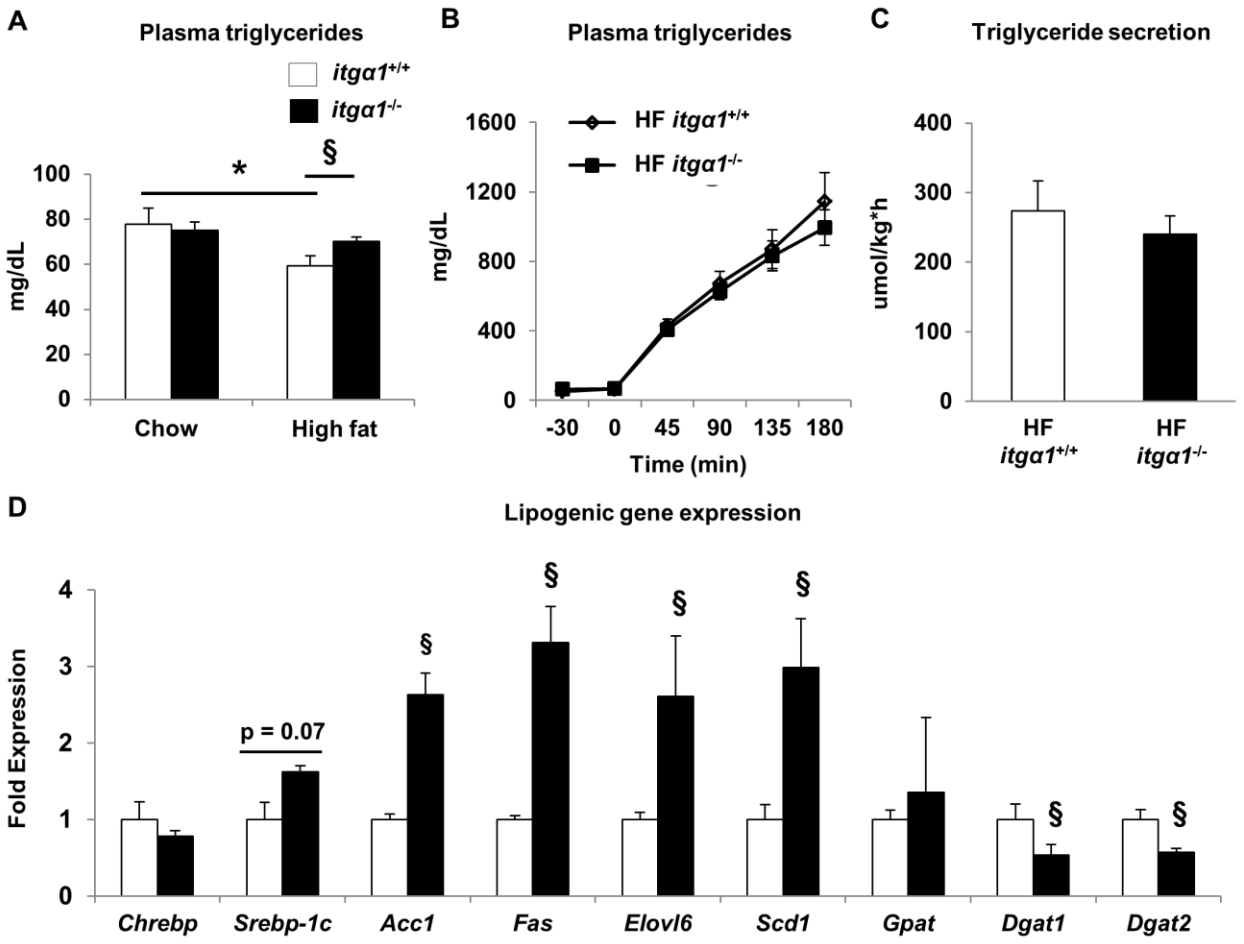

Figure 3.8 – Effect of whole-body integrin α1 deletion on triglyceride (TG) metabolism. (A) Circulating plasma TGs in basal 5-h fasted mice. (B) Hepatic TG secretion was determined using tyloxapol to block VLDL-TG clearance from the circulation. (C) Quantification of triglyceride secretion rates. (D) mRNA was extracted from basal 5-h fasted livers and qPCR was used to determine lipogenic gene expression. Data are represented as means ± SEM. $^{*}p < 0.05$ compared to chow-fed *itgα1*$^{+/+}$ mice. $^{§}p < 0.05$ compared to HF-fed *itgα1*$^{+/+}$ mice. (n = 5-8/group).

Srebp-1c, *Fas*, *Acc1*, *Scd1* and *Elovl6* were increased in HF-fed *itga1-/-* mice. In contrast, expression of *Dgat1* and *Dgat2* genes, the genes responsible for catalyzing the final step in TG biosynthesis, were decreased in HF-fed *itga1-/-* mice (Figure 3.8D).

Circulating free fatty acids (FFAs) are typically the major substrate for the accumulation of hepatic TGs (30). Thus we measured several markers of FFA metabolism in each mouse model. Basal 5-h fasting plasma FFAs were equal between the two genotypes (Figure 3.8A). Insulin suppressed plasma FFAs to a greater extent in HF-fed *itga1-/-* mice. Next we analyzed gene expression of several genes involved in the regulation of fatty acid metabolism including *Cd36*, *Pparα*, *Pparγ* and *Cpt-1α* (Figure 3.9B). Consistent with the finding that hepatic lipid accumulation was decreased in HF-fed *itga1-/-* mice, we found that gene expression for *Cd36* and *Pparγ* was decreased in HF-fed *itga1-/-* mice.

To determine the contribution of mitochondrial fatty acid supported respiration to TG and DAG accumulation in both chow and HF-fed $itg\alpha 1^{+/+}$ and *itga1-/-* mice we assessed mitochondrial oxygen consumption in mechanically permeabilized liver pieces. Mechanically permeabilized liver pieces were used in lieu of isolated mitochondria to ensure the cytoskeletal attachments are conserved and the mitochondria are not stressed during the functional measurements. ADP-stimulated (state 3) respiration in the presence of palmitoyl-carnitine and malate was increased in *itga1-/-* mice compared to $itg\alpha 1^{+/+}$ mice regardless of diet (Figure 3.9D). There was no difference in glutamate/malate stimulated state 3 respiration (Figure 3.9C) or citrate synthase activity (data not shown) between groups. Thus the observed decrease in TG and DAG accumulation in HF-fed *itga1-/-* mice is linked to increased capacity for mitochondrial fatty acid supported respiration.

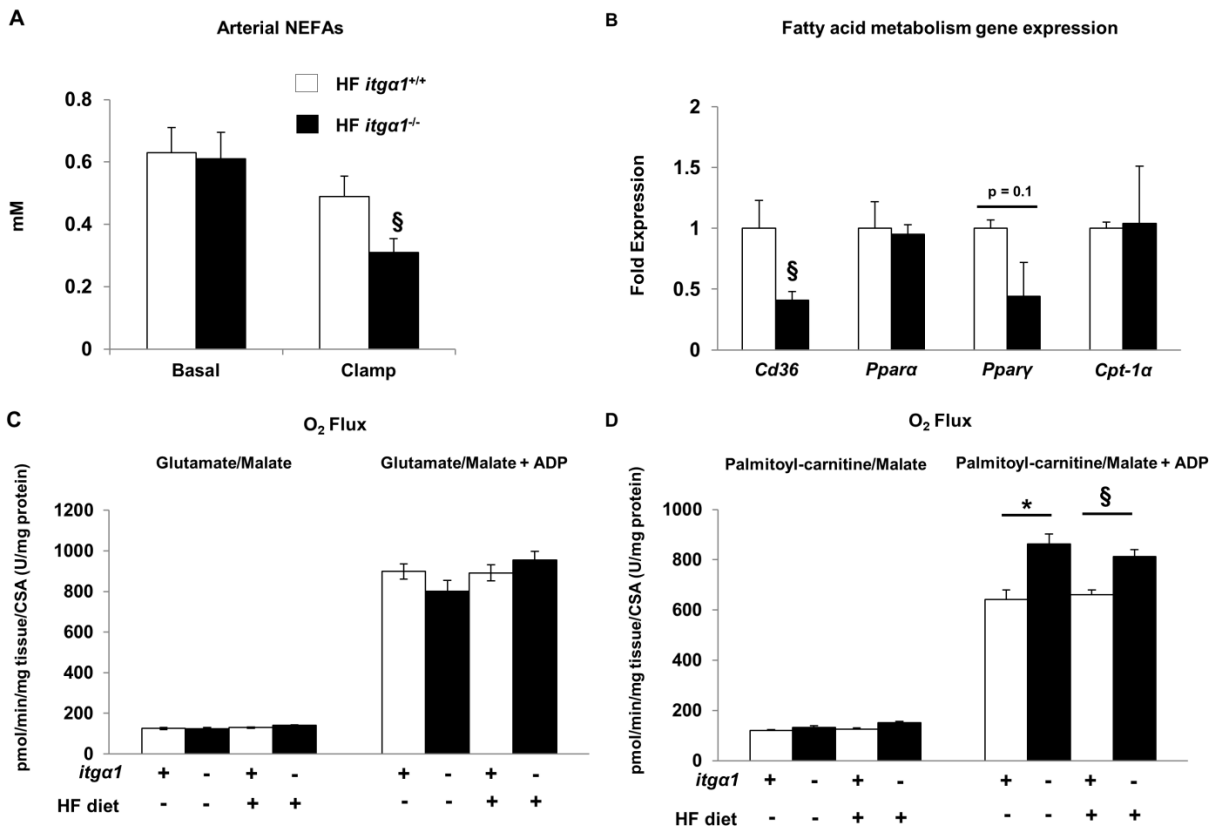

Figure 3.9 – Effect of integrin α1β1 on free fatty acid (FFA) metabolism. (A) Arterial non-esterified free fatty acids (NEFAs) in the basal 5-h fasted state and during the insulin clamp. (B) Gene expression of several genes implicated in the regulation of fatty acid metabolism. mRNA was extracted from 5-h fasted livers and qPCR was used to determine gene expression (n = 5-6/group). (C and D) High-resolution respirometry was performed on mechanically permeabilized liver pieces from 5-h fasted mice. Data are represented as means ± SEM. *$p < 0.05$ compared to chow-fed $itg\alpha1^{+/+}$ mice and $^{\S}p < 0.05$ compared to HF-fed $itg\alpha1^{+/+}$ mice.

Discussion

Integrin α1β1 is a collagen binding integrin found on the hepatocyte (102). Results from these studies show that integrin α1 protein expression is increased in hepatocytes with HF feeding. The goal of this study was to determine whether increased expression of the integrin α1 subunit with HF feeding would promote hepatic insulin action and protect against metabolic impairments in HF fed C57BL/6J mice. We found that integrin α1β1 signaling protects against diet-induced hepatic insulin resistance as it promotes hepatic insulin action. Insulin clamp studies showed that hepatic glucose production is completely resistant to suppression by an insulin stimulus in HF-fed *itga1-/-* mice and this is associated with decreased insulin signaling. Despite severe hepatic insulin resistance, HF-fed *itga1-/-* mice exhibit a 50% reduction in hepatic TG and DAG accumulation compared to their wild-type littermates. The reduction in hepatic lipids was associated with a combination of decreased FFA availability upon insulin stimulation, decreased gene expression of the fatty acid transporter *Cd36* and increased mitochondrial fatty acid utilization.

The hepatocyte is the most abundant cell type in the liver and is a major site of hepatic insulin action. Thus, it was important to determine the effects of HF feeding on integrin α1 protein expression in isolated hepatocytes. Our studies show that integrin α1 protein expression is increased in hepatocytes isolated from wild-type mice after 16 weeks of HF feeding.

To determine the role of integrin α1 in glucose and lipid metabolism, *itgα1*$^{+/+}$ and *itga1-/-* mice were fed either a chow or HF-diet for 16 weeks. The whole body deletion of integrin α1 in HF fed mice resulted in a small decrease in fat mass (~ 8%). Glucose transported into the fat cell provides the three carbon backbone essential for the esterification of FFAs (186). Previous studies from our lab show that HF-fed *itga1-/-* mice have decreased insulin-stimulated adipose

tissue glucose uptake (178). Thus, it is reasonable to propose that this reduction in glucose uptake contributes to the small decrease in fat mass in the HF-fed *itga1-/-* mice.

The measurement of basal 5-h fasting blood glucose and insulin revealed that fasting insulin was elevated in HF-fed *itga1-/-* mice indicating impaired glucose metabolism and potentially insulin resistance. Oral glucose tolerance was assessed in mice with an indwelling gastric catheter for glucose delivery and an arterial catheter for blood sampling. There was no difference in either the glycemic or insulin responses during the OGTT between genotypes. To determine whether the increase in integrin α1 protein expression improved hepatic insulin sensitivity in HF fed mice, insulin clamps were used to assess insulin action. Consistent with our previous report (178) HF-fed *itga1-/-* mice exhibited a lower glucose infusion rate (GIR) compared to HF-fed *itgα1*$^{+/+}$ mice. Hepatic glucose production was suppressed by ~50% in HF-fed *itgα1*$^{+/+}$, while it was not suppressed in *itga1-/-* mice. This indicates a more severe hepatic insulin resistance in HF-fed *itga1-/-* mice. There was no difference in R_d during the insulin clamp. This indicates that the difference in the GIR during the insulin clamp is due to complete loss of hepatic insulin sensitivity and not decreased insulin-stimulated glucose disposal from tissues such as the skeletal muscle. The absence of skeletal muscle insulin resistance in HF-fed *itga1-/-* mice supports a previous observation from our laboratory showing that there is no difference in skeletal muscle insulin sensitivity between HF-fed *itgα1*$^{+/+}$ and *itga1-/-* mice (178).

Glucose tolerance is determined by several factors in addition to insulin resistance. These include glucose effectiveness (i.e. the ability of glucose to suppress endogenous glucose production and stimulate glucose uptake (187)) and insulin secretion and clearance. Since insulin concentrations were equal between genotypes during the OGTT, it is probable that impaired insulin action is offset by differences in glucose effectiveness. Moreover, arterial insulin

concentrations are similar in the two genotypes, but the insulin levels at the liver are unknown. The liver is perfused by hepatic portal venous blood, which is unobtainable in the mouse. It is well-accepted that arterial insulin does not reflect insulin in the portal vein. Thus, one explanation for normal GTT, in the face of insulin resistance is different insulin concentrations at the liver. Overall, these studies highlight the value of considering both glucose tolerance and insulin action as distinct read outs when determining the metabolic phenotype of novel mouse models.

The complete lack of suppression of hepatic glucose production during the insulin clamp in HF-fed *itga1-/-* mice was associated with decreased insulin-stimulated IRS1 and Akt activation followed by no insulin-mediated suppression of *G6pc* gene expression and increased insulin-mediated *Pepck* gene expression. This occurred in the absence of differences in insulin-mediated Foxo1 phosphorylation at Ser^{253} in whole liver homogenate. There was also no difference in insulin receptor phosphorylation. This suggests that there may be some aspect of integrin α1β1 signaling that promotes hepatic insulin action downstream of the insulin receptor in HF-fed mice (142). To further investigate how the deletion of integrin α1 in HF-fed mice results in decreased IRS1 and Akt activation, we assessed activation of several signaling molecules in the MAPK signaling pathway including ERK1/2 and JNK1/2. Previous studies implicate a role for JNK activation in the development of hepatic insulin resistance by decreasing insulin-induced tyrosine phosphorylation IRS1 (188). In contrast, we found that activation of this pathway was downregulated in HF-fed *itga1-/-* mice compared to HF-fed $itg\alpha 1^{+/+}$ mice indicating that the absence of integrin α1 dampens MAPK signaling despite hepatic insulin resistance and JNK activation is not responsible for the observed decrease in IRS1 Tyr phosphorylation in HF-fed *itga1-/-* mice.

There is considerable crosstalk between the insulin and integrin signaling cascades (62,142,176,177). A potential mediator of this crosstalk is the integrin specific signaling molecule, FAK. FAK has been implicated in the regulation of hepatic insulin signaling (144,146,152). Decreased FAK signaling is associated with decreased hepatic IRS1 and Akt phosphorylation (144). Furthermore, *fa/fa* rats treated with a TNF-α neutralizing agent exhibited increased hepatic FAK phosphorylation associated with decreased hepatic glucose output (152). In contrast to these studies, our findings showed that down regulation of FAK phosphorylation is not essential for the severe insulin resistance in insulin clamped HF-fed *itga1-/-* mice compared to their wild-type littermates. There was a tendency for increased FAK activation in the basal 5-h fasted *itga1-/-* mice; however this trend was equivalent regardless of diet. It is notable however, that we do see a striking decrease in FAK phosphorylation in livers from 5-h fasted HF-fed mice compared to chow-fed mice regardless of genotype. This suggests that HF feeding facilitates an integrin α1β1 independent inhibition of FAK activation. Although the hepatic insulin resistance seen in the HF-fed *itga1-/-* mice cannot be attributed to decreased FAK phosphorylation, this may be an independent mechanism whereby HF feeding decreases hepatic insulin action in wild-type mice.

To further elucidate the mechanisms of the severe hepatic insulin resistance in the HF-fed *itga1-/-* mice, we measured hepatic lipid accumulation in our mouse models. Hepatic TG accumulation, or its lipogenic metabolites, can decrease hepatic insulin action (29,51). Surprisingly, we found that HF-fed *itga1-/-* mice exhibit a 50% reduction in hepatic TG and DAG accumulation compared to their wild-type littermates. This data is important for several reasons. First, it suggests that integrin α1β1 promotes TG and DAG accumulation in the liver. Second, hepatic steatosis is dissociated from insulin resistance in HF-fed *itga1-/-* mice. This

makes it a unique model of hepatic insulin resistance. It also supports other studies (28,56-58) that show that insulin resistance can be dissociated from lipid accumulation and can exist in the absence of increased TG and DAG.

To identify a potential mechanism whereby HF-fed *itga1-/-* mice exhibit decreased TG and DAG accumulation, we examined indices of TG synthesis and breakdown in both the HF-fed *itgα1*$^{+/+}$ and *itga1-/-* mice. These include lipogenesis, VLDL secretion, circulating FFAs and mitochondrial fatty acid respiration (28-30). Results from the present studies show that expression of the lipogenic genes *Srebp-1c, Fas, Acc1, Scd1* and *Elovl6* were increased. This indicates that the decrease in hepatic lipid accumulation is independent of decreased expression of these key lipogenic genes. We propose this is the result of a feedback mechanism that exists to upregulate lipogenic pathways when hepatic lipid stores are low. This supports the notion that the liver promotes the incorporation of lipid metabolites into neutral lipid droplets to protect against the deleterious effects of a HF diet. TG synthesis is regulated by the step-limiting enzyme, diglyceride acyltransferase (DGAT). Contrary to the increase in genes involved in lipogenesis, we found that gene expression for two predominant isoforms of DGAT (*Dgat1* and *Dgat2*) was decreased. This finding may explain, at least in part, why hepatic DAG and TG accumulation is decreased in HF-fed *itga1-/-* mice. This conclusion is supported by previously published work from Chen et al. (189). In this study, the global deletion of DGAT1 resulted in a decrease in hepatic DAG levels. To determine whether a critical substrate for the DGAT reaction was altered, we measured hepatic G3P levels. Our results indicate that G3P levels are increased in the livers of HF-fed *itga1-/-* mice (35.6 ± 4.7 and 48.4 ± 1.8 nmol/mg liver) suggesting that the observed decrease in lipid accumulation is independent of hepatic G3P levels.

The majority of liver TGs are derived from circulating FFAs (30,37). Here we show that HF-fed *itga1-/-* mice have decreased circulating FFAs compared to HF-fed *itgα1*$^{+/+}$ mice during the insulin clamp. This indicates that insulin suppresses circulating FFAs to a greater extent in HF-fed *itga1-/-* mice suggesting that insulin-mediated lipolysis (i.e. the hydrolysis of triacylglycerol in adipocytes) is blunted and this may account for the decreased lipid accumulation.

CD36 is key for FFA transport into the hepatocyte and CD36 expression is correlated with liver fat content (190,191). Our results show that liver *Cd36* gene expression was in fact decreased in *itga1-/-* mice consistent with the reduction in lipid accumulation. Additionally, CD36 is a known transcriptional target of PPARγ (192). In further support of the decrease in *Cd36* gene expression, our studies show that gene expression for *Pparγ* was also decreased.

FFAs are esterified into TGs or oxidized by the mitochondria in the hepatocyte (193). When the supply of FFAs exceeds the amount the mitochondria can oxidize, hepatic fat accumulation occurs. To determine the contribution of the mitochondria to fatty acid utilization in the chow and HF-fed *itgα1*$^{+/+}$ and *itga1-/-* mice, palmitoyl-carnitine/malate stimulated state 3 respiration was measured in mechanically permeabilized liver pieces. Results show that palmitoyl-carnitine stimulated state 3 respiration is higher in *itga1-/-* mice regardless of diet. This suggests that hepatic mitochondria in *itga1-/-* mice have a greater capacity to utilize fatty acid substrates. Hepatic mitochondrial oxygen flux was not different in chow and HF-fed mice. This result is supported by a study from Satapati et al. that also showed no difference in hepatic mitochondrial palmitoyl-carnitine/malate supported state 3 respiration at 16 weeks of HF feeding in mice (194). The differences in mitochondrial respiration (i.e. fatty acid utilization by the mitochondria) occurred in the absence of differences in the expression of genes involved in the

regulation of fatty acid oxidation (i.e. *Pparα* and *Cpt-1α*). Overall the results show that the decrease in hepatic lipid accumulation in the HF-fed *itga1-/-* mice is due to regulation at multiple sites. Hepatic FFA availability and uptake of FFAs are decreased while FFA utilization by the mitochondria is increased.

Here we introduce for the first time that integrin α1 is upregulated in hepatocytes as an important adaptive response to over nutrition and that this may protect against more severe insulin resistance. This novel concept is illustrated in Figure 3.10. In HF-fed wild-type mice, the combination of both insulin and integrin α1β1 signaling leads to IRS1 and Akt phosphorylation resulting in the partial suppression of hepatic glucose output. In contrast, when integrin α1 is absent, insulin-mediated IRS1 and Akt activation is decreased. This results in the complete absence of insulin-induced suppression of hepatic glucose production. Interestingly, the profound insulin resistance observed in HF-fed *itga1-/-* mice is not only independent of increased hepatic TG and DAG concentrations, it occurs in the presence of a striking decrease in these lipids. This is attributed to alterations in free fatty acid metabolism. In HF-fed wild-type mice, circulating FFAs are taken up by the liver and utilized for the synthesis of DAG and TG. In HF-fed *itga1-/-* mice, circulating FFAs are lower and those that are available within the hepatocyte are utilized to a greater extent by the mitochondria for mitochondrial respiration.

The mouse model utilized in these studies was a whole-body deletion of the integrin α1 subunit. The liver is a heterogeneous tissue comprised of many different cell types including, but not limited to, hepatocytes, sinusoidal lining cells, endothelial cells, stellate cells and Kupffer cells. The hepatocyte is the most abundant cell type, making up approximately 80% of the cells

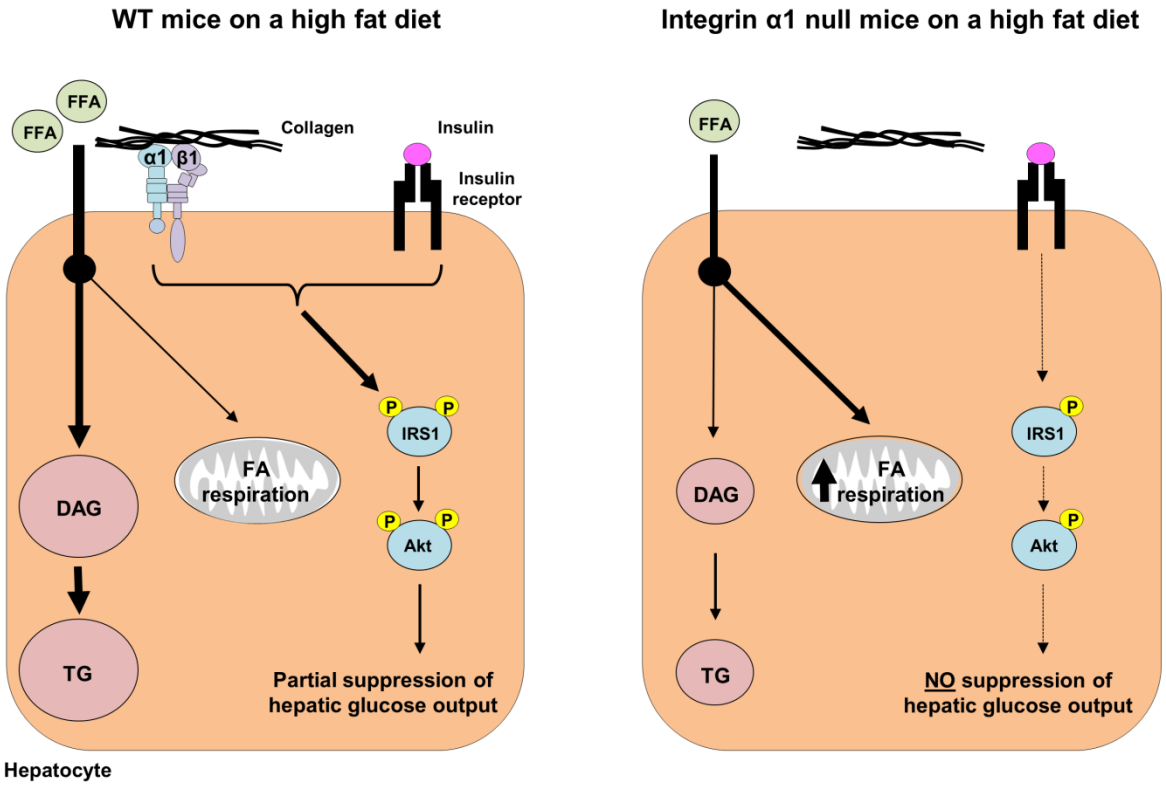

Figure 3.10 – Model whereby the integrin α1β1 protects against severe hepatic insulin resistance while promoting TG accumulation. Integrin α1 protein expression increases when wild-type (WT) mice are fed a high fat diet. This leads to increased integrin α1β1 cell signaling upon collagen binding. Upon insulin stimulation, the combination of both insulin and integrin α1β1 signaling leads to the phosphorylation and subsequent activation IRS1 and Akt. This results in the partial suppression of hepatic glucose output. Circulating free-fatty acids (FFAs) are taken up by the liver and utilized primarily for the synthesis of diglyceride (DAG) and triglyceride (TG) while some may be shunted towards the mitochondria for mitochondrial respiration. In contrast, when integrin α1 null mice are fed a high fat diet and insulin levels are high, the absence of integrin signaling leads to decreased IRS1 and Akt activation. This results in no suppression of hepatic glucose output. Circulating FFAs are lower and the available FFAs are utilized primarily by the mitochondria for mitochondrial respiration. This results in decreased DAG and TG levels.

in the liver, and is a major site of hepatic insulin action and lipid metabolism (60). Thus, it seems highly likely that the observed metabolic phenotype is a result of changes within the hepatocyte. In summary, this study shows for the first time the novel role of integrin α1β1 in the regulation of hepatic glucose and lipid metabolism under conditions of over nutrition *in vivo*. Furthermore, the interaction of integrin and insulin signaling is critical in determining the scope and severity of insulin resistance.

Acknowledgments

This work was supported by National Institutes of Health grants R37 DK050277 to DHW, R01 DK054902 to DHW, U24 DK059637 to DHW, R01 DK095761 to AP, and Veterans Affairs Merit Reviews 1I01BX002025-01 to AP. This work was also supported by DK20593 (the Diabetes Research and Training Center) and the Molecular Endocrinology Training Program at Vanderbilt. We would like to thank the Vanderbilt Mouse Metabolic Phenotyping Center Lipid Core for performing the liver DAG analysis and the Vanderbilt Mouse Metabolic Phenotyping Center Pathology Core for oil red o staining.

Chapter IV

INTEGRIN-LINKED KINASE IS A MAJOR CONTRIBUTOR TO HEPATIC INSULIN RESISTANCE IN HIGH FAT FED MICE

Aims

The results from Chapter III demonstrate that integrin α1 protein expression is upregulated in hepatocytes with HF feeding and this exerts a protective effect against the deleterious effects of a HF diet. The goal of Chapter IV was to determine whether integrin α1β1 signaling through integrin-linked kinase (ILK) protects against the development of hepatic insulin resistance in high fat (HF) fed mice. In this chapter, mice with a hepatocyte-specific deletion of ILK were generated and the metabolic effects of ILK deletion were assessed in both chow and HF-fed mice. In this Chapter, I hypothesize that the hepatocyte-specific deletion of ILK would impair hepatic insulin action in HF-fed mice.

Introduction

The prevalence of metabolic syndrome and Type 2 diabetes (T2D) have increased dramatically in recent years (195). Insulin resistance is a hallmark of metabolic syndrome and it precedes the development of T2D (1,2). The liver is integral to maintaining whole-body glucose homeostasis. Under normal conditions, insulin suppresses hepatic glucose production. In the insulin resistant state, insulin fails to suppress hepatic glucose production resulting in hyperglycemia. In addition to maintaining glucose homeostasis, insulin also promotes hepatic triglyceride (TG) synthesis and storage within the liver during nutrient overload. This results in increased hepatic lipid accumulation, liver damage and increases in extracellular matrix (ECM) proteins such as collagen (32,51,175).

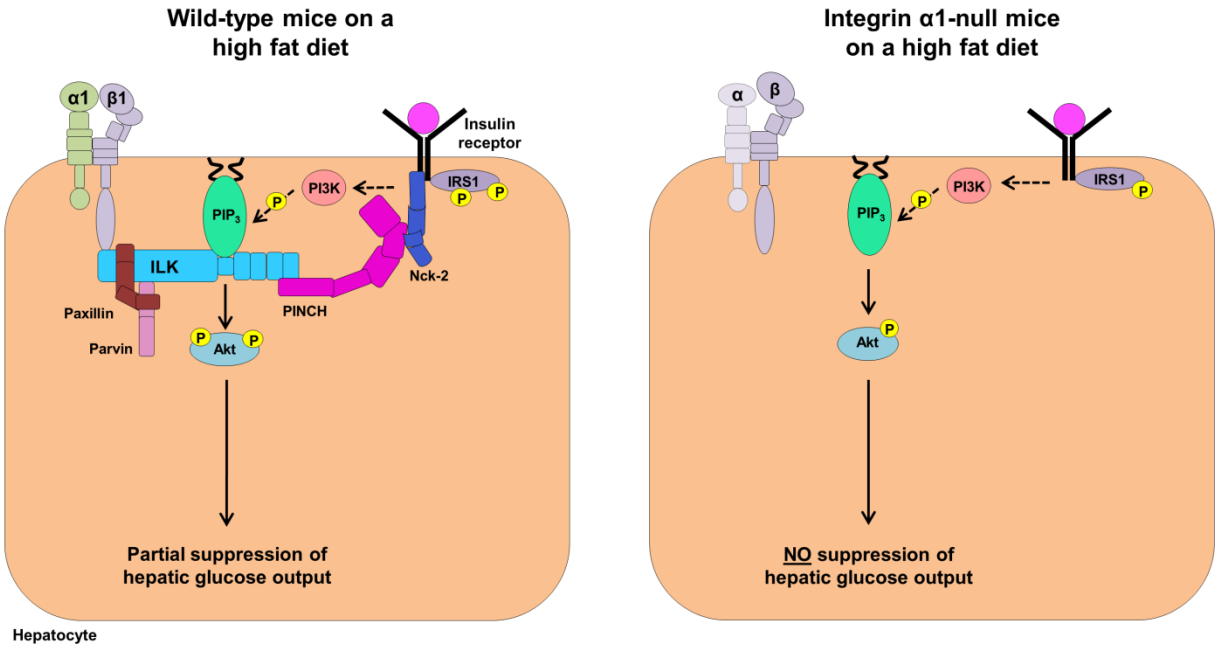

Figure 4.1 – Scheme of the hypothesis presented in Chapter IV. In high fat fed wild-type mice, insulin binds to the insulin receptor and the combination of both integrin and insulin signaling, stimulates the phosphorylation of IRS1 and Akt through integrin-linked kinase (ILK). This results in the partial suppression of hepatic glucose output during an insulin clamp. In high fat fed integrin α1-null mice, there is no signal transduction through either integrin α1β1 or ILK. When insulin binds its receptor this leads to the partial phosphorylation of IRS1 and Akt and results in no suppression of hepatic glucose output during the insulin clamp.

Integrins provide physical links to the ECM and transmit signals to the intracellular space through protein-protein interactions and signaling events (62). They lack enzymatic activity; therefore signal transduction by integrins occurs through the recruitment of signaling and/or adaptor proteins to their cytoplasmic tails (127). One such protein is integrin-linked kinase (ILK). ILK is a highly conserved intracellular scaffolding protein located at focal adhesions. It interacts with the β1, β2 and β3-integrin cytoplasmic domains and numerous cytoskeleton-associated proteins such as actin. Interestingly, ILK was originally identified as a kinase due to the significant sequence homology of the C-terminus to other Ser/Thr protein kinases (129). Since then, several lines of evidence have confirmed that ILK does not possess an active kinase domain and it is now classified as a *bona fide* pseudokinase (130,131). The pseudokinase domain of ILK is an essential domain for the recruitment of several adaptor proteins and signaling molecules including proteins involved in insulin action such as PKB/Akt, PDK1 and GSK-3β. Therefore although ILK lacks intrinsic kinase activity, it has been implicated in the regulation of numerous intracellular growth factor signaling cascades (135-137).

ILK is a major mediator of integrin signaling and is a key regulator of ECM-cell interactions. Extensive research has been conducted on ILK signaling and function in tissue culture cell systems (127,196,197). However few studies have focused on the role of ILK in the liver and even fewer have focused on the role of hepatic ILK *in vivo*. ILK protein expression is increased in a rodent model of liver fibrosis (158). ILK has been shown to be involved in the regulation of matrix-induced hepatocyte differentiation *in vitro* and *in vivo* (159). Studies in mice have described a role for ILK in the regulation of liver ECM response to liver injury (159,198-200). The genetic deletion of ILK from hepatocytes results in enhanced liver regeneration (198). ILK expression is upregulated during liver wound healing and has been shown to be involved in

the fibrotic response to liver injury. Collectively, these studies show that the interaction between hepatocytes and the ECM through ILK are critical for the liver regeneration and differentiation. Nonetheless, to date, no studies have investigated the role of ILK in the context of hepatic metabolic derangements that occurs as a result of HF feeding.

Hepatic insulin resistance is associated with increased collagen. Integrin α1β1 is the only collagen binding integrin shown to be expressed on the hepatocyte. The results presented in Chapter III show that the whole-body deletion of integrin α1 leads to severe hepatic insulin resistance in mice fed a HF diet compared to controls. Integrins lack intrinsic catalytic activity therefore they are reliant on the recruitment of signaling and/or adaptor proteins to their cytoplasmic tails to facilitate signal transduction. Two main integrin signaling proteins are the cytoplasmic tyrosine kinase, FAK, and the scaffolding protein, ILK. Results from Chapter III demonstrate that differences in FAK activation are not responsible for the observed phenotype in HF fed integrin α1-null mice. Thus it was hypothesized that integrin α1β1 signals through ILK to protect against diet-induced hepatic insulin resistance (Figure 4.1).

To test this hypothesis, mice with a hepatocyte-specific deletion and their wild-type littermates on a C57BL/6J background were generated and placed on either a chow or HF diet. Insulin sensitivity was assessed using the hyperinsulinemic-euglycemic (insulin) clamp. Contrary to the original hypothesis, here we show that the deletion of hepatocyte ILK results in the complete restoration of hepatic insulin sensitivity in HF-fed mice. This was evidenced by full insulin-mediated suppression of hepatic glucose production during the insulin clamp, increased insulin signaling and greater insulin-mediated suppression of gluconeogenic gene expression. There was no difference in the chow-fed mice between genotypes. The improvement in hepatic insulin action in HF-fed mice was associated with decreased hepatic lipid accumulation and

increased mitochondrial glucose oxidation. In summary, hepatic ILK deletion has no effect on insulin action in lean mice, but sensitizes the liver to insulin during the challenge of HF feeding.

Experimental Design

The global deletion of ILK is embryonic lethal due to defects in F-actin organization and epiblast polarity (160). Thus, mice with a hepatocyte-specific deletion of integrin-linked kinase (ILK) were used to determine the role of ILK in the regulation of hepatic insulin action in high fat (HF) fed mice. Mice carrying an ILK allele flanked by loxP sites ($ILK^{lox/lox}$, kindly provided by Dr. Roy Zent) (161) were crossed to transgenic mice expressing Cre recombinase under the control of the albumin (Alb) promoter (purchased from Jackson Laboratory) to generate $ILK^{lox/lox}$Alb*cre* mice and wild-type littermates, $ILK^{lox/lox}$ mice. Mice were fed either a standard chow diet (5.5% fat by weight; 5001 Purina Laboratory Rodent Diet) or HF diet (60% kcal from fat; F3282 BioServ) for 16 weeks. All studies were performed at 19 weeks of age. Insulin action was assessed using the insulin clamp combined with tracer techniques to determine sites of insulin resistance. See Chapter II for detailed methods.

Results

Components of the ILK-PINCH-parvin (IPP) complex are differentially expressed in hepatocytes with HF feeding

HF-feeding can differentially regulate protein expression in hepatocytes. To determine whether the expression of different components of the IPP complex are effected by HF-feeding, western blot analysis was used to determine ILK, PINCH and α-parvin protein expression in

hepatocytes isolated from chow and HF-fed mice. The results from this study show that ILK protein expression is decreased and PINCH and α-parvin protein expression was increased in hepatocytes isolated from HF-fed mice compared to chow-fed mice (Figure 4.2).

Adaptations to the genetic deletion of ILK from hepatocytes

Mice expressing Cre-recombinase under the Albumin promoter (purchased from Jackson Laboratory) were crossed with $ILK^{lox/lox}$ mice to generate mice with a hepatocyte specific deletion of ILK ($ILK^{lox/lox}$Alb*cre*) and wild-type littermates, $ILK^{lox/lox}$ mice (161). Livers were perfused with collagenase to isolate liver cells and differential centrifugation was used to separate hepatocytes from nonparenchymal cells. The deletion of ILK in hepatocytes was confirmed in $ILK^{lox/lox}$Alb*cre* mice by performing western blot analysis (Figure 4.3B). ILK was highly expressed in whole liver lysate and in the nonparenchymal cellular fraction (Figure 4.3A and C). This is consistent with another study confirming the high expression of ILK in other cell types in the liver including endothelial cells, Kupffer cells, stellate cells and biliary cells (201).
To determine the role of ILK in hepatic insulin action *in vivo*, $ILK^{lox/lox}$ and $ILK^{lox/lox}$Alb*cre* mice were placed on either a chow or HF diet. HF feeding increased body weight and adiposity (Table 4.1). There were no differences in body weight, adiposity or lean mass at 19 weeks of age between the genotypes on either a chow or HF diet.

Hepatic insulin action is improved in HF $ILK^{lox/lox}$Albcre mice

Insulin action was assessed in $ILK^{lox/lox}$ and $ILK^{lox/lox}$Alb*cre* mice on both a chow and HF diet using the hyperinsulinemic-euglycemic (insulin) clamp. During the insulin clamp, blood glucose was maintained between 130-140 mg/dL (Figure 4.4A and C). There was no difference

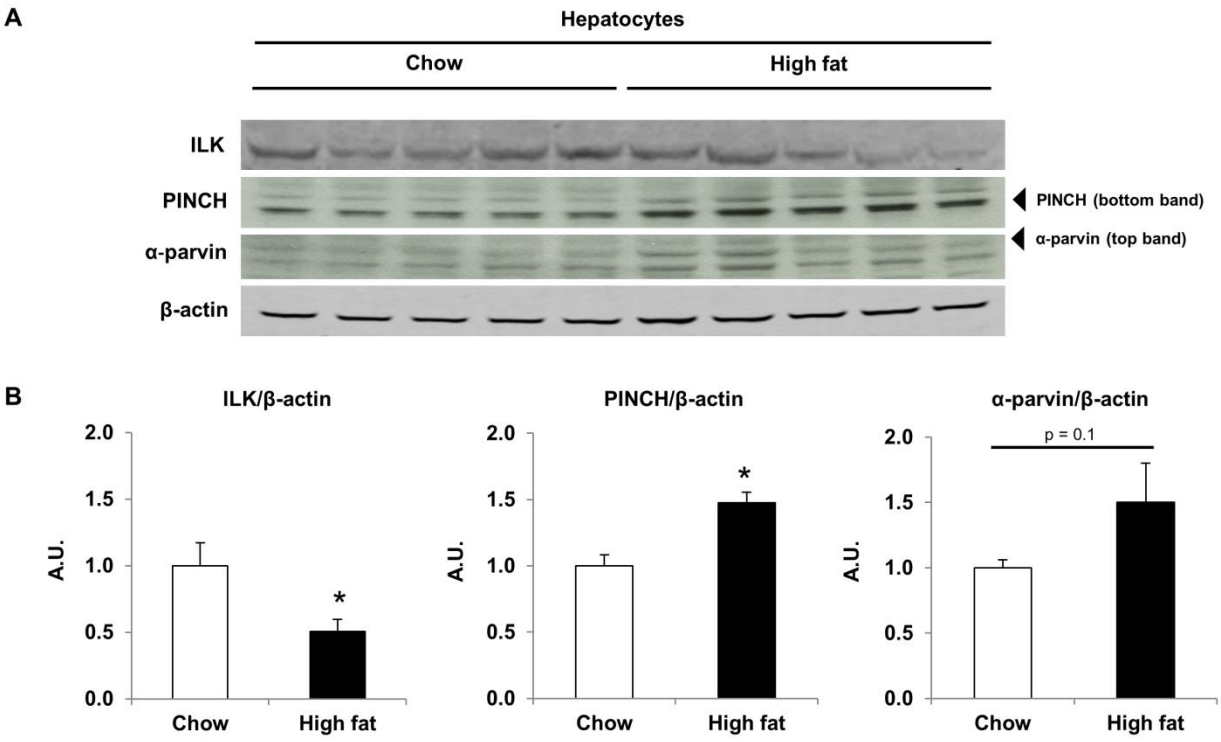

Figure 4.2 – Components of the Integrin-linked kinase (ILK)-PINCH-Parvin (IPP) complex are differentially expressed in hepatocytes isolated from high fat fed mice. (A) Western blot analysis in isolated hepatocytes. (B) Quantitative analysis of data from A. Integrated intensities were obtained by the Odyssey and Image J software. Protein expression was normalized to β-actin. Data are represented as means ± SEM; n = 5/group. *$p < 0.05$ chow vs. high fat fed.

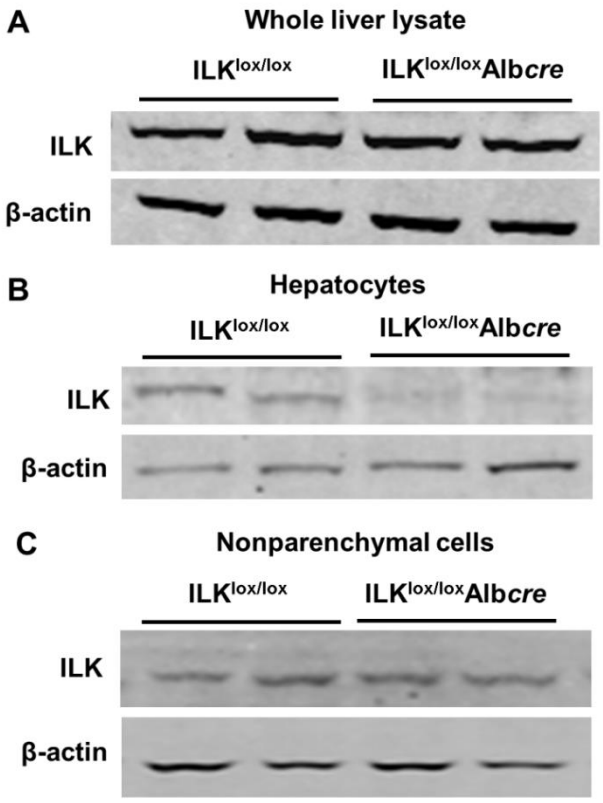

Figure 4.3 – Integrin-linked kinase (ILK) is absent in hepatocytes isolated from ILK$^{lox/lox}$Alb*cre* mice. Western blot analysis for ILK protein expression in (A) whole liver lysate, (B) hepatocytes and (C) nonparenchymal cells isolated from ILK$^{lox/lox}$ and ILK$^{lox/lox}$Alb*cre* mice.

in the glucose infusion rate (GIR), endoR_a or glucose utilization (R_d) (Figure 4.5A, B and C) during the insulin clamp between the chow fed ILK$^{lox/lox}$ and chow fed ILK$^{lox/lox}$Alb*cre* mice. The GIR was increased in HF-fed ILK$^{lox/lox}$Alb*cre* mice by 50% compared to HF-fed ILK$^{lox/lox}$ mice (Figure 4.4D). Basal endogenous glucose production (endoR_a) was not different between genotypes (Figure 4.5A and D). Suppression of endo R_a during the insulin clamp was attenuated in ILK$^{lox/lox}$ mice by the HF diet; while suppression of endo R_a was fully restored in ILK$^{lox/lox}$Alb*cre* mice demonstrating complete restoration of hepatic insulin sensitivity (Figure 4.5D). There was no difference in R_d during the insulin clamp (Figure 4.5B and E). Basal 5-h fasted plasma insulin values were not different between the genotypes and plasma insulin was raised during the insulin clamp (Figure 4.5C and F).

ILK has been shown to interact with several modulators of the insulin signaling cascade such as Akt (202). To determine whether the hepatocyte specific deletion of ILK affected insulin signaling, several markers of insulin signaling were assessed in basal 5-h fasted and insulin stimulated livers from HF-fed ILK$^{lox/lox}$ and ILK$^{lox/lox}$Alb*cre* mice using western blot analysis (Figure 4.6A, B, D and E). IRS1, Akt and FAK phosphorylation were all increased in the liver with an insulin stimulus regardless of genotype. There was a slight increase in the phosphorylation of IRS1 at Y612 in the basal 5-h fasted ILK$^{lox/lox}$Alb*cre* mice (Figure 4.6A and D). Consistent with the hepatic glucose flux measurements, Akt phosphorylation at S473 was elevated in the HF-fed ILK$^{lox/lox}$Alb*cre* mice with an insulin stimulus (Figure 4.6A and C). To further determine the role of ILK in insulin signaling within the liver, an antibody microarray was used to identify several proteins that were upregulated or downregulated in insulin-stimulated livers from HF-fed ILK$^{lox/lox}$Alb*cre* mice compared to HF-fed ILK$^{lox/lox}$ mice. These proteins are represented in Table 4.2. The upregulated proteins in the livers from HF-fed

Table 4.1
Metabolic characteristics of mice with a hepatocyte-specific deletion of ILK ($ILK^{lox/lox}$Alb*cre*) and wild-type mice ($ILK^{lox/lox}$) fed either a chow or high fat diet.

	Chow		High Fat	
	$ILK^{lox/lox}$	$ILK^{lox/lox}$Alb*cre*	$ILK^{lox/lox}$	$ILK^{lox/lox}$Alb*cre*
N	8	8	5	6
Weight (g)	29.5 ± 1.2	29.7 ± 1.1	41.3 ± 2.1*	38.0 ± 1.8†
Adiposity (%)	10.6 ± 1.8	7.4 ± 0.42	31.8 ± 2.0	32.3 ± 3.1
Absolute lean mass (g)	20.8 ± 0.7	22.6 ± 0.6	26.0 ± 0.9	24.1 ± 0.9
Age at study (wks)	19	19	19	19
Duration on diet (wks)	16	16	16	16
Blood glucose (mg/dL)				
Basal	136 ± 4	136 ± 3	146 ± 15	129 ± 7
Clamp	135 ± 2	140 ± 4	135 ± 2	130 ± 4

Fasting and insulin clamp characteristics of wild-type ($ILK^{lox/lox}$) and $ILK^{lox/lox}$Alb*cre* mice fed either a chow or high fat diet. Body weight, body composition and fasting blood glucose were determined in basal 5-h fasted mice. Data are represented as means ± SEM. *$p < 0.05$ compared to chow fed $ILK^{lox/lox}$ mice. †$p < 0.05$ compared to chow fed $ILK^{lox/lox}$Alb*cre* mice.

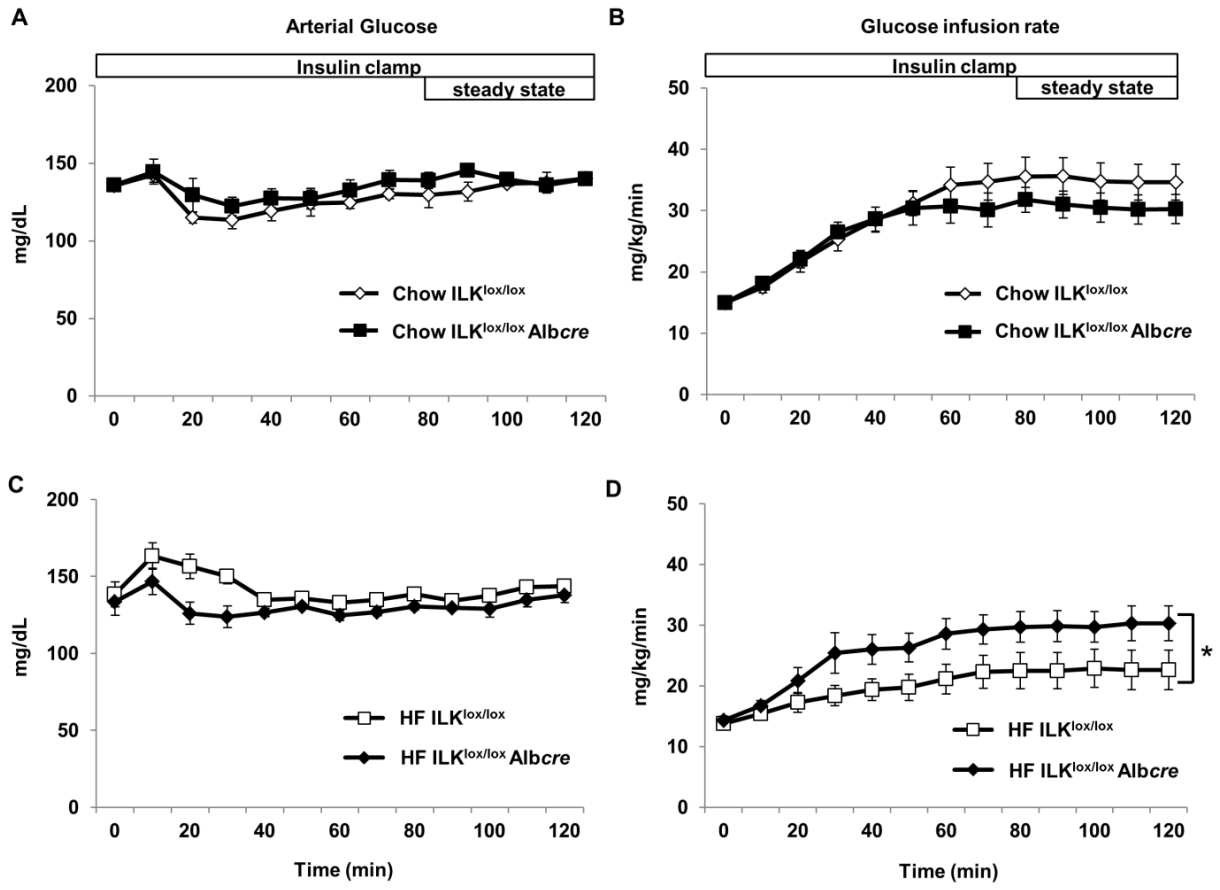

Figure 4.4 – Whole-body insulin sensitivity is greater in high fat (HF) fed ILK$^{lox/lox}$Alb*cre* mice compared to controls. Arterial glucose (A and C) and the glucose infusion rate (B and D) were measured during the hyperinsulinemic-euglycemic (insulin) clamp (n = 5-8/group). Mice were fasted for 5-h prior to the start of the insulin clamp. Blood glucose was maintained between 130-140 mg/dL during the steady state (80-120 min). Glucose (50%) was infused to maintain euglycemia. Data are represented as means ± SEM; n = 5-6/group. *$p < 0.1$.

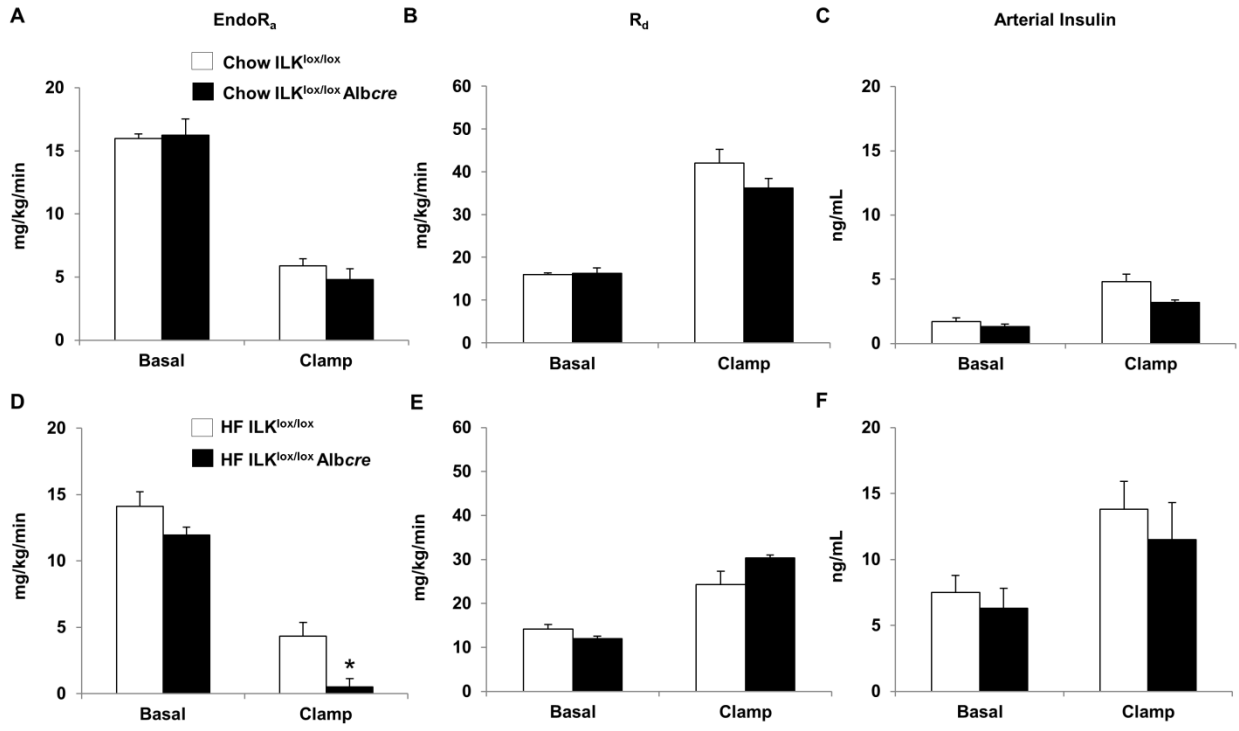

Figure 4.5 – Hepatic insulin sensitivity is improved in HF-fed ILK$^{lox/lox}$Alb*cre* mice. Endogenous glucose production (endoR_a)(A and D) and whole-body disappearance (R_d)(B and E) were determined during the steady state period of the insulin clamp (n = 5-8/group). Arterial insulin (C and F) was determined in the basal 5-h fasted state and during the insulin clamp. Data are represented at means ± SEM. *$p < 0.05$ compared to HF ILK$^{lox/lox}$Alb*cre*.

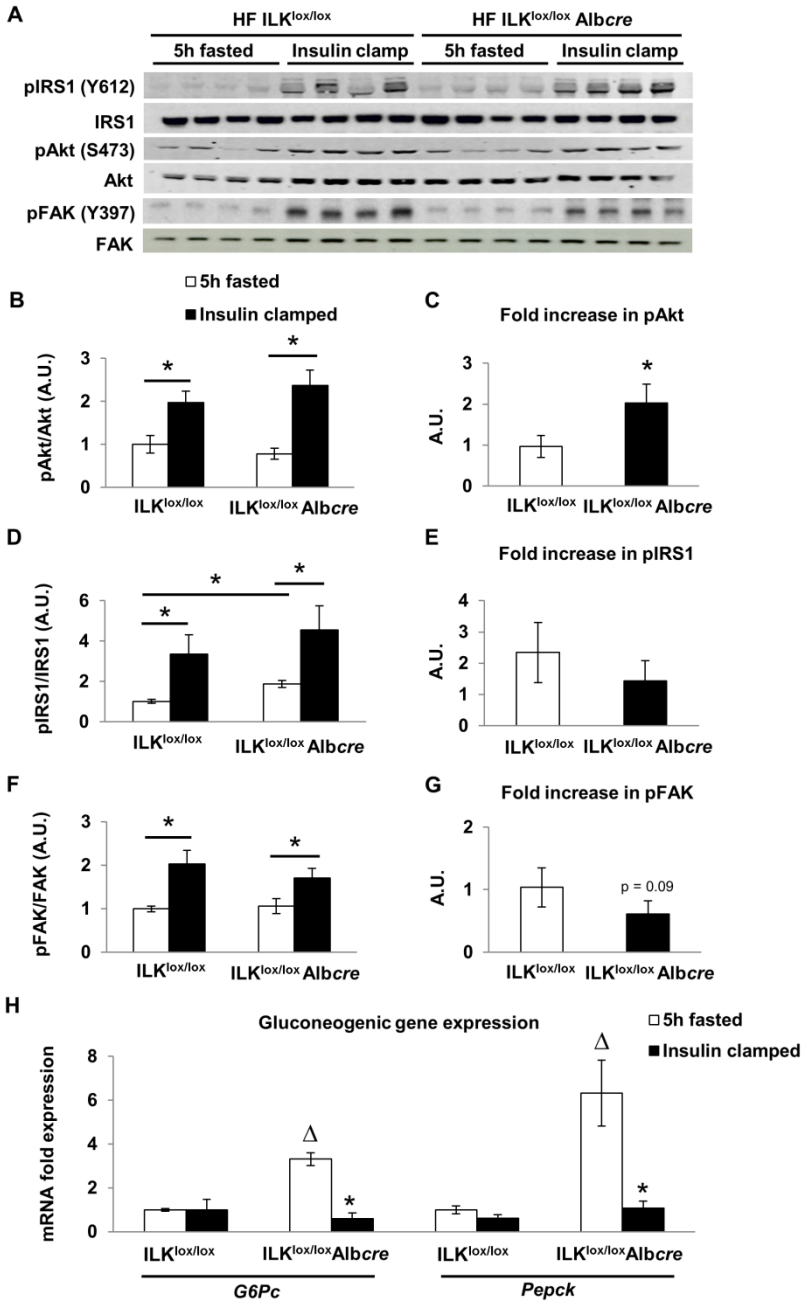

Figure 4.6 – Hepatic insulin action is increased in high fat (HF) fed ILK$^{lox/lox}$Alb*cre* mice. Western blot analysis was performed on liver homogenates from basal 5-h fasted and 5-h fasted insulin clamped mice (A)((n = 4/group). (B, D and E) Quantitative analysis of western blots. (C, E and G) Fold increase of insulin-stimulated activation was calculated relative to wild-type (ILK$^{lox/lox}$) mice. Integrated intensities were obtained by the odyssey and Image J software. (F) mRNA was extracted from both basal 5-h fasted and 5-h fasted insulin clamped livers. qPCR was performed to determine gene expression of the gluconeogenic genes *G6pc* and *Pepck*. Data are represented at means ± SEM. *$p < 0.05$. $^{\Delta}p < 0.05$ compared to 5-h fasted HF ILK$^{lox/lox}$ mice.

Table 4.2

Protein microarray data from high fat fed ILK$^{lox/lox}$ and ILK$^{lox/lox}$Alb*cre* mice.

Target Protein Name	Phospho Site	Full Target Protein Name	Z-ratio
Rb	S807	Retinoblastoma-associated protein 1	3.79
S6K	S424	p70 ribosomal protein-serine S6 kinase	2.46
Fyn	Pan-specific	Fyn proto-oncogene-encoded protein-tyrosine kinase	2.39
PKBb (Akt2)	Pan-specific	Protein-serine kinase B beta	2.37
TBK1	Pan-specific	Serine/threonine-protein kinase TBK1	2.35
Shc1	Y349	SH2 domain-containing transforming protein 1	2.16
PKBb (Akt2)	Pan-specific	Protein-serine kinase B beta	2.15
Syk	Y323	Spleen protein-tyrosine kinase	2.14
S6K	S411	p70 ribosomal protein-serine S6 kinase	2.14
MST1	Pan-specific	Mammalian STE20-like protein-serine kinase 1 (KRS2)	2.12
Myc	S373	Myc proto-oncogene protein	2.08
PKCh	Pan-specific	Protein kinase C eta type	1.97
Gab1	Y627	GRB2-associated binder 1	1.94
Raf1	Pan-specific	Raf1 proto-oncogene-encoded protein-serine kinase	1.92
JNK1/2/3	Pan-specific	Jun N-terminus protein-serine kinase (SAPK) 1/2/3	1.83
HDAC5	S498	Histone deacetylase 5	1.83
GSK3a	Pan-specific	Glycogen synthase-serine kinase 3 alpha	1.80
MEK7 (MAP2K7)	Pan-specific	MAPK/ERK protein-serine kinase 7 (MKK7)	1.77
DDIT3(CHOP)	Pan-specific	DNA damage-inducible transcript 3 protein	1.77
PAK2	Pan-specific	p21-activated kinase 2 (gamma) (serine/threonine-protein kinase 2)	1.75
Smac/DIABLO	Pan-specific	Second mitochondria-derived activator of caspase	1.71
IkBa	Pan-specific	Inhibitor of NF-kappa-B alpha (MAD3)	1.69
GroEL	Pan-specific	GroEL homolog (may correspond to Hsp60)	1.68
FKHR	S256	Forkhead box protein O1	1.64
MEK5 (MAP2K5)	Pan-specific	MAPK/ERK protein-serine kinase 5 (MKK5)	1.60
JAK1	Pan-specific	Janus protein-tyrosine kinase 1	1.57
GATA1	S142	Erythroid transcription factor	1.56
JNK2 (MAPK9)	Pan-specific	Jun N-terminus protein-serine kinase (SAPK) 2	1.53
Tubulin	Pan-specific	Tubulin	-1.51
MEK4 (MAP2K4)	S257+T261	MAPK/ERK protein-serine kinase 4 (MKK4)	-1.52
Bax	Pan-specific	Apoptosis regulator Bcl2-associated X protein	-1.53
4G10	pTyr	4G10	-1.58
Catenin b1	Pan-specific	Catenin (cadherin-associated protein) beta 1	-1.63
PKA Cb	S339	cAMP-dependent protein-serine kinase catalytic subunit beta	-1.65
MLK3	T277+S281	Mixed-lineage protein-serine kinase 3	-1.73
MEK3/6 (MAP2K3/6)	S218/S207	MAPK/ERK protein-serine kinase 3/6 (MKK3/6)	-1.74
BLNK	Y84	B-cell linker protein	-1.85
WIP1	Pan-specific	Protein phosphatase 1D	-1.90
ATF2	T69 + T71	Activating transcription factor 2 (CRE-BP1)	-2.58
Paxillin 1	Y118	Paxillin 1	-3.01

Protein and phosphoprotein expression in livers from 5-h fasted high fat fed ILK$^{lox/lox}$Alb*cre* mice compared to ILK$^{lox/lox}$ mice. A Z ratio of ± 1.2 to 1.5 is considered significant.

ILK$^{lox/lox}$Alb*cre* mice included Akt2, TBK1, and GSK3a as well as several proteins in the MAPK signaling cascade such as Raf1, MAP2K7, MAP2K5 and MAPK9. In support of the improved insulin sensitivity in HF-fed ILK$^{lox/lox}$Alb*cre* mice, FoxO1 phosphorylation at S256 was increased.

To determine the effect of ILK on hepatic gluconeogenic gene expression in the HF-fed state, qPCR was used to determine gene expression of glucose-6-phosphatase (*G6pc*) and phosphoenolpyruvate carboxylase (*Pepck*) in the livers from basal 5-h fasted and insulin clamped mice (Figure 4.6H). *G6pc* and *Pepck* gene expression were increased in 5-h fasted HF-fed ILK$^{lox/lox}$Alb*cre* mice. There was no suppression of either *G6pc* or *Pepck* gene expression in the HF-fed ILK$^{lox/lox}$ mice. In contrast, and in support of the insulin clamp data and Akt signaling, *G6pc* and *Pepck* expression were greatly suppressed with an insulin stimulus in HF-fed ILK$^{lox/lox}$Alb*cre* mice.

Liver glycogen was determined in basal 5-h fasted and insulin clamped livers from HF-fed ILK$^{lox/lox}$ and ILK$^{lox/lox}$Alb*cre* mice. Fasting glycogen levels were increased in HF-fed ILK$^{lox/lox}$Alb*cre* mice (Figure 4.7A). Insulin stimulated the accumulation of glycogen in the livers of insulin clamped HF-fed ILK$^{lox/lox}$ mice; however this accumulation was blunted in the HF-fed ILK$^{lox/lox}$Alb*cre* mice. There was no difference in the glycogen synthetic rate between the genotypes during the insulin clamp (Figure 4.7B). Mitochondrial dysfunction is associated with the development of diet-induced hepatic insulin resistance (203). To test the hypothesis that mitochondrial function was improved in the HF-fed ILK$^{lox/lox}$Alb*cre* mice, high-resolution respirometry was used to determine mitochondrial function in isolated mitochondria (Figure 4.8A and B). State 2 respiration with the substrates glutamate and malate was not different between the genotypes. Consistent with our hypothesis, glutamate/malate stimulated state 3

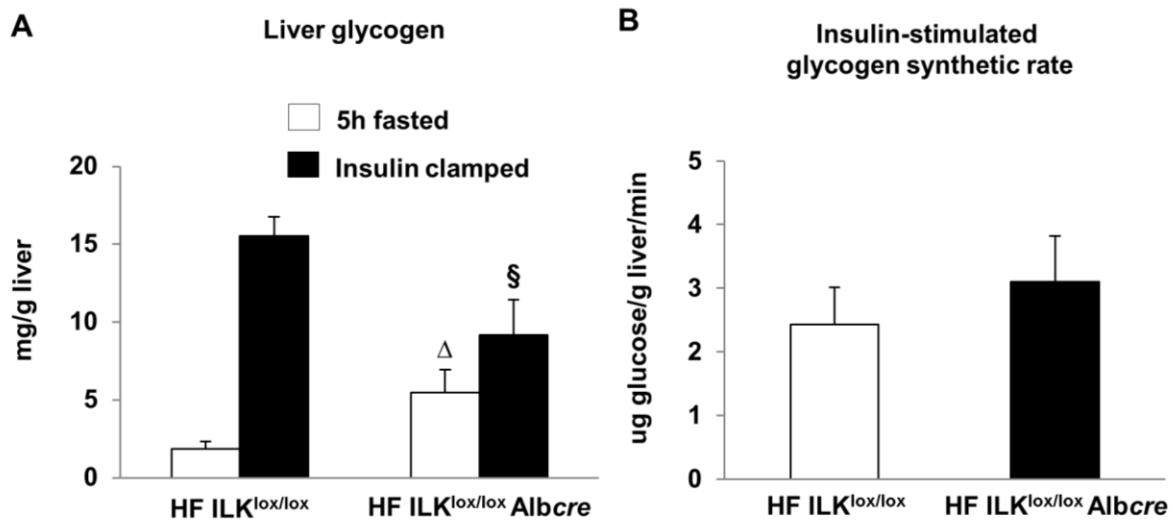

Figure 4.7 – Effect of hepatocyte ILK deletion on liver glycogen metabolism. Liver glycogen (A) was assessed in livers from basal 5-h fasted mice and in livers excised immediately after the insulin clamp. Liver insulin-stimulated glycogen synthetic rate (B) was determined in livers excised immediately after the insulin clamp. Data are represented at means ± SEM. $^{\Delta}p < 0.05$ compared to 5-h fasted HF ILK$^{lox/lox}$ mice. $^{\S}p < 0.05$ compared to insulin clamped ILK$^{lox/lox}$ mice.

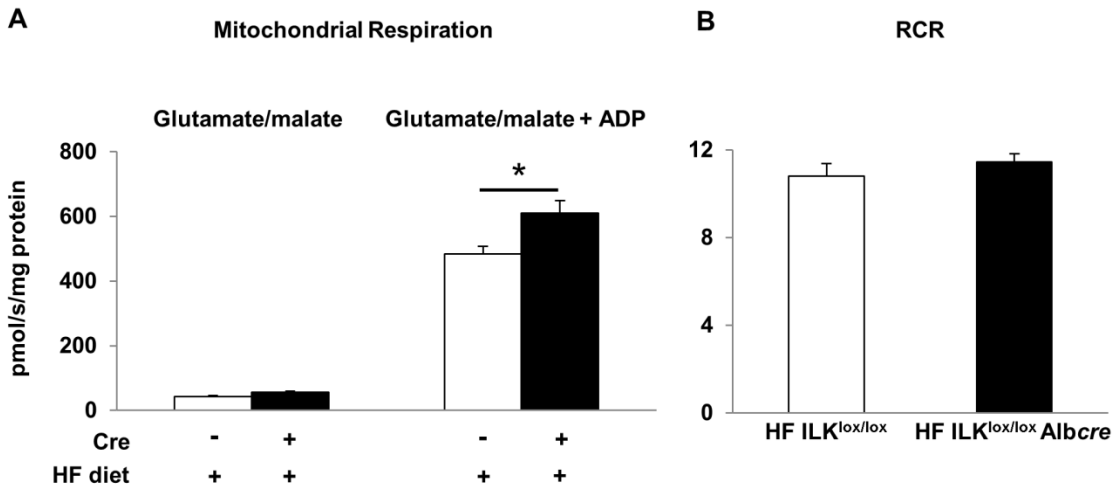

Figure 4.8 – Complex I supported mitochondrial respiration is higher in high fat (HF) fed ILK$^{lox/lox}$Alb*cre* mice. High-resolution respirometry (A) was performed on mitochondria isolated from livers of 5-h fasted mice. (B) The respiratory control ratio (RCR) was determined as state 3 /state 2 respiration. Data are represented at means ± SEM. *$p < 0.05$.

respiration was increased in ILK$^{lox/lox}$Alb*cre* mice. There was no difference in the respiratory control ratio (RCR) between the groups (Figure 4.8B).

Hepatic triglyceride content was decreased in mice with a genetic deletion of ILK

HF feeding leads to the development of fatty liver and hepatic insulin resistance (51). To test the hypothesis that improved hepatic insulin action in HF-fed ILK$^{lox/lox}$Alb*cre* mice was associated with decreased triglyceride (TG) accumulation; several markers of lipid metabolism were measured. Hepatic triglyceride (TG) content was decreased in livers from basal 5-h fasted HF-fed ILK$^{lox/lox}$Alb*cre* mice (Figure 4.9A). There was no difference in circulating basal 5-h fasted plasma TGs (Figure 4.9B). Lipogenic gene expression was determined using qPCR (Figure 4.8C). Despite decreased TG accumulation, gene expression for the lipogenic genes *Srebp-1c*, *Fas*, *Acc1*, *Dgat1* and *Dgat2* were increased. Circulating free fatty acids (FFAs) are the main substrate for the synthesis and accumulation of hepatic TGs (30). In support of decreased TG content, circulating FFAs were decreased in HF-fed ILK$^{lox/lox}$Alb*cre* mice in both the basal 5-h fasted and insulin clamped states (Figure 4.9D). There was no difference in the % suppression between the genotypes. To determine the contribution of mitochondrial fatty acid supported respiration to the observed decrease in hepatic TGs, mitochondrial function was determined in isolated mitochondria using the fatty acid substrates palmitoyl-carnitine and malate (Figure 4.9E). There was no difference in either state 2 or state 3 respiration between the genotypes or RCR (Figure 4.9F).

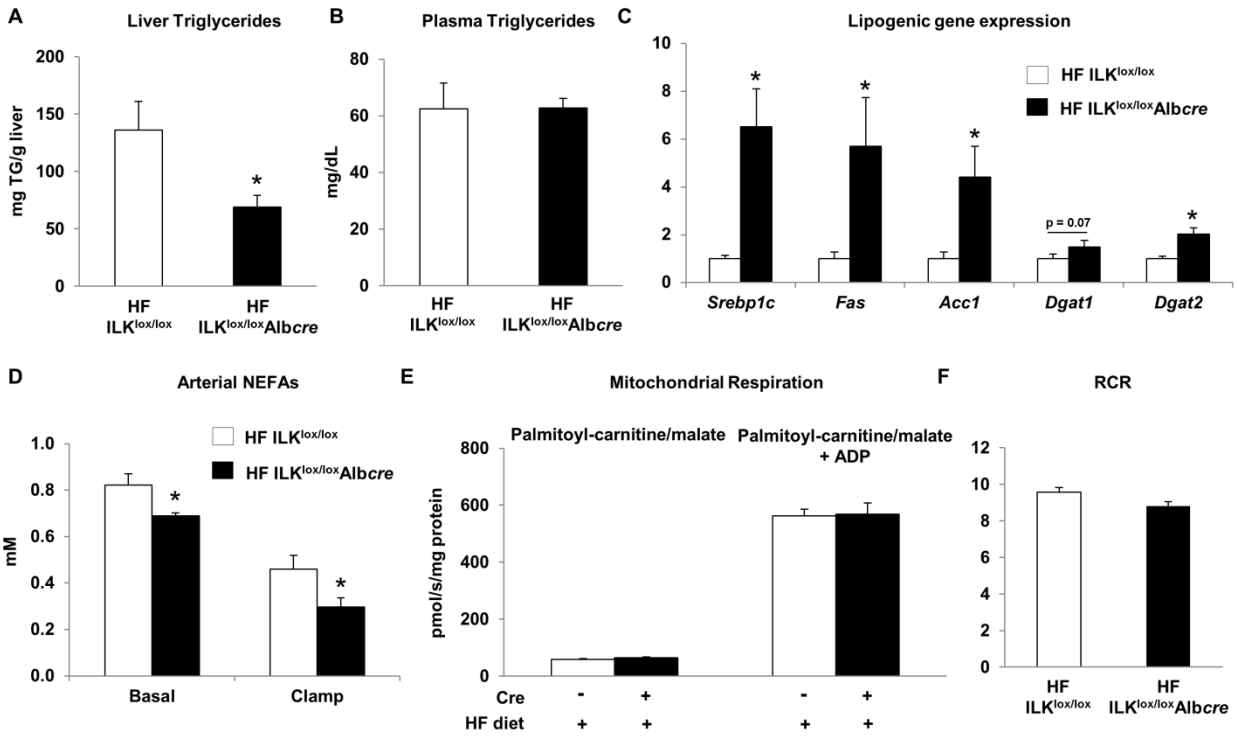

Figure 4.9 – Integrin-linked kinase (ILK) promotes hepatic lipid accumulation in high fat (HF) fed mice. Liver triglyceride content (A) was determined in livers from 5-h fasted mice. (B) Circulating plasma triglycerides in basal 5-h fasted mice. High-resolution respirometry (D) was performed on isolated mitochondria from livers of 5-h fasted mice. (C) mRNA was extracted from basal 5-h fasted livers and qPCR was used to determine gene expression of several lipogenic genes. (D) Arterial non-esterified free fatty acids (NEFAs) in basal 5-h fasted and insulin clamped mice. High-resolution respirometry (E) and respiratory control ratio (RCR) (F) from mitochondria isolated from livers of 5-h fasted mice. Data are represented at means ± SEM. *$p < 0.05$ compared to HF ILK$^{lox/lox}$Alb*cre*.

Discussion

Hepatic insulin resistance is associated with increased collagen. Integrin α1β1 is the only collagen binding integrin expressed on the hepatocyte. Integrins lack intrinsic catalytic activity therefore they rely on associated kinases and scaffolding proteins to transduce signals from the ECM to the inside of the cell. This suggests that the ECM may contribute to the pathogenesis of hepatic insulin resistance through integrin signaling.

The goal of this study was to determine whether integrin α1β1 signals through ILK to promote hepatic insulin action in HF fed mice. ILK is a major integrin signaling protein and facilitates communication from the ECM to the intracellular space. To eliminate this key effector of ECM-cell communication, we generated mice with a hepatocyte-specific deletion ($ILK^{lox/lox}$Alb*cre* mice) and their wild-type littermates ($ILK^{lox/lox}$ mice) on a C57BL/6J background. The mice were fed either a chow or HF diet and hepatic glucose and lipid metabolism were assessed *in vivo*. Contrary to our hypothesis, here we show for the first time that the selective deletion of hepatic ILK *in vivo* results in the complete restoration of hepatic insulin sensitivity in HF-fed, but not chow fed, C57BL/6J mice. The increase in insulin action in HF-fed mice corresponds to changes in the activation of key signaling pathways, a greater capacity for hepatic mitochondrial glucose oxidation and decreased hepatic lipid accumulation.

Hepatocytes are the most abundant cell type in the liver and a major site of hepatic insulin action and lipid metabolism (28). Thus, $ILK^{lox/lox}$Alb*cre* mice were generated to determine the metabolic effects of hepatic ILK deletion. Our data illustrate that ILK was selectively deleted from hepatocytes in the $ILK^{lox/lox}$Alb*cre* mice and not from the nonparenchymal cells of the liver. This occurred despite high expression of ILK protein in lysates prepared from the whole liver. The liver is composed of several different cell types

including stellate cells, Kupffer cells, and endothelial cells. This suggests that ILK is highly expressed in the nonparenchymal cells of the liver and may explain why ILK is still so highly expressed in lysates from whole livers. Our study is consistent with other studies reporting high expression of ILK in stellate cells and other hepatic cell types (158,201).

ILK protein expression was determined in hepatocytes isolated from chow and HF-fed mice. Here we show that ILK protein expression is decreased in hepatocytes isolated from HF-fed mice. In light of this finding, we propose that ILK protein expression is downregulated during times of over nutrition as mechanism to decrease integrin signaling and protect the hepatocyte against the deleterious effects of a HF-diet. The precise regulation of ILK expression is still unknown.

Hepatic insulin resistance is characterized by increased hepatic glucose output despite high levels of circulating insulin. In our studies, the hyperinsulinemic-euglycemic (insulin) clamp was used to assess insulin action to determine the role of ILK in hepatic insulin action *in vivo*. Here we show that the glucose infusion rate (GIR) was increased in HF-fed ILK$^{lox/lox}$Alb*cre* mice by 50% compared to HF-fed ILK$^{lox/lox}$ mice. There was no difference in the glucose infusion rate (GIR) or endoR_a in chow mice during the insulin clamp. In HF-fed mice, basal endogenous glucose production (endoR_a) was not different between genotypes. The insulin-mediated suppression of endo R_a during the insulin clamp was attenuated in ILK$^{lox/lox}$ mice by the HF diet, while suppression of endo R_a was fully restored in HF-fed ILK$^{lox/lox}$Alb*cre* mice. This demonstrates the complete restoration of hepatic insulin sensitivity in HF-fed ILK$^{lox/lox}$Alb*cre* mice. There was no difference in glucose utilization (R_d) during the insulin clamp indicating that the difference in GIR was solely attributed to differences in hepatic, and not peripheral, insulin action between the genotypes.

Mitochondrial dysfunction is a characteristic of the insulin resistant liver (203,204). In our study, we found that the increase in hepatic insulin sensitivity in HF-fed ILK$^{lox/lox}$Alb*cre* mice was associated with increased glutamate/malate stimulated state 3 respiration. Our data suggests that ILK decreases complex I based mitochondrial respiration in the presence of increased dietary lipids as a result of HF feeding. This is the first study to establish a role for ILK in the regulation of hepatic mitochondrial function.

ILK has been implicated in the regulation of both integrin and growth factor signaling (136,153,205). For some time, it was postulated that ILK was a Ser/Thr kinase capable of directly phosphorylating Akt and GSK3β (129,137). An original study showed that purified ILK from mammalian cell extracts resulted in Akt phosphorylation (137). The overexpression of ILK in 3T3 cells resulted in increased phosphorylation of Akt and GSK-3β while Akt Ser473 phosphorylation was diminished in cells transfected with kinase-deficient ILK (153). Moreover, the selective inhibition of ILK by siRNA reduced hepatic Akt phosphorylation in rats (158). Collectively, this led to the notion that ILK regulates Akt and GSK3β activation *in vitro* and *in vivo*. This has since been refuted. It is currently recognized that ILK is an adaptor protein that is part of a multiprotein complex that recruits kinases and promotes the phosphorylation of Akt and GSK3β through an indirect mechanism (136,205). However, no studies to date have addressed the role of ILK in the phosphorylation of hepatic Akt, or other key insulin signaling molecules such as IRS1, after a prolonged insulin stimulus *in vivo*. Here we show that there is no difference in the levels of Akt Ser473 phosphorylation between HF-fed ILK$^{lox/lox}$ and ILK$^{lox/lox}$Alb*cre* in the basal 5h fasted state. In support of the insulin clamp data, insulin-mediated phosphorylation of Akt Ser473 was enhanced in HF-fed ILK$^{lox/lox}$Alb*cre* mice. This finding is supported by a study

showing that treatment of ILK deficient cells with insulin resulted in the robust phosphorylation of Akt at Ser473 and Thr308 (160).

Focal adhesion kinase (FAK) is an integrin-associated cytoplasmic tyrosine kinase implicated in the regulation of hepatic insulin signaling (144,146,149). Thus we assessed FAK phosphorylation in livers from both basal 5h fasted and insulin clamped mice. Here we show that FAK Y397 phosphorylation is increased in the liver after an insulin clamp. This is consistent with other studies showing that insulin stimulates hepatic FAK phosphorylation (125,149).

Integrin engagement has been shown to stimulate IRS1 activation (142). In our studies we show that IRS1 phosphorylation was increased in the basal 5h fasted state in HF-fed $ILK^{lox/lox}$Alb*cre* mice compared to HF-fed $ILK^{lox/lox}$ mice. However, there was no difference in the fold increase in phosphorylated IRS1 between the genotypes. This indicates that the deletion of hepatic ILK improves insulin signaling downstream of IRS1 in insulin clamped livers. The increase in hepatic insulin signaling in HF-fed $ILK^{lox/lox}$Alb*cre* mice led to greater insulin-mediated suppression of the gluconeogenic genes *G6pc* and *Pepck*. Collectively, our data show that hepatocyte ILK deletion improves hepatic insulin action during the challenge of HF feeding.

Hepatic insulin resistance is associated with elevated hepatic lipid accumulation (51). Three days of HF feeding in mice results in a 3-fold increase in hepatic triglyceride (TG) accumulation and decreased suppression of hepatic glucose production during an insulin clamp (51). Here we show that hepatic TG accumulation is decreased in HF-fed $ILK^{lox/lox}$Alb*cre* mice compared to HF-fed $ILK^{lox/lox}$ mice. A large fraction of liver TGs are derived from circulating free fatty acids (FFAs) (30,37), thus we measured circulating FFAs in our study. In accordance with decreased TG accumulation, circulating FFAs were decreased in both the basal 5h fasted state and during the insulin clamp in the HF-fed $ILK^{lox/lox}$Alb*cre* mice compared to HF-fed

ILK$^{lox/lox}$ mice. There was no difference in the percent suppression with an insulin stimulus between the genotypes. It is important to note that the decrease in liver TGs in HF-fed ILK$^{lox/lox}$Alb*cre* mice occurred in the presence of increased gene expression for the lipogenic genes *Srebp1c*, *Fas, Acc1*, *Dgat1* and *Dgat2*. This is in accordance with the studies in Chapter III where we reported that hepatic TG accumulation is reduced in HF-fed integrin α1 null mice despite increased lipogenic gene expression. We propose this is attributed to a feedback mechanism that upregulates lipogenic pathways when hepatic lipid stores are low. Collectively, these studies show that ILK promotes hepatic lipid accumulation via decreased availability of circulating FFAs in HF-fed mice.

In summary, we demonstrate for the first time that hepatic ILK desensitizes the liver to insulin during the challenge of HF feeding and promotes hepatic lipid accumulation *in vivo* (Figure 4.10). The selective deletion of ILK from hepatocytes leads to a marked improvement in hepatic insulin action in HF-fed, but not chow fed, mice. This improvement was associated with increased insulin signaling, a greater capacity for hepatic mitochondrial glucose oxidation and decreased hepatic lipid accumulation. This study further emphasizes the importance of the ECM and integrin signaling in hepatic insulin action and lipid metabolism in HF-fed mice.

Acknowledgments

This work was supported by National Institutes of Health grants R37 DK050277 to DHW, R01 DK054902 to DHW, U24 DK059637 to DHW, R01 DK095761 to AP, and Veterans Affairs Merit Reviews 1I01BX002025-01 to AP. This work was also supported by DK20593 (the Diabetes Research and Training Center) and the Molecular Endocrinology Training Program at Vanderbilt. We would like to thank Dr. Roy Zent for generously providing the ILK floxed mice in addition to the PINCH and α-parvin antibodies for western blot analysis.

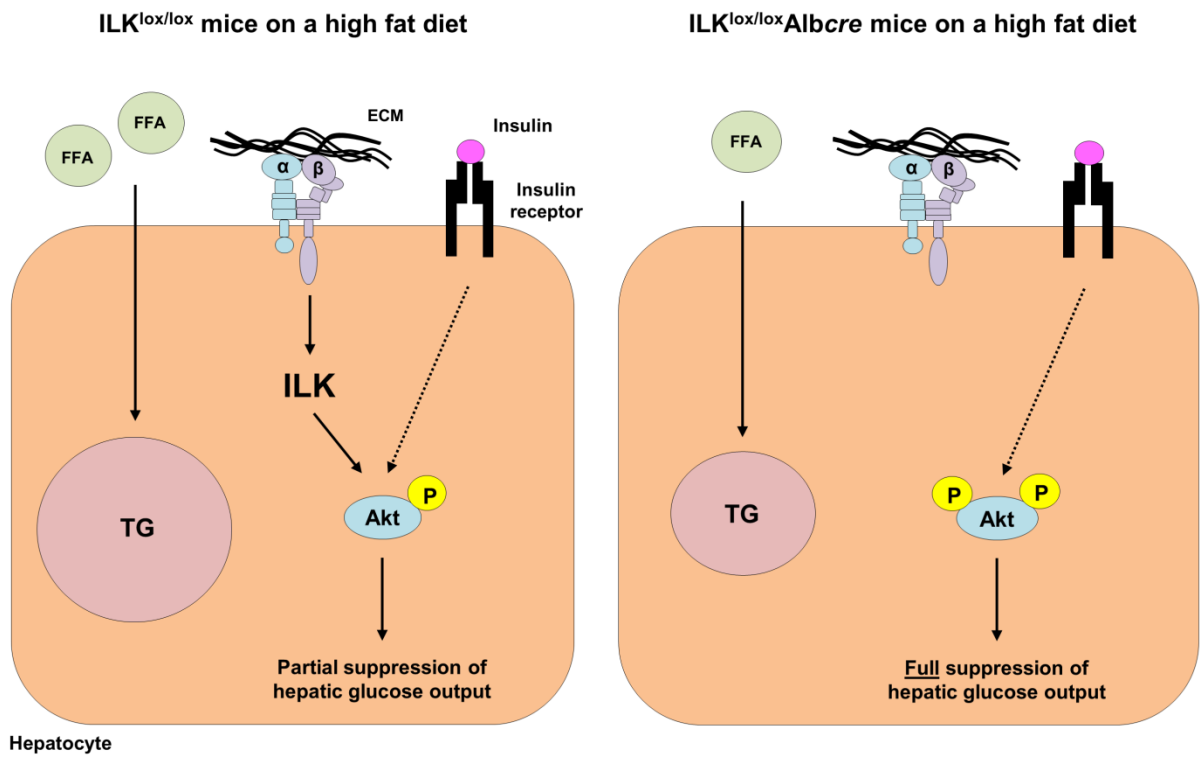

Figure 4.10 – Model whereby the hepatocyte-specific deletion of ILK facilitates insulin action and decreases lipid accumulation in the liver. Upon insulin stimulation, the combination of both insulin and integrin signaling through ILK leads to the phosphorylation and subsequent activation Akt. This results in the partial suppression of hepatic glucose output. Circulating free-fatty acids (FFAs) are taken up by the liver and utilized for the synthesis of triglycerides (TG). In contrast, when ILK is absent and insulin levels are high, the absence of integrin signaling through ILK leads to increased Akt activation. This results in the full suppression of hepatic glucose output. Circulating FFAs are lower and this results in decreased hepatic TG levels.

Chapter V

SUMMARY AND FUTURE DIRECTIONS

The data presented within the Dissertation provide the first demonstration that integrins contribute to the regulation of hepatic insulin action and lipid metabolism in HF fed mice. The hepatocellular mechanisms of insulin resistance and lipid accumulation in the diet-induced obese mouse model have been characterized. The studies described herein add to the present understanding of insulin resistance by bridging hepatocyte metabolism and the ECM through plasma membrane associated integrin receptors. In Chapter III, I show that the integrin α1 subunit is upregulated in hepatocytes during times of nutritional overload and this exerts a protective effect against the development of diet-induced hepatic insulin resistance while promoting lipid accumulation. In Chapter IV, I show that a downstream integrin signaling molecule, ILK, is also involved in the regulation of hepatic insulin action and lipid accumulation. The association between integrins and insulin signaling has not been well-studied. The studies in the Dissertation are amongst the first to demonstrate a mechanistic link between integrins and hepatic insulin action *in vivo*. The results from these studies open new avenues for investigation in a novel area of metabolic research and identify innovative therapeutic targets to treat the underlying insulin resistance associated with Type 2 diabetes.

The ECM is a dynamic structure that is constantly changing and remodeling during times of injury and repair (72). Results from these studies demonstrate that the liver ECM expands with HF feeding. This was evidenced by increased gene expression for several collagen chains in addition to increased hydroxyproline content in livers from HF fed mice compared to chow fed mice. The ECM communicates with cells through integrins. Integrins are unique as they

transduce signals from the ECM to the inside of the cell. Pathological states are associated with ECM remodeling and changes in integrin expression. The Dissertation studies are the first to describe changes in protein expression of an integrin and downstream integrin signaling proteins in hepatocytes from wild-type C57BL/6J HF-fed mice compared to chow-fed littermates. Collectively, the results in Chapter III show that integrin α1 protein expression is upregulated in hepatocytes with HF feeding, while the results in Chapter IV show that ILK protein expression is downregulated in hepatocytes with HF feeding. This indicates that the expression of hepatic integrins and integrin signaling proteins fluctuate as an adaptation to over nutrition, but that the directionality is specific.

Cell-matrix adhesions through integrins are critical for normal liver function. They are responsible for many cellular processes including hepatocyte survival and differentiation. Several studies have described a role for integrins in the regulation of insulin signaling in adipocytes (142,176) and a large majority of these studies utilized a variety of tissue culture cell systems. To date, only two studies have assessed the contribution of integrins to insulin action *in vivo* (177,178). The focus of both of these studies was on the regulation of skeletal muscle glucose uptake by integrins. Yet, prior to the studies described herein, the mechanistic contribution of integrins to hepatic insulin action *in vivo* had never been assessed. In the Dissertation studies, two integrin mouse models were utilized to establish a role for integrins in hepatic insulin action *in vivo*. These were the integrin α1-null mouse model and mice with a hepatocyte-specific deletion of ILK. Each model provided valuable insight into the regulation of hepatic insulin action by integrins.

The studies described in Chapter III demonstrate that integrin α1-null mice exhibit severe hepatic insulin resistance when fed a HF diet. This is evidenced by the absence of a suppressive effect of insulin on hepatic glucose production during an insulin clamp compared to a 50% suppression in HF-fed wild-type littermates. The lack of suppression of hepatic glucose production was accompanied by decreased IRS1 and Akt phosphorylation indicating that integrin α1β1 facilitates insulin signaling and promotes hepatic insulin action.

Integrins transduce signals to the inside of the cell through scaffolding proteins and downstream kinases (92). FAK and ILK are two prominent proteins described to facilitate integrin signal transduction. Several studies have established a role for FAK in the regulation of insulin signaling, thus it was hypothesized that integrin α1β1 promotes insulin action through FAK. To test this hypothesis, FAK phosphorylation was assessed in livers from HF fed integrin α1-null mice and their wild-type littermates. There was no difference in FAK phosphorylation between the genotypes in livers from either 5-h fasted or insulin-clamped mice. This strongly suggests that FAK activation was not responsible for the observed phenotype. In an attempt to test the hypothesis that α1β1 promotes hepatic insulin action in HF fed mice through a mechanism that requires ILK, mice with a hepatocyte-specific deletion of ILK were studied. The hypothesis was not correct. The results in Chapter IV show that the deletion of ILK from the hepatocyte actually improves hepatic insulin action in HF fed mice, suggesting that ILK contributes to diet-induced hepatic insulin resistance.

These opposing effects of the two gene deletions on hepatic glucose production emphasize the complexity of the integrin signaling system. The integrin α1β1 studies described in Chapter III were conducted on mice with a whole-body deletion of the integrin α1 subunit. In contrast, the studies in Chapter IV were performed using mice with a hepatocyte-specific

deletion of ILK. The liver is a heterogeneous tissue comprised of several different cell types including hepatocytes, endothelial lining cells, Kupffer cells, and stellate cells. The hepatocyte is the major cell type involved in the regulation of hepatic insulin action. Nonetheless, other cell types such as Kupffer cells have also been shown to contribute to the pathogenesis of diet-induced hepatic insulin resistance. For example, the depletion of Kupffer cells in male Wistar rats fed either a high sucrose or HF diet exhibit improved hepatic insulin sensitivity (206). Thus the ILK studies in Chapter IV can be isolated to insulin action within the hepatocyte, while the severe insulin resistance observed in the HF fed integrin α1-null mice described in Chapter III could be attributed to a combination of hepatic and extrahepatic effects.

Moreover, there are 2 integrins known to be expressed on the hepatocyte, integrin α1β1 and integrin α5β1. The whole-body deletion of integrin α1 eliminated hepatocellular integrin α1β1 signaling; however integrin α5β1 signaling remained intact. ILK interacts with several different integrin beta subunits including β1, β2 and β3. Integrin β1 is the only β integrin subunit known to interact with ILK that is expressed on hepatocytes (102). Integrin β2 is expressed on lymphocytes and while integrin β3 is highly expressed in the liver, no information exists regarding the expression of integrin β3 in hepatocytes. In integrin α1-null mice, integrin α1β1 is no longer able to signal, however integrin α5β1 is still present in hepatocytes and can signal through ILK. Hence, it is plausible that in the absence of integrin α1β1, integrin α5β1 is signaling through ILK and this promotes the development of severe hepatic insulin resistance in the presence of nutrient overload. This is depicted in Figure 5.1. It is also possible that there is some unidentified integrin α1 subunit binding partner that is modulating the protective effect observed in Chapter III. This unidentified binding partner could be identified experimentally in future studies via immunoprecipitation, SILAC and/or the yeast two-hybrid system.

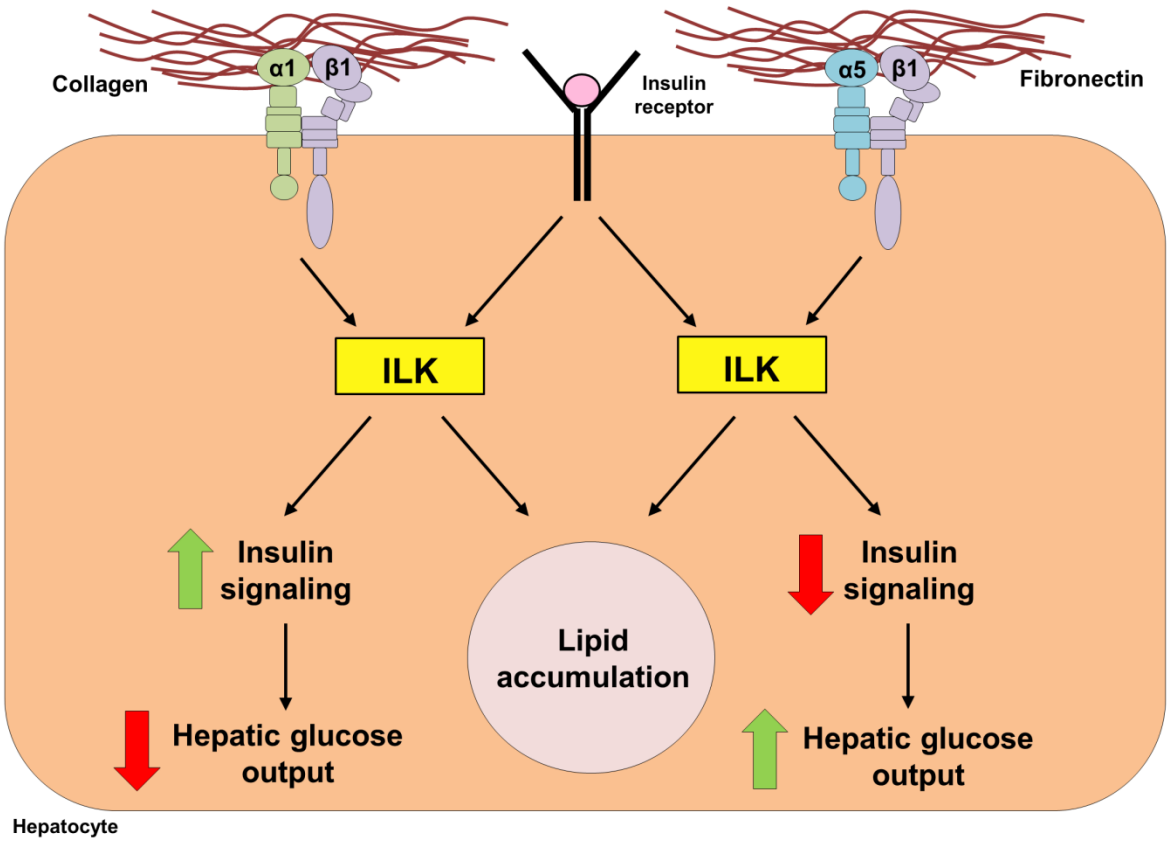

Figure 5.1 – Proposed model whereby integrins regulate hepatic glucose and lipid metabolism in high fat fed mice. Upon insulin stimulation, integrin signaling through integrin α1β1 and ILK results in improved insulin action and decreased hepatic glucose output. In the absence of integrin α1β1 and in the presence of insulin, signaling through integrin α5β1 and ILK results in impaired insulin action and increased hepatic glucose output. Moreover, integrin signaling through integrins α1β1 and α5β1 and ILK results in hepatic lipid accumulation.

The studies conducted in Chapter III are noteworthy as they serve to refine what is currently known about the insulin resistant liver. Most strikingly, the severe hepatic insulin resistance observed in the integrin α1-null mouse model was present in the absence of TG and DAG accumulation. Not only were the hepatic lipids reduced, they were actually normalized to chow fed levels. Prior to this study, several lines of research (29,51-53) concluded that hepatic lipid accumulation directly causes hepatic insulin resistance. The results of the integrin α1β1 studies indicate that hepatic insulin resistance can be completely dissociated from lipid accumulation.

The severe hepatic insulin resistance observed in the HF fed integrin α1-null mice also occurred in the absence of differences in glucose tolerance. The liver is a major insulin sensitive organ and defects in liver insulin action contribute to the dysregulation of glucose homeostasis. Insulin resistance is one of several factors that can influence glucose tolerance. It is often assumed that in rodent models, impaired glucose tolerance combined with impairments in a separate, and often completely disparate, measurement of hepatic insulin action (i.e. insulin signaling) signifies the presence of hepatic insulin resistance. This is not necessarily the case. The 'gold standard' for assessing hepatic insulin action is through the insulin clamp combined with isotopes of glucose to measure glucose fluxes. Other commonly used tests are not able to accurately assess hepatic insulin sensitivity. There are several other factors in addition to insulin resistance that can influence glucose tolerance. These include glucose effectiveness (i.e. the ability of glucose to suppress endogenous glucose production and stimulate glucose uptake) and insulin secretion and clearance. Thus it is plausible that impaired insulin action is offset by differences in glucose effectiveness. Measurements of arterial insulin concentration do not accurately reflect the insulin concentration in the portal vein; hence it is unknown whether

insulin concentrations at the liver are different and this could also contribute to the normal GTT results in the face of hepatic insulin resistance. Taken together this emphasizes the need to assess both glucose tolerance and insulin sensitivity as independent measurements when determining the metabolic phenotype of a novel rodent model.

Focal adhesion kinase (FAK) is a key integrin-mediated regulator of insulin signaling (125,143-145). The phosphorylation of FAK at Tyr397 is associated with its activation. The studies conducted in Chapter III show that FAK Tyr397 phosphorylation is greatly reduced in the livers of HF fed wild-type mice compared to chow fed littermates. This is the first study to establish that FAK activation is decreased in whole liver homogenate with HF feeding. This suggests that diminished FAK activation may contribute to decreased hepatic insulin action in HF fed wild-type mice. Future studies should be designed to test this hypothesis.

Hepatic lipid content was decreased in both mouse models suggesting that integrins regulate hepatic lipid accumulation independent of specific pathways of insulin-signaling. The decrease in hepatic lipid accumulation in both mouse models was attributed to altered free fatty acid (FFA) metabolism. However, each model had its own unique features. The reduction in hepatic lipids in HF-fed integrin α1-null mice was attributed to a combination of decreased FFA availability upon insulin stimulation, decreased gene expression of the fatty acid transporter *Cd36*, and increased mitochondrial FFA utilization. In contrast, the observed decrease in lipid accumulation in mice with a hepatocyte-specific deletion of ILK was exclusively attributed to decreased circulating FFAs in the 5-h fasted and insulin clamped states. There was no difference in mitochondrial FFA oxidation observed in this model. It is important to note that the observed increase in mitochondrial FFA oxidation in integrin α1-null mice was present irrespective of diet. This suggests that the presence of integrin α1β1 decreases mitochondrial fatty acid supported

respiration. Additionally, in support of increased insulin action, mice with a hepatocyte-specific deletion of ILK on a HF diet exhibit increased complex I supported mitochondrial respiration. These studies establish for the first time a role for integrins in the regulation of mitochondrial function.

Notably, expression of several genes implicated in de novo lipogenesis such as *Srebp-1c*, *Fas* and *Acc1* were in fact increased despite decreased lipid accumulation. These are amongst the first studies to openly describe this observation. This suggests that a feedback mechanism exists to up-regulate lipogenic pathways when hepatic lipid stores are low and future studies could be conducted to monitor protein expression of key lipogenic proteins as well as rates of de novo lipogenesis using D_2O to confirm this hypothesis. Moreover, this supports the broader view that lipid metabolites in the liver are shunted into neutral lipid droplets to protect against the deleterious effect of a HF diet. Collectively, the results from both mouse models reinforce the concept that circulating FFA concentrations contributes to hepatic lipid accumulation in the HF fed state.

The studies outlined in the Dissertation are the beginning of an important new line of research that seeks to understand how integrins regulate hepatic insulin action *in vivo*. One goal of this work was to establish new therapeutic targets to ameliorate hepatic insulin action. The results in Chapter III show that integrin α1β1 promotes hepatic insulin action and lipid accumulation in the presence of over nutrition. This suggests that molecular activators of integrin α1β1 may improve hepatic insulin sensitivity but also increase lipid accumulation. In contrast, the results in Chapter IV show that the deletion of hepatic ILK improves hepatic insulin sensitivity and reduces lipid accumulation in high fat fed mice. This suggests that ILK inhibitors would be beneficial in the treatment of both hepatic insulin resistance and fatty liver disease.

In light of this, the role of integrins on insulin action and lipid metabolism within the hepatocyte warrants further investigation. It was noted earlier that the phenotype in the integrin α1-null mouse model may not be attributed to insulin action within the hepatocyte alone. At the time of the Dissertation studies, integrin α1 floxed mice did not exist, however integrin α1floxed mice have been recently generated by Dr. Ambra Pozzi. To address the contribution of hepatocyte integrin α1β1 to the described phenotype in Chapter III, further research is needed in mice with a hepatocyte-specific deletion of the integrin α1 subunit.

Integrin β1 is the only known β integrin subunit expressed on the hepatocyte. In an early attempt to determine a role for hepatocyte integrin β1, integrin β1floxed mice (kindly provided by Dr. Roy Zent) were crossed with mice expressing Cre-recombinase under the albumin promoter. After much effort to generate mice with a hepatocyte-specific deletion of integrin β1, it was determined that this mouse model was embryonic lethal. This is supported in a recent study by Speicher et al. (207). The role of integrin β1 in mediating hepatic insulin action *in vivo* is critical for understanding the regulation of hepatic insulin action by integrins. To address this, future studies will be conducted in the laboratory using an inducible model of hepatocyte integrin β1 deletion.

Considering that integrins α1β1 and α5β1 are the only known integrins expressed on the hepatocyte, it will also be important to establish whether integrin α5β1 also influences hepatic insulin action. Integrin α5β1 is a receptor for fibronectin. Preliminary studies from our laboratory suggest that fibronectin gene and protein expression is increased in the livers of HF-fed mice. This suggests that integrin α5β1 signaling may be increased in the diet-induced obese state and this contributes to decreased hepatic insulin action. The role of integrin α5β1 and fibronectin in

the pathogenesis of diet-induced hepatic insulin resistance will be examined in future studies in the laboratory.

In conclusion, the studies described in the Dissertation establish for the first time a novel role for integrins in the regulation of hepatic insulin action and lipid accumulation *in vivo*. A strength of these studies is the emphasis on monitoring the *in vivo* pathways that regulate hepatic metabolism in a mouse model of metabolic disease. The regulation of hepatic insulin action in the diet-induced obese state is quite complex. Key metabolic pathways are not able to be measured accurately in tissue culture systems or in perfused livers. Many questions remain as to how metabolic disease develops and persists over time. The current work addresses the contribution of integrins to alterations in hepatic metabolism in the presence of nutritional overload. These studies emphasize the potential utility of molecular activators or inhibitors of integrin signaling as therapeutic targets to treat the underlying insulin resistance associated with Type 2 diabetes.

Chapter VI

CONCLUSIONS AND IMPLICATIONS

The data contained within this Dissertation are the first to describe a role for integrins in the regulation of hepatic insulin action and lipid accumulation *in vivo*. The results from these studies emphasize that integrins represent a novel therapeutic target to treat the underlying hepatic insulin resistance associated with Type 2 diabetes. The fundamental conclusions of this cumulative work include: integrin α1β1 protects against diet-induced hepatic insulin resistance while promoting lipid accumulation and a downstream integrin signaling molecule, integrin-linked kinase, is a major contributor to hepatic insulin resistance and lipid accumulation in high fat fed mice.

REFERENCES

1. Pehling, G., Tessari, P., Gerich, J. E., Haymond, M. W., Service, F. J., and Rizza, R. A. (1984) Abnormal meal carbohydrate disposition in insulin-dependent diabetes. Relative contributions of endogenous glucose production and initial splanchnic uptake and effect of intensive insulin therapy. *J. Clin. Invest.* **74**, 985-991

2. DeFronzo, R. A., and Del Prato, S. (1996) Insulin resistance and diabetes mellitus. *J. Diabetes Complications* **10**, 243-245

3. Postic, C., Shiota, M., Niswender, K. D., Jetton, T. L., Chen, Y., Moates, J. M., Shelton, K. D., Lindner, J., Cherrington, A. D., and Magnuson, M. A. (1999) Dual roles for glucokinase in glucose homeostasis as determined by liver and pancreatic beta cell-specific gene knock-outs using Cre recombinase. *J. Biol. Chem.* **274**, 305-315

4. Cherrington, A. D. (1999) Banting Lecture 1997. Control of glucose uptake and release by the liver in vivo. *Diabetes* **48**, 1198-1214

5. Basu, R., Basu, A., Johnson, C. M., Schwenk, W. F., and Rizza, R. A. (2004) Insulin dose-response curves for stimulation of splanchnic glucose uptake and suppression of endogenous glucose production differ in nondiabetic humans and are abnormal in people with type 2 diabetes. *Diabetes* **53**, 2042-2050

6. Basu, R., Schwenk, W. F., and Rizza, R. A. (2004) Both fasting glucose production and disappearance are abnormal in people with "mild" and "severe" type 2 diabetes. *American journal of physiology. Endocrinology and metabolism* **287**, E55-62

7. Madison, L. L., Combes, B., Strickland, W., Unger, R., and Adams, R. (1959) Evidence for a direct effect of insulin on hepatic glucose output. *Metabolism.* **8**, 469-471

8. Duckworth, W. C., Bennett, R. G., and Hamel, F. G. (1998) Insulin degradation: progress and potential. *Endocr. Rev.* **19**, 608-624

9. Field, J. B. (1973) Extraction of insulin by liver. *Annu. Rev. Med.* **24**, 309-314

10. Bonora, E., Zavaroni, I., Coscelli, C., and Butturini, U. (1983) Decreased hepatic insulin extraction in subjects with mild glucose intolerance. *Metabolism.* **32**, 438-446

11. Karakash, C., Assimacopoulos-Jeannet, F., and Jeanrenaud, B. (1976) An anomaly of insulin removal in perfused livers of obese-hyperglycemic (ob/ob) mice. *J. Clin. Invest.* **57**, 1117-1124

12. Ebina, Y., Ellis, L., Jarnagin, K., Edery, M., Graf, L., Clauser, E., Ou, J. H., Masiarz, F., Kan, Y. W., Goldfine, I. D., and et al. (1985) The human insulin receptor cDNA: the structural basis for hormone-activated transmembrane signalling. *Cell* **40**, 747-758

13. Sun, X. J., Crimmins, D. L., Myers, M. G., Jr., Miralpeix, M., and White, M. F. (1993) Pleiotropic insulin signals are engaged by multisite phosphorylation of IRS-1. *Mol. Cell. Biol.* **13**, 7418-7428

14. Boulton, T. G., Nye, S. H., Robbins, D. J., Ip, N. Y., Radziejewska, E., Morgenbesser, S. D., DePinho, R. A., Panayotatos, N., Cobb, M. H., and Yancopoulos, G. D. (1991) ERKs: a family of protein-serine/threonine kinases that are activated and tyrosine phosphorylated in response to insulin and NGF. *Cell* **65**, 663-675

15. Easton, R. M., Cho, H., Roovers, K., Shineman, D. W., Mizrahi, M., Forman, M. S., Lee, V. M., Szabolcs, M., de Jong, R., Oltersdorf, T., Ludwig, T., Efstratiadis, A., and Birnbaum, M. J. (2005) Role for Akt3/protein kinase Bgamma in attainment of normal brain size. *Mol. Cell. Biol.* **25**, 1869-1878

16. Matsumoto, M., Han, S., Kitamura, T., and Accili, D. (2006) Dual role of transcription factor FoxO1 in controlling hepatic insulin sensitivity and lipid metabolism. *J. Clin. Invest.* **116**, 2464-2472

17. Biddinger, S. B., and Kahn, C. R. (2006) From mice to men: insights into the insulin resistance syndromes. *Annu. Rev. Physiol.* **68**, 123-158

18. Boucher, J., Kleinridders, A., and Kahn, C. R. (2014) Insulin receptor signaling in normal and insulin-resistant states. *Cold Spring Harbor perspectives in biology* **6**

19. Michael, M. D., Kulkarni, R. N., Postic, C., Previs, S. F., Shulman, G. I., Magnuson, M. A., and Kahn, C. R. (2000) Loss of insulin signaling in hepatocytes leads to severe insulin resistance and progressive hepatic dysfunction. *Mol. Cell* **6**, 87-97

20. Dong, X. C., Copps, K. D., Guo, S., Li, Y., Kollipara, R., DePinho, R. A., and White, M. F. (2008) Inactivation of hepatic Foxo1 by insulin signaling is required for adaptive nutrient homeostasis and endocrine growth regulation. *Cell metabolism* **8**, 65-76

21. Altomonte, J., Richter, A., Harbaran, S., Suriawinata, J., Nakae, J., Thung, S. N., Meseck, M., Accili, D., and Dong, H. (2003) Inhibition of Foxo1 function is associated with improved fasting glycemia in diabetic mice. *American journal of physiology. Endocrinology and metabolism* **285**, E718-728

22. Jitrapakdee, S. (2012) Transcription factors and coactivators controlling nutrient and hormonal regulation of hepatic gluconeogenesis. *Int. J. Biochem. Cell Biol.* **44**, 33-45

23. Lu, M., Wan, M., Leavens, K. F., Chu, Q., Monks, B. R., Fernandez, S., Ahima, R. S., Ueki, K., Kahn, C. R., and Birnbaum, M. J. (2012) Insulin regulates liver metabolism in vivo in the absence of hepatic Akt and Foxo1. *Nat. Med.* **18**, 388-395

24. Duckworth, W. C., Runyan, K. R., Wright, R. K., Halban, P. A., and Solomon, S. S. (1981) Insulin degradation by hepatocytes in primary culture. *Endocrinology* **108**, 1142-1147

25. Carpentier, J. L., Gorden, P., Freychet, P., Le Cam, A., and Orci, L. (1979) Lysosomal association of internalized 125I-insulin in isolated rat hepatocytes. Direct demonstration by quantitative electron microscopic autoradiography. *J. Clin. Invest.* **63**, 1249-1261

26. Carpentier, J. L., Gorden, P., Barazzone, P., Freychet, P., Le Cam, A., and Orci, L. (1979) Intracellular localization of 125I-labeled insulin in hepatocytes from intact rat liver. *Proc. Natl. Acad. Sci. U. S. A.* **76**, 2803-2807

27. Hovorka, R., Powrie, J. K., Smith, G. D., Sonksen, P. H., Carson, E. R., and Jones, R. H. (1993) Five-compartment model of insulin kinetics and its use to investigate action of chloroquine in NIDDM. *Am. J. Physiol.* **265**, E162-175

28. Postic, C., and Girard, J. (2008) Contribution of de novo fatty acid synthesis to hepatic steatosis and insulin resistance: lessons from genetically engineered mice. *J. Clin. Invest.* **118**, 829-838

29. Stefan, N., Staiger, H., and Haring, H. U. (2011) Dissociation between fatty liver and insulin resistance: the role of adipose triacylglycerol lipase. *Diab tologia* **54**, 7-9

30. Donnelly, K. L., Smith, C. I., Schwarzenberg, S. J., Jessurun, J., Boldt, M. D., and Parks, E. J. (2005) Sources of fatty acids stored in liver and secreted via lipoproteins in patients with nonalcoholic fatty liver disease. *J. Clin. Invest.* **115**, 1343-1351

31. Zhang, J., Zhao, Y., Xu, C., Hong, Y., Lu, H., Wu, J., and Chen, Y. (2014) Association between serum free fatty acid levels and nonalcoholic fatty liver disease: a cross-sectional study. *Scientific reports* **4**, 5832

32. Sanyal, A. J. (2001) Insulin resistance and nonalcoholic steatohepatitis: fat or fiction? *Am. J. Gastroenterol.* **96**, 274-276

33. Ruan, H., and Lodish, H. F. (2003) Insulin resistance in adipose tissue: direct and indirect effects of tumor necrosis factor-alpha. *Cytokine Growth Factor Rev.* **14**, 447-455

34. Voshol, P. J., Haemmerle, G., Ouwens, D. M., Zimmermann, R., Zechner, R., Teusink, B., Maassen, J. A., Havekes, L. M., and Romijn, J. A. (2003) Increased hepatic insulin sensitivity together with decreased hepatic triglyceride stores in hormone-sensitive lipase-deficient mice. *Endocrinology* **144**, 3456-3462

35. Greco, D., Kotronen, A., Westerbacka, J., Puig, O., Arkkila, P., Kiviluoto, T., Laitinen, S., Kolak, M., Fisher, R. M., Hamsten, A., Auvinen, P., and Yki-Jarvinen, H. (2008) Gene expression in human NAFLD. *American journal of physiology. Gastrointestinal and liver physiology* **294**, G1281-1287

36. Koonen, D. P., Jacobs, R. L., Febbraio, M., Young, M. E., Soltys, C. L., Ong, H., Vance, D. E., and Dyck, J. R. (2007) Increased hepatic CD36 expression contributes to dyslipidemia associated with diet-induced obesity. *Diabetes* **56**, 2863-2871

37. Murthy, V. K., and Shipp, J. C. (1979) Synthesis and accumulation of triglycerides in liver of diabetic rats. Effects of insulin treatment. *Diabetes* **28**, 472-478

38. Ma, L., Robinson, L. N., and Towle, H. C. (2006) ChREBP*Mlx is the principal mediator of glucose-induced gene expression in the liver. *J. Biol. Chem.* **281**, 28721-28730

39. Ma, L., Sham, Y. Y., Walters, K. J., and Towle, H. C. (2007) A critical role for the loop region of the basic helix-loop-helix/leucine zipper protein Mlx in DNA binding and glucose-regulated transcription. *Nucleic Acids Res* **35**, 35-44

40. Foretz, M., Guichard, C., Ferre, P., and Foufelle, F. (1999) Sterol regulatory element binding protein-1c is a major mediator of insulin action on the hepatic expression of glucokinase and lipogenesis-related genes. *Proc. Natl. Acad. Sci. U. S. A.* **96**, 12737-12742

41. Horton, J. D., Shimomura, I., Brown, M. S., Hammer, R. E., Goldstein, J. L., and Shimano, H. (1998) Activation of cholesterol synthesis in preference to fatty acid synthesis in liver and adipose tissue of transgenic mice overproducing sterol regulatory element-binding protein-2. *J. Clin. Invest.* **101**, 2331-2339

42. Benhamed, F., Denechaud, P. D., Lemoine, M., Robichon, C., Moldes, M., Bertrand-Michel, J., Ratziu, V., Serfaty, L., Housset, C., Capeau, J., Girard, J., Guillou, H., and Postic, C. (2012) The lipogenic transcription factor ChREBP dissociates hepatic steatosis from insulin resistance in mice and humans. *J. Clin. Invest.* **122**, 2176-2194

43. Shimano, H., Shimomura, I., Hammer, R. E., Herz, J., Goldstein, J. L., Brown, M. S., and Horton, J. D. (1997) Elevated levels of SREBP-2 and cholesterol synthesis in livers of mice homozygous for a targeted disruption of the SREBP-1 gene. *J. Clin. Invest.* **100**, 2115-2124

44. Liang, G., Yang, J., Horton, J. D., Hammer, R. E., Goldstein, J. L., and Brown, M. S. (2002) Diminished hepatic response to fasting/refeeding and liver X receptor agonists in mice with selective deficiency of sterol regulatory element-binding protein-1c. *J. Biol. Chem.* **277**, 9520-9528

45. Sunny, N. E., Parks, E. J., Browning, J. D., and Burgess, S. C. (2011) Excessive hepatic mitochondrial TCA cycle and gluconeogenesis in humans with nonalcoholic fatty liver disease. *Cell metabolism* **14**, 804-810

46. Ibdah, J. A., Perlegas, P., Zhao, Y., Angdisen, J., Borgerink, H., Shadoan, M. K., Wagner, J. D., Matern, D., Rinaldo, P., and Cline, J. M. (2005) Mice heterozygous for a

defect in mitochondrial trifunctional protein develop hepatic steatosis and insulin resistance. *Gastroenterology* **128**, 1381-1390

47. Zhou, M., Xu, A., Tam, P. K., Lam, K. S., Chan, L., Hoo, R. L., Liu, J., Chow, K. H., and Wang, Y. (2008) Mitochondrial dysfunction contributes to the increased vulnerabilities of adiponectin knockout mice to liver injury. *Hepatology* **48**, 1087-1096

48. Rector, R. S., Thyfault, J. P., Uptergrove, G. M., Morris, E. M., Naples, S. P., Borengasser, S. J., Mikus, C. R., Laye, M. J., Laughlin, M. H., Booth, F. W., and Ibdah, J. A. (2010) Mitochondrial dysfunction precedes insulin resistance and hepatic steatosis and contributes to the natural history of non-alcoholic fatty liver disease in an obese rodent model. *J. Hepatol.* **52**, 727-736

49. Schonfeld, G., Patterson, B. W., Yablonskiy, D. A., Tanoli, T. S., Averna, M., Elias, N., Yue, P., and Ackerman, J. (2003) Fatty liver in familial hypobetalipoproteinemia: triglyceride assembly into VLDL particles is affected by the extent of hepatic steatosis. *J. Lipid Res.* **44**, 470-478

50. Choi, S. H., and Ginsberg, H. N. (2011) Increased very low density lipoprotein (VLDL) secretion, hepatic steatosis, and insulin resistance. *Trends in endocrinology and metabolism: TEM* **22**, 353-363

51. Samuel, V. T., Liu, Z. X., Qu, X., Elder, B. D., Bilz, S., Befroy, D., Romanelli, A. J., and Shulman, G. I. (2004) Mechanism of hepatic insulin resistance in non-alcoholic fatty liver disease. *J. Biol. Chem.* **279**, 32345-32353

52. Dentin, R., Denechaud, P. D., Benhamed, F., Girard, J., and Postic, C. (2006) Hepatic gene regulation by glucose and polyunsaturated fatty acids: a role for ChREBP. *J. Nutr.* **136**, 1145-1149

53. Kraegen, E. W., Clark, P. W., Jenkins, A. B., Daley, E. A., Chisholm, D. J., and Storlien, L. H. (1991) Development of muscle insulin resistance after liver insulin resistance in high-fat-fed rats. *Diabetes* **40**, 1397-1403

54. Kim, J. K., Fillmore, J. J., Chen, Y., Yu, C., Moore, I. K., Pypaert, M., Lutz, E. P., Kako, Y., Velez-Carrasco, W., Goldberg, I. J., Breslow, J. L., and Shulman, G. I. (2001) Tissue-specific overexpression of lipoprotein lipase causes tissue-specific insulin resistance. *Proc. Natl. Acad. Sci. U. S. A.* **98**, 7522-7527

55. Leavens, K. F., Easton, R. M., Shulman, G. I., Previs, S. F., and Birnbaum, M. J. (2009) Akt2 is required for hepatic lipid accumulation in models of insulin resistance. *Cell metabolism* **10**, 405-418

56. Monetti, M., Levin, M. C., Watt, M. J., Sajan, M. P., Marmor, S., Hubbard, B. K., Stevens, R. D., Bain, J. R., Newgard, C. B., Farese, R. V., Sr., Hevener, A. L., and

Farese, R. V., Jr. (2007) Dissociation of hepatic steatosis and insulin resistance in mice overexpressing DGAT in the liver. *Cell metabolism* **6**, 69-78

57. Yamaguchi, K., Yang, L., McCall, S., Huang, J., Yu, X. X., Pandey, S. K., Bhanot, S., Monia, B. P., Li, Y. X., and Diehl, A. M. (2007) Inhibiting triglyceride synthesis improves hepatic steatosis but exacerbates liver damage and fibrosis in obese mice with nonalcoholic steatohepatitis. *Hepatology* **45**, 1366-1374

58. Matsuzaka, T., Shimano, H., Yahagi, N., Kato, T., Atsumi, A., Yamamoto, T., Inoue, N., Ishikawa, M., Okada, S., Ishigaki, N., Iwasaki, H., Iwasaki, Y., Karasawa, T., Kumadaki, S., Matsui, T., Sekiya, M., Ohashi, K., Hasty, A. H., Nakagawa, Y., Takahashi, A., Suzuki, H., Yatoh, S., Sone, H., Toyoshima, H., Osuga, J., and Yamada, N. (2007) Crucial role of a long-chain fatty acid elongase, Elovl6, in obesity-induced insulin resistance. *Nat. Med.* **13**, 1193-1202

59. Nakamura, A., and Terauchi, Y. (2013) Lessons from mouse models of high-fat diet-induced NAFLD. *International journal of molecular sciences* **14**, 21240-21257

60. Postic, C., and Magnuson, M. A. (2000) DNA excision in liver by an albumin-Cre transgene occurs progressively with age. *Genesis* **26**, 149-150

61. Brock, R. W., and Dorman, R. B. (2007) Obesity, insulin resistance and hepatic perfusion. *Microcirculation* **14**, 339-347

62. Hynes, R. O. (2009) The extracellular matrix: not just pretty fibrils. *Science* **326**, 1216-1219

63. Martinez-Hernandez, A., and Amenta, P. S. (1995) The extracellular matrix in hepatic regeneration. *FASEB J.* **9**, 1401-1410

64. Schuppan, D. (1990) Structure of the extracellular matrix in normal and fibrotic liver: collagens and glycoproteins. *Semin. Liver Dis.* **10**, 1-10

65. Liu, X., Wu, H., Byrne, M., Krane, S., and Jaenisch, R. (1997) Type III collagen is crucial for collagen I fibrillogenesis and for normal cardiovascular development. *Proc. Natl. Acad. Sci. U. S. A.* **94**, 1852-1856

66. Hahn, E., Wick, G., Pencev, D., and Timpl, R. (1980) Distribution of basement membrane proteins in normal and fibrotic human liver: collagen type IV, laminin, and fibronectin. *Gut* **21**, 63-71

67. Setty, S., Kim, Y., Fields, G. B., Clegg, D. O., Wayner, E. A., and Tsilibary, E. C. (1998) Interactions of type IV collagen and its domains with human mesangial cells. *J. Biol. Chem.* **273**, 12244-12249

68. Sun, M., Chen, S., Adams, S. M., Florer, J. B., Liu, H., Kao, W. W., Wenstrup, R. J., and Birk, D. E. (2011) Collagen V is a dominant regulator of collagen fibrillogenesis: dysfunctional regulation of structure and function in a corneal-stroma-specific Col5a1-null mouse model. *J. Cell Sci.* **124**, 4096-4105

69. Velling, T., Risteli, J., Wennerberg, K., Mosher, D. F., and Johansson, S. (2002) Polymerization of type I and III collagens is dependent on fibronectin and enhanced by integrins alpha 11beta 1 and alpha 2beta 1. *J. Biol. Chem.* **277**, 37377-37381

70. Colognato, H., Winkelmann, D. A., and Yurchenco, P. D. (1999) Laminin polymerization induces a receptor-cytoskeleton network. *J. Cell Biol.* **145**, 619-631

71. Sasaki, T., Giltay, R., Talts, U., Timpl, R., and Talts, J. F. (2002) Expression and distribution of laminin alpha1 and alpha2 chains in embryonic and adult mouse tissues: an immunochemical approach. *Exp. Cell Res.* **275**, 185-199

72. Pozzi, A., and Zent, R. (2003) Integrins: sensors of extracellular matrix and modulators of cell function. *Nephron. Experimental nephrology* **94**, e77-84

73. Day, C. P., and James, O. F. (1998) Steatohepatitis: a tale of two "hits"? *Gastroenterology* **114**, 842-845

74. Gressner, O. A., Lahme, B., Demirci, I., Gressner, A. M., and Weiskirchen, R. (2007) Differential effects of TGF-beta on connective tissue growth factor (CTGF/CCN2) expression in hepatic stellate cells and hepatocytes. *J. Hepatol.* **47**, 699-710

75. Gressner, A. M., Weiskirchen, R., Breitkopf, K., and Dooley, S. (2002) Roles of TGF-beta in hepatic fibrosis. *Front. Biosci.* **7**, d793-807

76. Friedman, S. L. (2000) Molecular regulation of hepatic fibrosis, an integrated cellular response to tissue injury. *J. Biol. Chem.* **275**, 2247-2250

77. Eng, F. J., and Friedman, S. L. (2000) Fibrogenesis I. New insights into hepatic stellate cell activation: the simple becomes complex. *American journal of physiology. Gastrointestinal and liver physiology* **279**, G7-G11

78. Weiner, F. R., Giambrone, M. A., Czaja, M. J., Shah, A., Annoni, G., Takahashi, S., Eghbali, M., and Zern, M. A. (1990) Ito-cell gene expression and collagen regulation. *Hepatology* **11**, 111-117

79. Czaja, M. J., Weiner, F. R., Flanders, K. C., Giambrone, M. A., Wind, R., Biempica, L., and Zern, M. A. (1989) In vitro and in vivo association of transforming growth factor-beta 1 with hepatic fibrosis. *J. Cell Biol.* **108**, 2477-2482

80. Annoni, G., Weiner, F. R., and Zern, M. A. (1992) Increased transforming growth factor-beta 1 gene expression in human liver disease. *J. Hepatol.* **14**, 259-264

81. McCuskey, R. S., Ito, Y., Robertson, G. R., McCuskey, M. K., Perry, M., and Farrell, G. C. (2004) Hepatic microvascular dysfunction during evolution of dietary steatohepatitis in mice. *Hepatology* **40**, 386-393

82. Bataller, R., and Brenner, D. A. (2001) Hepatic stellate cells as a target for the treatment of liver fibrosis. *Semin. Liver Dis.* **21**, 437-451

83. Friedman, S. L., Roll, F. J., Boyles, J., and Bissell, D. M. (1985) Hepatic lipocytes: the principal collagen-producing cells of normal rat liver. *Proc. Natl. Acad. Sci. U. S. A.* **82**, 8681-8685

84. Maher, J. J., Bissell, D. M., Friedman, S. L., and Roll, F. J. (1988) Collagen measured in primary cultures of normal rat hepatocytes derives from lipocytes within the monolayer. *J. Clin. Invest.* **82**, 450-459

85. Sorrentino, P., Terracciano, L., D'Angelo, S., Ferbo, U., Bracigliano, A., and Vecchione, R. (2010) Predicting fibrosis worsening in obese patients with NASH through parenchymal fibronectin, HOMA-IR, and hypertension. *Am. J. Gastroenterol.* **105**, 336-344

86. Wada, T., Miyashita, Y., Sasaki, M., Aruga, Y., Nakamura, Y., Ishii, Y., Sasahara, M., Kanasaki, K., Kitada, M., Koya, D., Shimano, H., Tsuneki, H., and Sasaoka, T. (2013) Eplerenone ameliorates the phenotypes of metabolic syndrome with NASH in liver-specific SREBP-1c Tg mice fed high-fat and high-fructose diet. *American journal of physiology. Endocrinology and metabolism* **305**, E1415-1425

87. Dixon, L. J., Flask, C. A., Papouchado, B. G., Feldstein, A. E., and Nagy, L. E. (2013) Caspase-1 as a central regulator of high fat diet-induced non-alcoholic steatohepatitis. *PloS one* **8**, e56100

88. Jaskiewicz, K., Rzepko, R., and Sledzinski, Z. (2008) Fibrogenesis in fatty liver associated with obesity and diabetes mellitus type 2. *Dig. Dis. Sci.* **53**, 785-788

89. Harrison, S. A. (2006) Liver disease in patients with diabetes mellitus. *J. Clin. Gastroenterol.* **40**, 68-76

90. Kang, L., Lantier, L., Kennedy, A., Bonner, J. S., Mayes, W. H., Bracy, D. P., Bookbinder, L. H., Hasty, A. H., Thompson, C. B., and Wasserman, D. H. (2013) Hyaluronan accumulates with high-fat feeding and contributes to insulin resistance. *Diabetes* **62**, 1888-1896

91. Farrell, G. C., Teoh, N. C., and McCuskey, R. S. (2008) Hepatic microcirculation in fatty liver disease. *Anat Rec (Hoboken)* **291**, 684-692

92. Hynes, R. O. (2002) Integrins: bidirectional, allosteric signaling machines. *Cell* **110**, 673-687

93. Barczyk, M., Carracedo, S., and Gullberg, D. (2010) Integrins. *Cell Tissue Res.* **339**, 269-280

94. Heino, J., Ignotz, R. A., Hemler, M. E., Crouse, C., and Massague, J. (1989) Regulation of cell adhesion receptors by transforming growth factor-beta. Concomitant regulation of integrins that share a common beta 1 subunit. *J. Biol. Chem.* **264**, 380-388

95. Hemler, M. E., Sanchez-Madrid, F., Flotte, T. J., Krensky, A. M., Burakoff, S. J., Bhan, A. K., Springer, T. A., and Strominger, J. L. (1984) Glycoproteins of 210,000 and 130,000 m.w. on activated T cells: cell distribution and antigenic relation to components on resting cells and T cell lines. *J. Immunol.* **132**, 3011-3018

96. Kern, A., Briesewitz, R., Bank, I., and Marcantonio, E. E. (1994) The role of the I domain in ligand binding of the human integrin alpha 1 beta 1. *J. Biol. Chem.* **269**, 22811-22816

97. Stamatoglou, S. C., Bawumia, S., Johansson, S., Forsberg, E., and Hughes, R. C. (1991) Affinity of integrin alpha 1 beta 1 from liver sinusoidal membranes for type IV collagen. *FEBS Lett.* **288**, 241-243

98. Gardner, H., Kreidberg, J., Koteliansky, V., and Jaenisch, R. (1996) Deletion of integrin alpha 1 by homologous recombination permits normal murine development but gives rise to a specific deficit in cell adhesion. *Dev. Biol.* **175**, 301-313

99. Pozzi, A., Wary, K. K., Giancotti, F. G., and Gardner, H. A. (1998) Integrin alpha1beta1 mediates a unique collagen-dependent proliferation pathway in vivo. *J. Cell Biol.* **142**, 587-594

100. Suzuki, K., Okuno, T., Yamamoto, M., Pasterkamp, R. J., Takegahara, N., Takamatsu, H., Kitao, T., Takagi, J., Rennert, P. D., Kolodkin, A. L., Kumanogoh, A., and Kikutani, H. (2007) Semaphorin 7A initiates T-cell-mediated inflammatory responses through alpha1beta1 integrin. *Nature* **446**, 680-684

101. Gardner, H. (2014) Integrin alpha1beta1. *Adv. Exp. Med. Biol.* **819**, 21-39

102. Volpes, R., van den Oord, J. J., and Desmet, V. J. (1991) Distribution of the VLA family of integrins in normal and pathological human liver tissue. *Gastroenterology* **101**, 200-206

103. Racine-Samson, L., Rockey, D. C., and Bissell, D. M. (1997) The role of alpha1beta1 integrin in wound contraction. A quantitative analysis of liver myofibroblasts in vivo and in primary culture. *J. Biol. Chem.* **272**, 30911-30917

104. Gardner, H., Broberg, A., Pozzi, A., Laato, M., and Heino, J. (1999) Absence of integrin alpha1beta1 in the mouse causes loss of feedback regulation of collagen synthesis in normal and wounded dermis. *J. Cell Sci.* **112 (Pt 3)**, 263-272

105. Pozzi, A., Moberg, P. E., Miles, L. A., Wagner, S., Soloway, P., and Gardner, H. A. (2000) Elevated matrix metalloprotease and angiostatin levels in integrin alpha 1 knockout mice cause reduced tumor vascularization. *Proc. Natl. Acad. Sci. U. S. A.* **97**, 2202-2207

106. Rossino, P., Defilippi, P., Silengo, L., and Tarone, G. (1991) Up-regulation of the integrin alpha 1/beta 1 in human neuroblastoma cells differentiated by retinoic acid: correlation with increased neurite outgrowth response to laminin. *Cell Regul.* **2**, 1021-1033

107. Santala, P., and Heino, J. (1991) Regulation of integrin-type cell adhesion receptors by cytokines. *J. Biol. Chem.* **266**, 23505-23509

108. Defilippi, P., Bozzo, C., Geuna, M., Rossino, P., Silengo, L., and Tarone, G. (1992) Modulation of extracellular matrix receptors (integrins) on human endothelial cells by cytokines. *EXS* **61**, 193-197

109. Kagami, S., Kuhara, T., Yasutomo, K., Okada, K., Loster, K., Reutter, W., and Kuroda, Y. (1996) Transforming growth factor-beta (TGF-beta) stimulates the expression of beta1 integrins and adhesion by rat mesangial cells. *Exp. Cell Res.* **229**, 1-6

110. Nejjari, M., Couvelard, A., Mosnier, J. F., Moreau, A., Feldmann, G., Degott, C., Marcellin, P., and Scoazec, J. Y. (2001) Integrin up-regulation in chronic liver disease: relationship with inflammation and fibrosis in chronic hepatitis C. *J. Pathol.* **195**, 473-481

111. Schaffert, C. S., Sorrell, M. F., and Tuma, D. J. (2001) Expression and cytoskeletal association of integrin subunits is selectively increased in rat perivenous hepatocytes after chronic ethanol administration. *Alcohol. Clin. Exp. Res.* **25**, 1749-1757

112. Yuan, S. T., Hu, X. Q., Lu, J. P., KeiKi, H., Zhai, W. R., and Zhang, Y. E. (2000) Changes of integrin expression in rat hepatocarcinogenesis induced by 3'-Me-DAB. *World journal of gastroenterology : WJG* **6**, 231-233

113. Moser, M., Legate, K. R., Zent, R., and Fassler, R. (2009) The tail of integrins, talin, and kindlins. *Science* **324**, 895-899

114. Shattil, S. J., Kim, C., and Ginsberg, M. H. (2010) The final steps of integrin activation: the end game. *Nature reviews. Molecular cell biology* **11**, 288-300

115. Critchley, D. R., and Gingras, A. R. (2008) Talin at a glance. *J. Cell Sci.* **121**, 1345-1347

116. Ussar, S., Wang, H. V., Linder, S., Fassler, R., and Moser, M. (2006) The Kindlins: subcellular localization and expression during murine development. *Exp. Cell Res.* **312**, 3142-3151

117. Zaidel-Bar, R., Itzkovitz, S., Ma'ayan, A., Iyengar, R., and Geiger, B. (2007) Functional atlas of the integrin adhesome. *Nature cell biology* **9**, 858-867

118. Hildebrand, J. D., Schaller, M. D., and Parsons, J. T. (1993) Identification of sequences required for the efficient localization of the focal adhesion kinase, pp125FAK, to cellular focal adhesions. *J. Cell Biol.* **123**, 993-1005

119. Hanks, S. K., Calalb, M. B., Harper, M. C., and Patel, S. K. (1992) Focal adhesion protein-tyrosine kinase phosphorylated in response to cell attachment to fibronectin. *Proc. Natl. Acad. Sci. U. S. A.* **89**, 8487-8491

120. Kornberg, L., Earp, H. S., Parsons, J. T., Schaller, M., and Juliano, R. L. (1992) Cell adhesion or integrin clustering increases phosphorylation of a focal adhesion-associated tyrosine kinase. *J. Biol. Chem.* **267**, 23439-23442

121. Calalb, M. B., Polte, T. R., and Hanks, S. K. (1995) Tyrosine phosphorylation of focal adhesion kinase at sites in the catalytic domain regulates kinase activity: a role for Src family kinases. *Mol. Cell. Biol.* **15**, 954-963

122. Loster, K., Vossmeyer, D., Hofmann, W., Reutter, W., and Danker, K. (2001) alpha1 Integrin cytoplasmic domain is involved in focal adhesion formation via association with intracellular proteins. *Biochem. J.* **356**, 233-240

123. Plows, L. D., Cook, R. T., Davies, A. J., and Walker, A. J. (2006) Integrin engagement modulates the phosphorylation of focal adhesion kinase, phagocytosis, and cell spreading in molluscan defence cells. *Biochim. Biophys. Acta* **1763**, 779-786

124. Schlaepfer, D. D., Hanks, S. K., Hunter, T., and van der Geer, P. (1994) Integrin-mediated signal transduction linked to Ras pathway by GRB2 binding to focal adhesion kinase. *Nature* **372**, 786-791

125. Huang, D., Cheung, A. T., Parsons, J. T., and Bryer-Ash, M. (2002) Focal adhesion kinase (FAK) regulates insulin-stimulated glycogen synthesis in hepatocytes. *J. Biol. Chem.* **277**, 18151-18160

126. Ilic, D., Furuta, Y., Kanazawa, S., Takeda, N., Sobue, K., Nakatsuji, N., Nomura, S., Fujimoto, J., Okada, M., and Yamamoto, T. (1995) Reduced cell motility and enhanced focal adhesion contact formation in cells from FAK-deficient mice. *Nature* **377**, 539-544

127. Wickstrom, S. A., Lange, A., Montanez, E., and Fassler, R. (2010) The ILK/PINCH/parvin complex: the kinase is dead, long live the pseudokinase! *EMBO J.* **29**, 281-291

128. Legate, K. R., and Fassler, R. (2009) Mechanisms that regulate adaptor binding to beta-integrin cytoplasmic tails. *J. Cell Sci.* **122**, 187-198

129. Hannigan, G. E., Leung-Hagesteijn, C., Fitz-Gibbon, L., Coppolino, M. G., Radeva, G., Filmus, J., Bell, J. C., and Dedhar, S. (1996) Regulation of cell adhesion and anchorage-dependent growth by a new beta 1-integrin-linked protein kinase. *Nature* **379**, 91-96

130. Lange, A., Wickstrom, S. A., Jakobson, M., Zent, R., Sainio, K., and Fassler, R. (2009) Integrin-linked kinase is an adaptor with essential functions during mouse development. *Nature* **461**, 1002-1006

131. Fukuda, K., Gupta, S., Chen, K., Wu, C., and Qin, J. (2009) The pseudoactive site of ILK is essential for its binding to alpha-Parvin and localization to focal adhesions. *Mol. Cell* **36**, 819-830

132. Zervas, C. G., Gregory, S. L., and Brown, N. H. (2001) Drosophila integrin-linked kinase is required at sites of integrin adhesion to link the cytoskeleton to the plasma membrane. *J. Cell Biol.* **152**, 1007-1018

133. Mackinnon, A. C., Qadota, H., Norman, K. R., Moerman, D. G., and Williams, B. D. (2002) C. elegans PAT-4/ILK functions as an adaptor protein within integrin adhesion complexes. *Curr. Biol.* **12**, 787-797

134. Vaynberg, J., and Qin, J. (2006) Weak protein-protein interactions as probed by NMR spectroscopy. *Trends Biotechnol.* **24**, 22-27

135. Qian, F., Zhang, Z. C., Wu, X. F., Li, Y. P., and Xu, Q. (2005) Interaction between integrin alpha(5) and fibronectin is required for metastasis of B16F10 melanoma cells. *Biochem. Biophys. Res. Commun.* **333**, 1269-1275

136. Hill, M. M., Feng, J., and Hemmings, B. A. (2002) Identification of a plasma membrane Raft-associated PKB Ser473 kinase activity that is distinct from ILK and PDK1. *Curr. Biol.* **12**, 1251-1255

137. Persad, S., Attwell, S., Gray, V., Mawji, N., Deng, J. T., Leung, D., Yan, J., Sanghera, J., Walsh, M. P., and Dedhar, S. (2001) Regulation of protein kinase B/Akt-serine 473 phosphorylation by integrin-linked kinase: critical roles for kinase activity and amino acids arginine 211 and serine 343. *J. Biol. Chem.* **276**, 27462-27469

138. Miyamoto, S., Teramoto, H., Gutkind, J. S., and Yamada, K. M. (1996) Integrins can collaborate with growth factors for phosphorylation of receptor tyrosine kinases and MAP kinase activation: roles of integrin aggregation and occupancy of receptors. *J. Cell Biol.* **135**, 1633-1642

139. Vuori, K., and Ruoslahti, E. (1994) Association of insulin receptor substrate-1 with integrins. *Science* **266**, 1576-1578

140. Zheng, B., and Clemmons, D. R. (1998) Blocking ligand occupancy of the alphaVbeta3 integrin inhibits insulin-like growth factor I signaling in vascular smooth muscle cells. *Proc. Natl. Acad. Sci. U. S. A.* **95**, 11217-11222

141. Schneller, M., Vuori, K., and Ruoslahti, E. (1997) Alphavbeta3 integrin associates with activated insulin and PDGFbeta receptors and potentiates the biological activity of PDGF. *EMBO J.* **16**, 5600-5607

142. Guilherme, A., and Czech, M. P. (1998) Stimulation of IRS-1-associated phosphatidylinositol 3-kinase and Akt/protein kinase B but not glucose transport by beta1-integrin signaling in rat adipocytes. *J. Biol. Chem.* **273**, 33119-33122

143. Huang, D., Khoe, M., Befekadu, M., Chung, S., Takata, Y., Ilic, D., and Bryer-Ash, M. (2007) Focal adhesion kinase mediates cell survival via NF-kappaB and ERK signaling pathways. *American journal of physiology. Cell physiology* **292**, C1339-1352

144. Bisht, B., Srinivasan, K., and Dey, C. S. (2008) In vivo inhibition of focal adhesion kinase causes insulin resistance. *The Journal of physiology* **586**, 3825-3837

145. Gupta, A., and Dey, C. S. (2009) PTEN and SHIP2 regulates PI3K/Akt pathway through focal adhesion kinase. *Mol. Cell. Endocrinol.* **309**, 55-62

146. Lebrun, P., Mothe-Satney, I., Delahaye, L., Van Obberghen, E., and Baron, V. (1998) Insulin receptor substrate-1 as a signaling molecule for focal adhesion kinase pp125(FAK) and pp60(src). *J. Biol. Chem.* **273**, 32244-32253

147. Bisht, B., Goel, H. L., and Dey, C. S. (2007) Focal adhesion kinase regulates insulin resistance in skeletal muscle. *Diab tologia* **50**, 1058-1069

148. Huang, D., Khoe, M., Ilic, D., and Bryer-Ash, M. (2006) Reduced expression of focal adhesion kinase disrupts insulin action in skeletal muscle cells. *Endocrinology* **147**, 3333-3343

149. Cheung, A. T., Wang, J., Ree, D., Kolls, J. K., and Bryer-Ash, M. (2000) Tumor necrosis factor-alpha induces hepatic insulin resistance in obese Zucker (fa/fa) rats via interaction of leukocyte antigen-related tyrosine phosphatase with focal adhesion kinase. *Diabetes* **49**, 810-819

150. Bisht, B., and Dey, C. S. (2008) Focal Adhesion Kinase contributes to insulin-induced actin reorganization into a mesh harboring Glucose transporter-4 in insulin resistant skeletal muscle cells. *BMC cell biology* **9**, 48

151. El Annabi, S., Gautier, N., and Baron, V. (2001) Focal adhesion kinase and Src mediate integrin regulation of insulin receptor phosphorylation. *FEBS Lett.* **507**, 247-252

152. Cheung, A. T., Ree, D., Kolls, J. K., Fuselier, J., Coy, D. H., and Bryer-Ash, M. (1998) An in vivo model for elucidation of the mechanism of tumor necrosis factor-alpha (TNF-alpha)-induced insulin resistance: evidence for differential regulation of insulin signaling by TNF-alpha. *Endocrinology* **139**, 4928-4935

153. Delcommenne, M., Tan, C., Gray, V., Rue, L., Woodgett, J., and Dedhar, S. (1998) Phosphoinositide-3-OH kinase-dependent regulation of glycogen synthase kinase 3 and protein kinase B/AKT by the integrin-linked kinase. *Proc. Natl. Acad. Sci. U. S. A.* **95**, 11211-11216

154. Troussard, A. A., Mawji, N. M., Ong, C., Mui, A., St -Arnaud, R., and Dedhar, S. (2003) Conditional knock-out of integrin-linked kinase demonstrates an essential role in protein kinase B/Akt activation. *J. Biol. Chem.* **278**, 22374-22378

155. Wang, H. V., Chang, L. W., Brixius, K., Wickstrom, S. A., Montanez, E., Thievessen, I., Schwander, M., Muller, U., Bloch, W., Mayer, U., and Fassler, R. (2008) Integrin-linked kinase stabilizes myotendinous junctions and protects muscle from stress-induced damage. *J. Cell Biol.* **180**, 1037-1049

156. White, D. E., Coutu, P., Shi, Y. F., Tardif, J. C., Nattel, S., St Arnaud, R., Dedhar, S., and Muller, W. J. (2006) Targeted ablation of ILK from the murine heart results in dilated cardiomyopathy and spontaneous heart failure. *Genes Dev.* **20**, 2355-2360

157. Tan, C., Cruet-Hennequart, S., Troussard, A., Fazli, L., Costello, P., Sutton, K., Wheeler, J., Gleave, M., Sanghera, J., and Dedhar, S. (2004) Regulation of tumor angiogenesis by integrin-linked kinase (ILK). *Cancer cell* **5**, 79-90

158. Zhang, Y., Ikegami, T., Honda, A., Miyazaki, T., Bouscarel, B., Rojkind, M., Hyodo, I., and Matsuzaki, Y. (2006) Involvement of integrin-linked kinase in carbon tetrachloride-induced hepatic fibrosis in rats. *Hepatology* **44**, 612-622

159. Gkretsi, V., Mars, W. M., Bowen, W. C., Barua, L., Yang, Y., Guo, L., St-Arnaud, R., Dedhar, S., Wu, C., and Michalopoulos, G. K. (2007) Loss of integrin linked kinase from mouse hepatocytes in vitro and in vivo results in apoptosis and hepatitis. *Hepatology* **45**, 1025-1034

160. Sakai, T., Li, S., Docheva, D., Grashoff, C., Sakai, K., Kostka, G., Braun, A., Pfeifer, A., Yurchenco, P. D., and Fassler, R. (2003) Integrin-linked kinase (ILK) is required for polarizing the epiblast, cell adhesion, and controlling actin accumulation. *Genes Dev.* **17**, 926-940

161. Terpstra, L., Prud'homme, J., Arabian, A., Takeda, S., Karsenty, G., Dedhar, S., and St-Arnaud, R. (2003) Reduced chondrocyte proliferation and chondrodysplasia in mice lacking the integrin-linked kinase in chondrocytes. *J. Cell Biol.* **162**, 139-148

162. Ayala, J. E., Bracy, D. P., Malabanan, C., James, F. D., Ansari, T., Fueger, P. T., McGuinness, O. P., and Wasserman, D. H. (2011) Hyperinsulinemic-euglycemic clamps in conscious, unrestrained mice. *Journal of visualized experiments : JoVE*

163. Finegood, D. T., Bergman, R. N., and Vranic, M. (1988) Modeling error and apparent isotope discrimination confound estimation of endogenous glucose production during euglycemic glucose clamps. *Diabetes* **37**, 1025-1034

164. Ayala, J. E., Bracy, D. P., McGuinness, O. P., and Wasserman, D. H. (2006) Considerations in the design of hyperinsulinemic-euglycemic clamps in the conscious mouse. *Diabetes* **55**, 390-397

165. Steele, R., Wall, J. S., De Bodo, R. C., and Altszuler, N. (1956) Measurement of size and turnover rate of body glucose pool by the isotope dilution method. *Am. J. Physiol.* **187**, 15-24

166. Folch, J., Lees, M., and Sloane Stanley, G. H. (1957) A simple method for the isolation and purification of total lipides from animal tissues. *J. Biol. Chem.* **226**, 497-509

167. Morrison, W. R., and Smith, L. M. (1964) Preparation of Fatty Acid Methyl Esters and Dimethylacetals from Lipids with Boron Fluoride--Methanol. *J. Lipid Res.* **5**, 600-608

168. Kuznetsov, A. V., Strobl, D., Ruttmann, E., Konigsrainer, A., Margreiter, R., and Gnaiger, E. (2002) Evaluation of mitochondrial respiratory function in small biopsies of liver. *Anal. Biochem.* **305**, 186-194

169. Pallotti, F., and Lenaz, G. (2007) Isolation and subfractionation of mitochondria from animal cells and tissue culture lines. *Methods Cell Biol.* **80**, 3-44

170. Hepple, R. T., Baker, D. J., Kaczor, J. J., and Krause, D. J. (2005) Long-term caloric restriction abrogates the age-related decline in skeletal muscle aerobic function. *FASEB J.* **19**, 1320-1322

171. Chan, T. M., and Exton, J. H. (1976) A rapid method for the determination of glycogen content and radioactivity in small quantities of tissue or isolated hepatocytes. *Anal. Biochem.* **71**, 96-105

172. Koliwad, S. K., Streeper, R. S., Monetti, M., Cornelissen, I., Chan, L., Terayama, K., Naylor, S., Rao, M., Hubbard, B., and Farese, R. V., Jr. (2010) DGAT1-dependent triacylglycerol storage by macrophages protects mice from diet-induced insulin resistance and inflammation. *J. Clin. Invest.* **120**, 756-767

173. Livak, K. J., and Schmittgen, T. D. (2001) Analysis of relative gene expression data using real-time quantitative PCR and the 2(-Delta Delta C(T)) Method. *Methods* **25**, 402-408

174. Cheadle, C., Vawter, M. P., Freed, W. J., and Becker, K. G. (2003) Analysis of microarray data using Z score transformation. *The Journal of molecular diagnostics : JMD* **5**, 73-81

175. Puri, P., Baillie, R. A., Wiest, M. M., Mirshahi, F., Choudhury, J., Cheung, O., Sargeant, C., Contos, M. J., and Sanyal, A. J. (2007) A lipidomic analysis of nonalcoholic fatty liver disease. *Hepatology* **46**, 1081-1090

176. Guilherme, A., Torres, K., and Czech, M. P. (1998) Cross-talk between insulin receptor and integrin alpha5 beta1 signaling pathways. *J. Biol. Chem.* **273**, 22899-22903

177. Zong, H., Bastie, C. C., Xu, J., Fassler, R., Campbell, K. P., Kurland, I. J., and Pessin, J. E. (2009) Insulin resistance in striated muscle-specific integrin receptor beta1-deficient mice. *J. Biol. Chem.* **284**, 4679-4688

178. Kang, L., Ayala, J. E., Lee-Young, R. S., Zhang, Z., James, F. D., Neufer, P. D., Pozzi, A., Zutter, M. M., and Wasserman, D. H. (2011) Diet-induced muscle insulin resistance is associated with extracellular matrix remodeling and interaction with integrin alpha2beta1 in mice. *Diabetes* **60**, 416-426

179. Carmiel-Haggai, M., Cederbaum, A. I., and Nieto, N. (2005) A high-fat diet leads to the progression of non-alcoholic fatty liver disease in obese rats. *FASEB J.* **19**, 136-138

180. Chen, X., Abair, T. D., Ibanez, M. R., Su, Y., Frey, M. R., Dise, R. S., Polk, D. B., Singh, A. B., Harris, R. C., Zent, R., and Pozzi, A. (2007) Integrin alpha1beta1 controls reactive oxygen species synthesis by negatively regulating epidermal growth factor receptor-mediated Rac activation. *Mol. Cell. Biol.* **27**, 3313-3326

181. Best, J. D., Kahn, S. E., Ader, M., Watanabe, R. M., Ni, T. C., and Bergman, R. N. (1996) Role of glucose effectiveness in the determination of glucose tolerance. *Diabetes Care* **19**, 1018-1030

182. Mattila, E., Pellinen, T., Nevo, J., Vuoriluoto, K., Arjonen, A., and Ivaska, J. (2005) Negative regulation of EGFR signalling through integrin-alpha1beta1-mediated activation of protein tyrosine phosphatase TCPTP. *Nature cell biology* **7**, 78-85

183. Vulin, A. I., Jacob, K. K., and Stanley, F. M. (2005) Integrin activates receptor-like protein tyrosine phosphatase alpha, Src, and Rho to increase prolactin gene expression through a final phosphatidylinositol 3-kinase/cytoskeletal pathway that is additive with insulin. *Endocrinology* **146**, 3535-3546

184. Fujita, M., Ieguchi, K., Davari, P., Yamaji, S., Taniguchi, Y., Sekiguchi, K., Takada, Y. K., and Takada, Y. (2012) Cross-talk between integrin alpha6beta4 and insulin-like growth factor-1 receptor (IGF1R) through direct alpha6beta4 binding to IGF1 and subsequent alpha6beta4-IGF1-IGF1R ternary complex formation in anchorage-independent conditions. *J. Biol. Chem.* **287**, 12491-12500

185. Shi, M., Pedchenko, V., Greer, B. H., Van Horn, W. D., Santoro, S. A., Sanders, C. R., Hudson, B. G., Eichman, B. F., Zent, R., and Pozzi, A. (2012) Enhancing integrin alpha1 inserted (I) domain affinity to ligand potentiates integrin alpha1beta1-mediated down-regulation of collagen synthesis. *J. Biol. Chem.* **287**, 35139-35152

186. Summers, L. K., Barnes, S. C., Fielding, B. A., Beysen, C., Ilic, V., Humphreys, S. M., and Frayn, K. N. (2000) Uptake of individual fatty acids into adipose tissue in relation to their presence in the diet. *Am. J. Clin. Nutr.* **71**, 1470-1477

187. Tonelli, J., Kishore, P., Lee, D. E., and Hawkins, M. (2005) The regulation of glucose effectiveness: how glucose modulates its own production. *Current opinion in clinical nutrition and metabolic care* **8**, 450-456

188. Hirosumi, J., Tuncman, G., Chang, L., Gorgun, C. Z., Uysal, K. T., Maeda, K., Karin, M., and Hotamisligil, G. S. (2002) A central role for JNK in obesity and insulin resistance. *Nature* **420**, 333-336

189. Chen, H. C., Stone, S. J., Zhou, P., Buhman, K. K., and Farese, R. V., Jr. (2002) Dissociation of obesity and impaired glucose disposal in mice overexpressing acyl coenzyme a:diacylglycerol acyltransferase 1 in white adipose tissue. *Diabetes* **51**, 3189-3195

190. Buque, X., Cano, A., Miquilena-Colina, M. E., Garcia-Monzon, C., Ochoa, B., and Aspichueta, P. (2012) High insulin levels are required for FAT/CD36 plasma membrane translocation and enhanced fatty acid uptake in obese Zucker rat hepatocytes. *American journal of physiology. Endocrinology and metabolism* **303**, E504-514

191. He, J., Lee, J. H., Febbraio, M., and Xie, W. (2011) The emerging roles of fatty acid translocase/CD36 and the aryl hydrocarbon receptor in fatty liver disease. *Exp Biol Med (Maywood)* **236**, 1116-1121

192. Chawla, A., Barak, Y., Nagy, L., Liao, D., Tontonoz, P., and Evans, R. M. (2001) PPAR-gamma dependent and independent effects on macrophage-gene expression in lipid metabolism and inflammation. *Nat. Med.* **7**, 48-52

193. Begriche, K., Massart, J., Robin, M. A., Bonnet, F., and Fromenty, B. (2013) Mitochondrial adaptations and dysfunctions in nonalcoholic fatty liver disease. *Hepatology* **58**, 1497-1507

194. Satapati, S., Sunny, N. E., Kucejova, B., Fu, X., He, T. T., Mendez-Lucas, A., Shelton, J. M., Perales, J. C., Browning, J. D., and Burgess, S. C. (2012) Elevated TCA cycle function in the pathology of diet-induced hepatic insulin resistance and fatty liver. *J. Lipid Res.* **53**, 1080-1092

195. Merlotti, C., Morabito, A., and Pontiroli, A. E. (2014) Prevention of type 2 diabetes; a systematic review and meta-analysis of different intervention strategies. *Diabetes, obesity & metabolism* **16**, 719-727

196. Di-Poi, N., Tan, N. S., Michalik, L., Wahli, W., and Desvergne, B. (2002) Antiapoptotic role of PPARbeta in keratinocytes via transcriptional control of the Akt1 signaling pathway. *Mol. Cell* **10**, 721-733

197. Plante, I., Charbonneau, M., and Cyr, D. G. (2006) Activation of the integrin-linked kinase pathway downregulates hepatic connexin32 via nuclear Akt. *Carcinogenesis* **27**, 1923-1929

198. Apte, U., Gkretsi, V., Bowen, W. C., Mars, W. M., Luo, J. H., Donthamsetty, S., Orr, A., Monga, S. P., Wu, C., and Michalopoulos, G. K. (2009) Enhanced liver regeneration following changes induced by hepatocyte-specific genetic ablation of integrin-linked kinase. *Hepatology* **50**, 844-851

199. Shafiei, M. S., and Rockey, D. C. (2006) The role of integrin-linked kinase in liver wound healing. *J. Biol. Chem.* **281**, 24863-24872

200. Gkretsi, V., Bowen, W. C., Yang, Y., Wu, C., and Michalopoulos, G. K. (2007) Integrin-linked kinase is involved in matrix-induced hepatocyte differentiation. *Biochem. Biophys. Res. Commun.* **353**, 638-643

201. Gkretsi, V., Apte, U., Mars, W. M., Bowen, W. C., Luo, J. H., Yang, Y., Yu, Y. P., Orr, A., St-Arnaud, R., Dedhar, S., Kaestner, K. H., Wu, C., and Michalopoulos, G. K. (2008) Liver-specific ablation of integrin-linked kinase in mice results in abnormal histology, enhanced cell proliferation, and hepatomegaly. *Hepatology* **48**, 1932-1941

202. Wu, C., and Dedhar, S. (2001) Integrin-linked kinase (ILK) and its interactors: a new paradigm for the coupling of extracellular matrix to actin cytoskeleton and signaling complexes. *J. Cell Biol.* **155**, 505-510

203. Vial, G., Dubouchaud, H., Couturier, K., Cottet-Rousselle, C., Taleux, N., Athias, A., Galinier, A., Casteilla, L., and Leverve, X. M. (2011) Effects of a high-fat diet on energy metabolism and ROS production in rat liver. *J. Hepatol.* **54**, 348-356

204. Vial, G., Dubouchaud, H., and Leverve, X. M. (2010) Liver mitochondria and insulin resistance. *Acta Biochim. Pol.* **57**, 389-392

205. Lynch, D. K., Ellis, C. A., Edwards, P. A., and Hiles, I. D. (1999) Integrin-linked kinase regulates phosphorylation of serine 473 of protein kinase B by an indirect mechanism. *Oncogene* **18**, 8024-8032

206. Huang, W., Metlakunta, A., Dedousis, N., Zhang, P., Sipula, I., Dube, J. J., Scott, D. K., and O'Doherty, R. M. (2010) Depletion of liver Kupffer cells prevents the development of diet-induced hepatic steatosis and insulin resistance. *Diabetes* **59**, 347-357
207. Speicher, T., Siegenthaler, B., Bogorad, R. L., Ruppert, R., Petzold, T., Padrissa-Altes, S., Bachofner, M., Anderson, D. G., Koteliansky, V., Fassler, R., and Werner, S. (2014) Knockdown and knockout of beta1-integrin in hepatocytes impairs liver regeneration through inhibition of growth factor signalling. *Nature communications* **5**, 3862